To the Graduate Council:

I am submitting herewith a thesis written by Richard H. Eskridge entitled "Prediction of Blast Induced Overpressure on Isolated and Shielded Structures." I recommend that it be accepted in partial fulfillment of the requirements for the degree of Master of Science, with a major in Engineering Science.

Dennis Keefer

Dennis R. Keefer, Major Professor

We have read this thesis
and recommend its acceptance:

Kenneth E. Harwell

R L Young

Accepted for the Council:

L. E. vanSloth

Vice Chancellor
Graduate Studies and Research

B

PREDICTION OF BLAST INDUCED OVERPRESSURE ON ISOLATED AND SHIELDED STRUCTURES

A Thesis
Presented for the
Master of Science
Degree
The University of Tennessee, Knoxville

Richard H. Eskridge

March 1981

ACKNOWLEDGEMENT

The author expresses his sincere appreciation to Dr. Dennis R. Keefer, Professor of Engineering Science, and Dr. Rush E. Elkins, Research Engineer, at the University of Tennessee Space Institute for their guidance and advice during the course of this investigation. Thanks are also given to Melody Ward for her patient and conscientious efforts in the typing of the manuscript.

The author is especially grateful to his wife, Kathy, for the continuing understanding and support which she has provided throughout his college career.

ABSTRACT

A simple model has been developed to predict the overpressure on a building exposed to blast waves created by large scale chemical or nuclear explosions. This model may be used to predict the blast loading on buildings which are either isolated or shielded by nearby structures. The model is based on a simple linear formulation for the equalization of pressure on the building face with that of the free-field. Dynamic effects are included in the model by the use of an empirical drag coefficient. The effects of reflected shock waves between adjacent buildings have also been taken into account, together with diffraction losses incurred by the blast wave due to interactions with adjacent structures. Comparison of the model with data from both shock tube and free-field experiments indicate reasonable agreement for several test configurations. This model should prove to be useful as input for existing models which predict the structural damage to buildings exposed to blast waves.

TABLE OF CONTENTS

LIST OF TABLES

LIST OF FIGURES

Figure | Page

Figure | Page

Figure | Page

LIST OF SYMBOLS

SYMBOL

A	=	Empirical Function of Time, Overpressure, and R (Appendix B).
A_N	=	Slope of the nth Input Segment.
a_o	=	Ambient Speed of Sound.
a_5	=	Speed of Sound Behind a Reflected Shock.
B	=	Empirical Function of Time, Overpressure, and R (Appendix B)
c	=	Velocity of Rarefaction Waves (or Compression Waves) on a Surface.
C_D	=	"Drag Coefficient" for a Building Face.
C_N	=	Arbitrary Constant on the Nth Segment.
D	=	Diffracted Overpressure Ratio (P_d/P_A) or the Distance Between Buildings Used to Calculate the Transit Time of Reflected Shocks.
F	=	Overpressure Ratio of Incident Shock (P_s/P_A).
h	=	Height of a Building Wall.
F_N	=	Reflected Overpressure of the Nth Reflected Shock on the Front Wall.
$I(t)$	=	Input Wave Adjusted for Dynamic Effects.
I_N	=	Overpressure of the Nth Data Point on the Input Wave Adjusted for Dynamic Effects.
ℓ	=	Distance Between Buildings or the Length of a Building.
M_o	=	Mach Number of the Incident Shock (u_o/a_o).
M_o'	=	Mach Number of a Reflected Shock.

SYMBOL

M_w	=	Mach Number of a Diffracted Shock, on the wall.
$p(t,N)$	=	Solution for the Overpressure on a Surface.
P_A	=	Ambient Atmospheric Pressure.
P_d	=	Overpressure of a Diffracted Shock
P_I	=	Initial Overpressure Used for Calculation of the Magnitudes of Subsequent Reflected Shocks.
P_L	=	Overpressure Approached as a Limit (Appendix B).
p_N	=	Value of Overpressure on the Solution at the Beginning of the Nth Input Segment.
p_o	=	Initial Value of Overpressure on a Surface.
P_q	=	Peak Value of the Dynamic Overpressure in the Free-field.
$p_q(t)$	=	Time Dependent Overpressure in the Free-field.
P_r	=	Overpressure of a Shock Reflected from a Surface.
P_s	=	Peak Overpressure of the Incident Shock.
P_{STAG}	=	Stagnation Overpressure on a Front Surface (Appendix B).
ps_N	=	Overpressure of the Nth Sampled Data Point in the Free-field at time t_N .
$ps(t)$	=	Time Dependent Side-on Overpressure of the Incident Shock Wave.
$q(t)$	=	Dynamic Component of Overpressure On a Surface.
R	=	Ratio of the Edges S_1 , S_2 of the Minimum Area to be Examined for Calculation Purposes (Appendix B).
R_N	=	Overpressure of the Nth Reflected Shock on a Rear Wall.

SYMBOL

s	=	Dummy Variable of Integration.
S	=	Characteristic Distance for a Surface.
S_1, S_2	=	Two Possible Choices for the Characteristic Distance of a Rectangular Surface.
t	=	Time.
t_c	=	Time Required for Shock Waves to Merge on the Rear Wall.
t_N	=	Time of the Nth Sampled Data Point on the Input Wave.
$\hat{t}_N$	=	Elapsed Time on an Input Segment $(t-t_N)$.
t_r	=	"Recovery Time" for a Diffracted Shock Wave.
t_s	=	Time of Arrival of a Reflected Shock.
t_t	=	Transit Time of a Shock Wave Across the Space Between Adjacent Buildings.
u_o	=	Velocity of the Incident Shock Wave.
u_d	=	Velocity of a Diffracted Shock Wave.
u'	=	Diffracted to Incident Shock Velocity Ratio (u_d/u_o).
w	=	Width of a Building.
W_N	=	Overpressure of a Reflected Shock at the End of the Nth Transit Between Buildings.
x	=	Spatial Co-ordinate (Distance).
z	=	Overpressure Ratio of the Incident Shock Wave (P_s/P_A) in Appendix B.
α	=	Shock Loss Coefficient.
γ	=	Ratio of Specific Heats.

SYMBOL

ζ	=	Normalized Time ($t \cdot a_o/S$) in Appendix B.
η	=	Normalized Time ($t \cdot a_5(1+R)/S$) in Appendix B.
Θ	=	Shock Turning Angle in Diffraction.
ξ	=	Angle of Incidence of Reflected Shock.
τ	=	Characteristic Time.

INTRODUCTION

Large scale chemical or nuclear explosions produce blast waves capable of causing damage to structures at great distances from the point of detonation. The ability to estimate the damage to a structure exposed to a blast wave has important military and civil defense applications. The interior and exterior blast loading on the structure must be known before the degree of damage can be determined. Estimation of the loading on a building which is shielded by nearby structures is of particular concern, although it has received little attention in the past.

Techniques have been developed to predict the loading on the exterior of an isolated block structure exposed to a blast wave at normal incidence. A crude approximation for this loading is given in "The Effects of Nuclear Weapons" [1]. Etheridge [2] has developed an improved method of estimating the blast loading using empirical curve fits to shock tube data. Calculations have also been made by Gentry [3] for the isolated block structure using a finite difference scheme. However, none of these models provide an estimate for the loading on the building when it is surrounded by other structures.

A model for the interior loading of a structure with openings exposed to a blast wave has been developed by Rempel [4]. This model is based on the bulk "filling" of the room due to inflow of air through the opening. An improved model by Keefer [5] considers the acoustic response of the interior. This model incorporates the results of Rempel [4] with a model developed by Vaidya [6] for the acoustic response of rooms to sonic booms.

The mechanical response of a structure of arbitrary plan has also been modeled by Rempel [7]. This model determines the degree of damage to the structure, given the internal and external pressure histories.

Experimental results have been obtained by Coulter [8] for two configurations of shielded model buildings exposed to blast waves of approximately 4 psi overpressure. Records from these experiments reveal significant differences between the shielded and isolated cases. These differences are sufficient to affect the assessment of structural damage in some cases. A model which accounts for these differences is needed if an accurate determination of blast damage is to be made for shielded structures.

A model for the blast loading on a building surrounded by nearby structures has been developed using simple physical concepts. This model is developed for the isolated building at arbitrary orientation to the incident blast in Chapter I. In Chapter II, this model is extended for use in the shieleded case. The results are summarized in Chapter III, together with comments on the possible applications and limitations of the model.

CHAPTER I

BLAST INTERACTIONS WITH ISOLATED STRUCTURES

1. Background

A shock wave passing over an isolated structure interacts differently with each face of the building, depending on the orientation of the face with respect to the direction of shock propagation. A forward oriented face will experience a discontinuous jump in overpressure due to reflection of the shock. Following reflection, rarefaction waves sweeping from the edge to the center of the building face will eventually reduce the overpressure on the wall to the peak-side-on overpressure plus a dynamic pressure component. A rearward oriented face will experience a continuous rise in overpressure from essentially zero to some maximum value and then will begin to decrease due to the propagation of rarefaction waves. A face oriented parallel to the direction of shock propagation will experience the peak side-on overpressure reduced by a dynamic component, and perturbations caused by local vortex shedding and rarefaction waves propagating from the rear. These differences in blast loading are illustrated graphically in Figure (1-1) below.

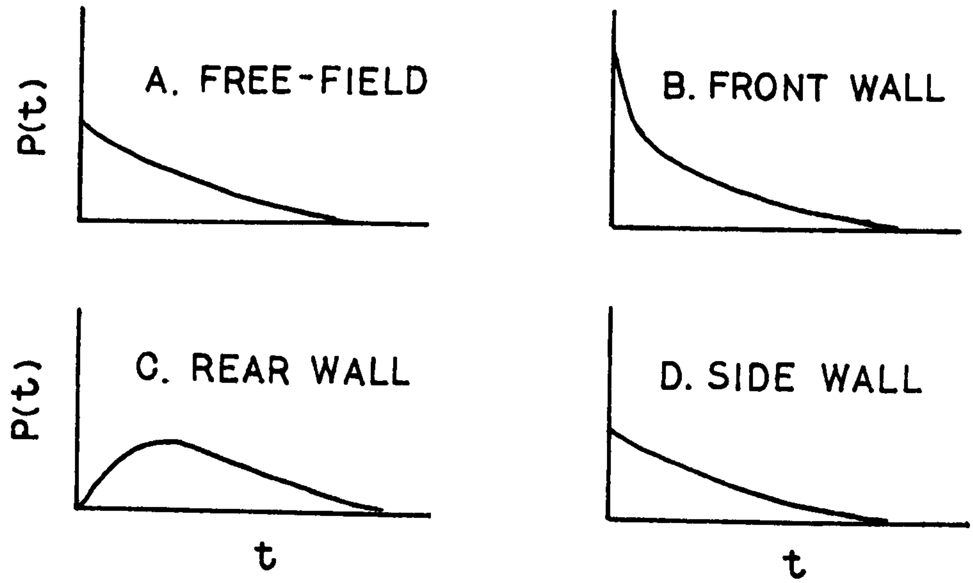

Figure 1-1. Idealized Overpressure on an Isolated Block Structure. (Normal Incidence)

Empirical models are given in "The Effects of Nuclear Weapons"[1] for these phenomena. These models provide a rough estimate of the general aspects of the loading and yield approximations for the peak overpressure on the building face. It is desirable, however, to obtain a more refined model which considers the problem in greater detail. Such a model has been developed and is presented in the following section.

2. Formulation of the Problem

Consider a blast wave incident on a finite surface in air (Figure 1-2).

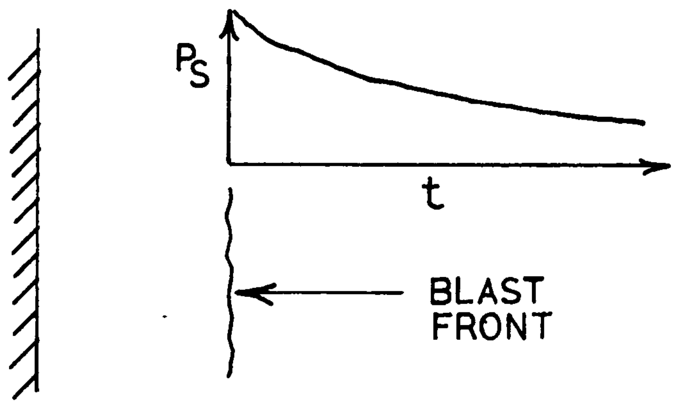

Figure 1-2. Blast Wave Incident on a Surface.

Upon reflection of the shock value from the surface at time t = 0, the pressure will instantaneously assume the value P_R . Let the overpressure of the incident wave be given by $p_s(t)$ and the overpressure on the wall be given by p(t). It will be assumed that the rate of change of pressure on the wall is directly proportional to the difference between the wall overpressure and the overpressure in the free-field. Mathematically, this statement becomes,

$$\frac{dp(t)}{dt} \propto (ps(t) - p(t)) \ . \qquad (1.1)$$

Introducing the constant of proportionality (or "characteristic time"), τ , gives

$$\frac{dp(t)}{dt} = \frac{1}{\tau}\,(ps(t) - p(t)) \;, \tag{1.2}$$

where:

p(t) = time dependent overpressure on the surface

ps(t) = free-field overpressure

τ = proportionality constant having units of time

This differential equation may be integrated if a mathematical form is given for ps(t). Often, it is convenient to approximate the input wave by a series of line segments connecting sampled data points. This process is illustrated graphically in Figure 1-3.

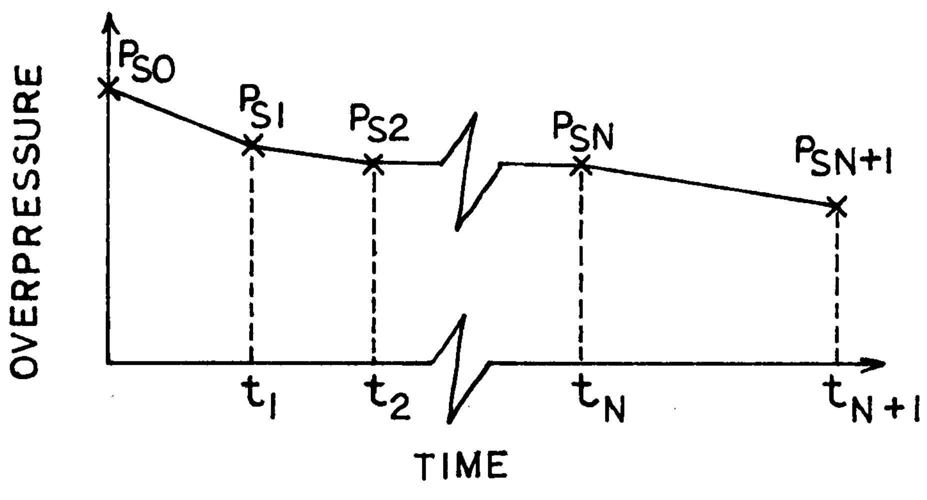

Figure 1-3. Approximation of the Input Wave by Line Segments.

Each point on the line segment may be represented in terms of the particular time under consideration and the end points of the segment. For

$$t_N \leq t < t_{N+1} \quad ,$$

$$ps(t) = A_N \; (t - t_N) + ps_N \quad , \tag{1.3}$$

Where A_N is the slope of the segment given by,

$$A_N = (ps_{N+1} - ps_N)/(t_{N+1} - t_N) \quad , \tag{1.4}$$

and ps_N is the overpressure of the input wave at time t_N . Define a quantity $\hat{t}_N$ on the Nth input segment so that

$$\hat{t}_N = (t - t_N) \tag{1.5}$$

In terms of $\hat{t}_N$ the input wave on the Nth segment becomes,

$$ps(\hat{t}_N) = A_N \; \hat{t}_N + ps_N \quad , \tag{1.6}$$

and the differential equation 1.2 may be written for the Nth input segment as,

$$\frac{dp}{d\hat{t}_N} + \frac{1}{\tau}\,p(\hat{t}_N) = \frac{1}{\tau}\,(A_N\hat{t}_N + ps_N) \tag{1.7}$$

This equation has the solution,

$$p(\hat{t}_N) = \frac{1}{\tau}\,e^{-\hat{t}_N/\tau}\int e^{s/\tau}\,(A_N s + ps_N)\,ds + C_N e^{-\hat{t}_N/\tau}, \tag{1.8}$$

where s is a dummy variable of integration and C_N is an arbitrary constant.

When this integral is evaluated, Equation (1.8) becomes,

$$p(\hat{t}_N) = ps_N + C_N e^{-\hat{t}_N/\tau} + A_N(\hat{t}_N - \tau) \quad . \tag{1.9}$$

At the beginning of each segment $t = t_N$ and $\hat{t}_N = 0$. Substituting this result in Equation 1.9 we obtain

$$p_N = p(t_N) = ps_N + C_N - A_N\tau \quad . \tag{1.10}$$

The arbitrary constant C_N is given by,

$$C_N = (p_N - ps_N) + A_N\tau \quad . \tag{1.11}$$

Substituting this value for C_N is Equation 1.9 we obtain,

$$p(\hat{t}_N) = ps_N + \left[(p_N - ps_N) + A_N\tau\right] e^{-\hat{t}_N/\tau} + A_N(\hat{t}_N - \tau) \ . \tag{1.12}$$

The overpressure of any time, t, is obtained by noting that $\hat{t}_N = t - t_N$,

$$p(t,N) = ps_N + \Big((p_N - ps_N) + A_N\,\tau\Big)e^{-(t-t_N)/\tau} + A_N(t-t_N-\tau) \qquad (1.13)$$

<u>where</u>:

$p(t,N)$ = overpressure on the surface at time t on the Nth Input interval $t_N < t \leq t_{N+1}$

ps_N = overpressure of the input wave at time t_N.

A_N = slope of the Nth segment of the input wave (Equation 1.4)

p_N = overpressure on the surface at time t_N as determined by the final calculations for the previous segment.

τ = "characteristic time" for the process.

This equation provides a solution for any desired sequence of input segments. When the solution is started at time t = 0 using the first segment of the input wave, the value of P_o is the initial condition on the wall. At the beginning of each succeeding segment, the value of the parameters are reinitialized to insure continuity of the solution across the segments. The solution is then continued on the new segment and the process is repeated.

The procedure is illustrated graphically in Figure 1-4 below.

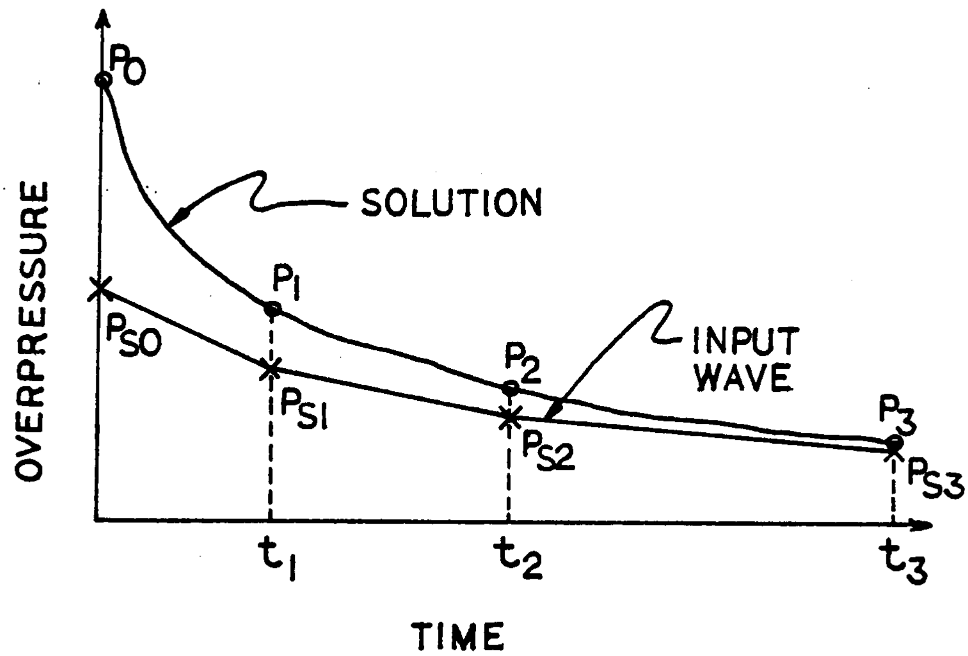

Figure 1—4. Illustration of the Solution for Segmented Input.

Equation 1.13 may be used for either front or back walls by choosing the appropriate initial pressure. For a front surface, the initial pressure P_0 is equal to the reflected overpressure P_R as given by the relation for normal reflection of a shock (Equation A.1). Measurements on the rear walls of structures indicate that for weak shocks, the average initial overpressure P_0 is approximately zero. Substitution of these initial conditions in Equation 1.13 for a classical blast wave, as shown in Figure 1-1(a), results in a solution which exhibits the general behavior for the front and rear walls as shown in Figures 1-1(b) and 1-1(c) respectively.

The "characteristic time", τ , may be chosen through consideration of the mechanism responsible for the pressure reduction. As previously mentioned, the reduction and buildup of pressure on the wall is controlled by rarefaction waves (or compression waves) sweeping across the building face from edge to center. Intuitively, it is the time required for these waves to propagate across the surface which determines how quickly equilibrium may be reached. This suggests the following form for the characteristic time,

$$\tau = S/c \ , \tag{1.14}$$

where:

S is the characteristic distance (center to edge),

c is the rate at which waves travel on the face.

For a rectangular building there are two choices, S_1 and S_2, which can be made for the characteristic distance (Figure 1-5). These distances are determined by the location of the planes of symmetry peculiar to the problem. In this case the ground acts as one plane of symmetry due to stagnation at the foot of the wall. The other plane of symmetry is vertical, extending upward through the center of the building, since the flow must part to both right and left to pass around the building[2].

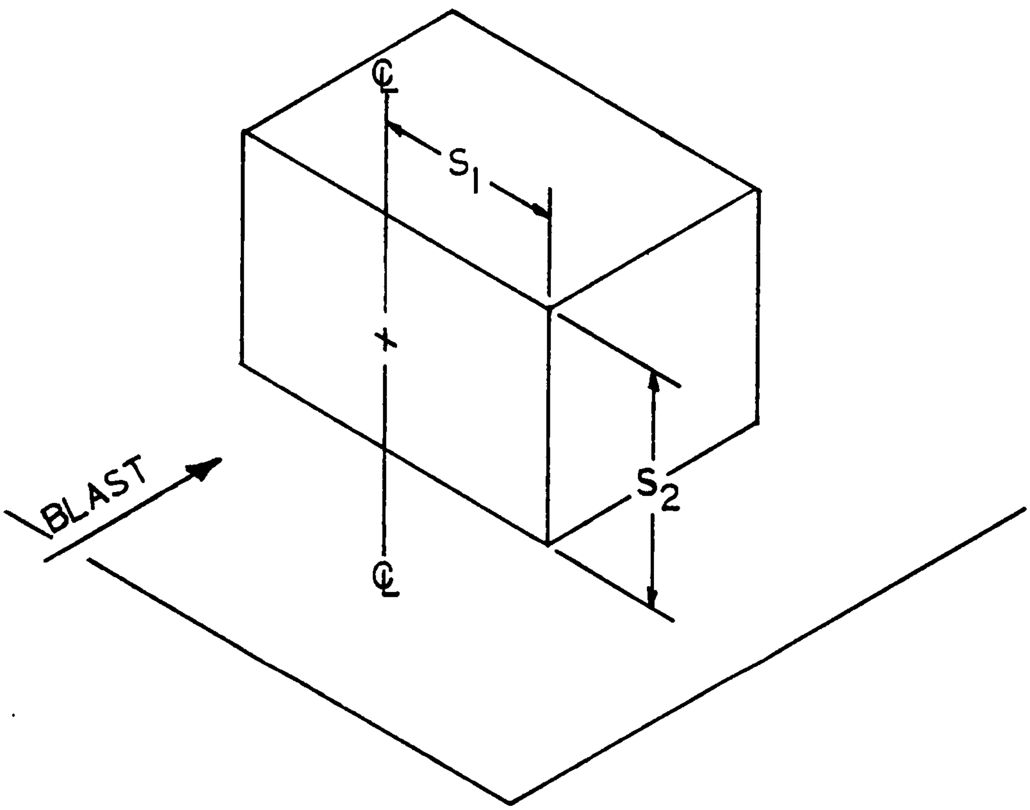

Figure 1-5. Two Possible Choices (S_1, S_2) for the Characteristic Distance (Normal Incidence).

The characteristic distances S_1 and S_2 are the perpendicular distances from each plane to the corresponding parallel edge. The smaller of the two is taken for use in Equation 1.14. The smaller is chosen because the rarefaction wave arrives from the nearest edge first, thus dominating the rate of reduction on the wall.

The rate at which waves sweep across the face, c, is different for the front and rear walls. On the front wall, the shock reaches the reflected pressure P_R and the speed of sound is changed from a_o to a higher speed, a_5. On the rear wall, the shock is weakened due to flow separation and extreme shock curvature as it diffracts around the corner of the building. Thus, after traveling a very short distance on the rear, the shock approximates an acoustic wave propagating at essentially the ambient sound velocity a_o. For the two cases, front and rear, Equation (1.14) becomes,

$$\tau = S/a_5 \text{ on the front wall, and} \tag{1.15}$$

$$\tau = S/a_0 \text{ on the rear wall,} \tag{1.16}$$

where:

S = minimum distance from an edge to the corresponding parallel plane of symmetry

a_5 = speed of sound behind the reflected shock wave (Equation A.2)

a_o = ambient speed of sound

Thus far, the analysis has neglected dynamic effects associated with the "afterwind" or air movement associated with the blast. For all but exceptionally weak shocks, this flow will induce a dynamic component of overpressure on the building which must be considered. It is possible to alter the analysis to include this effect as shown in the next section.

3. Calculation of Dynamic Effects

The air movement associated with the passage of a blast wave will induce a dynamic component of pressure on any structure immersed in the flow. It is the sum of the dynamic and interacting shock overpressure which comprises the total overpressure on the structure. Therefore, dynamic effects must be considered in order to provide a more accurate estimate of the overpressure on the building.

It is possible to estimate the dynamic pressure on any surface of the structure using a model based on an empirical drag co-efficient, and the assumption of uniform parallel flow in the free-field [1]. Consider a structure immersed in a flow where the free-field dynamic pressure is given by $p_q(t)$. The dynamic pressure $q(t)$, on any particular face of the building is given by,

$$q(t) = C_D p_q(t) , \tag{1.17}$$

where:

$q(t)$ is the dynamic component of overpressure on a given face of the building

$p_q(t)$ is the dynamic pressure of the free-field

C_D is the empirical drag co-efficient for the building face.

The dynamic component ($q(t)$) of the overpressure on the wall is easily calculated if the free-field dynamic overpressure is known. It will be assumed in this analysis that the free-field static and dynamic overpressure waveforms are approximately similar in time. With this assumption, it is possible to write $p_q(t)$ in the form,

$$p_q(t) = \frac{P_q}{P_s} ps(t) , \tag{1.18}$$

where P_q is the peak dynamic pressure of the free-field (Equation A.3) and P_s is the peak-side-on overpressure of the incident blast. The dynamic component of overpressure incident on the wall is then,

$$q(t) = C_D \frac{P_q}{P_s} ps(t) . \tag{1.19}$$

The model developed in the previous section is linear; therefore, it is possible to account for the dynamic component of the overpressure by simple modification of the input wave, $ps(t)$. Let

$$I(t) = ps(t) + p_q(t) \quad . \tag{1.20}$$

Then

$$I(t) = \left[C_D \frac{P_q}{P_s} + 1 \right] ps(t) \quad , \tag{1.21}$$

where I(t) is the input wave modified to include dynamic effects. A segmented input as described in Section 2 may be used to approximate I(t) by applying the transformation,

$$I_N = \left[C_D \frac{P_q}{P_s} + 1 \right] ps_N \quad , \tag{1.22}$$

to each input data point ps_N at time t_N on the input waveform. The segment slope, A_N, becomes,

$$A_N = (I_{N+1} - I_N)/(t_{N+1} - t_N) \quad . \tag{1.23}$$

Substitution of I_N for ps_N in Equation 1.13 gives,

$$P(t,N) = I_N + \left((p_N - I_N) + A_N\tau\right) e^{-(t-t_N)/\tau} + A_N(t-t_N-\tau) . \tag{1.24}$$

Equation 1.24 gives the overpressure on the surface of a building, including both static and dynamic effects. This overpressure may be larger or smaller than the corresponding solution for the static overpressure given by Equation 1.13, depending on the value of the drag co-efficient. When the drag co-efficient is positive (forward facing wall) the pressure is larger due to the addition of a positive dynamic component. For a rearward facing wall, the drag co-efficient is negative and the pressure is reduced due to the negative dynamic component of the flow. Approximate drag co-efficients are given in Appendix C for the faces of a strucure with a gabled roof.

4. Shocks at Oblique Incidence

The previous analysis has been based on the assumption that the blast wave strikes the building at normal incidence; however, it is possible to extend these results for use in the oblique case. Consider a plane shock wave incident at an oblique angle on a forward facing surface (Figure 1-6).

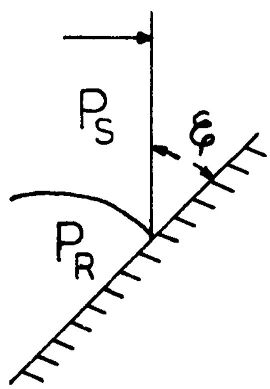

Figure 1-6. Plane Shock Wave Striking a Surface at Oblique Incidence.

Unlike the case for normal incidence, all points on the surface are not loaded at the same instant of time. Therefore, the time scale of the problem must be shifted to account for the delay in wave front arrival. The reflected overpressure on the surface will also differ from normal shock reflection.

Porzel [10] has compiled values of reflected overpressures for a wide range of incident shock strengths as a function of the angle of incidence. These results are particularly useful for predicting reflected overpressures in the regime of transition and mach reflection. For all practical purposes, the reflected overpressures corresponding to angles of incidence less than 40^{o} are well approximated by the value for normal reflection (Equation A.1).

Equation 1.24 may be used to calculate the overpressure on the surface if the value of reflected overpressure, P_R , is substituted for the initial overpressure on the wall, p_0 , and if the time delay for wave arrival is accounted for. The value of the characteristic time, τ , is determined in the same manner as the case for normal incidence. It is important to note that the drag co-efficients will also differ for the oblique case and thus must be chosen accordingly.

It previously has been assumed that the initial overpressure on a rearward facing surface is effectively zero. This assumption was based on the fact that the shock is degraded due to flow separation and other effects. However, for shallow oblique angles on the rear (such as the case of a sloped roof) it is possible for the shock wave to diffract with very little loss, providing an initial pressure which is non-zero. Simple models are available to predict this loss due to shock diffraction.

Consider a shock wave propagating around a convex corner (Figure 1-7).

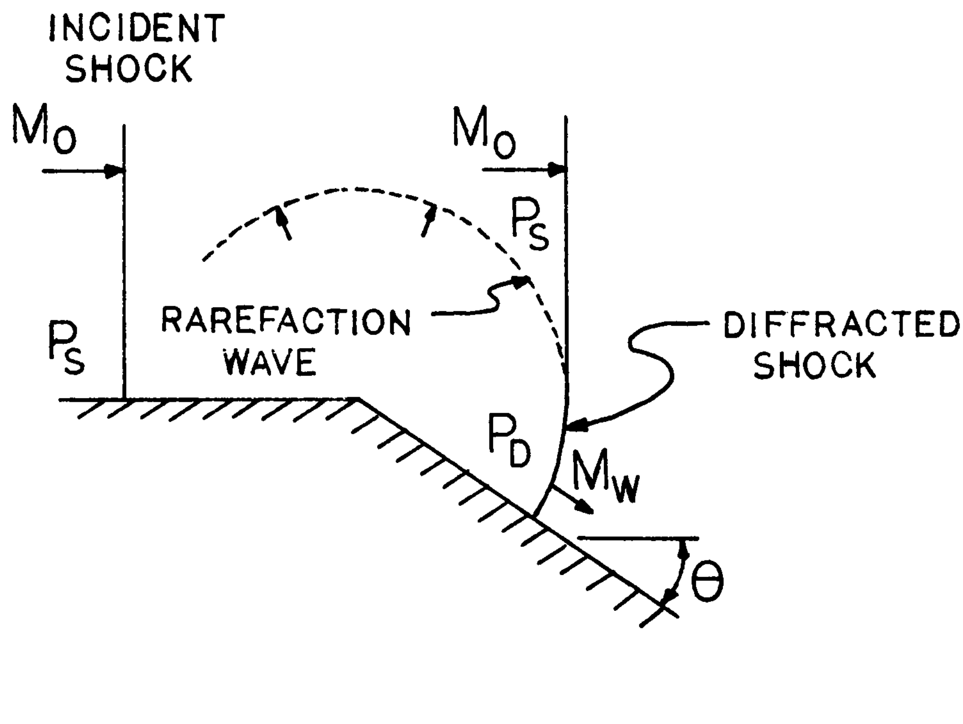

Figure 1-7. Shock Wave Propagation Around a Convex Corner.

When the shock wave arrives at the corner, a rarefaction wave is generated behind the shock front due to the expansion of the flow. This rarefaction wave interacts with the shock, causing it to diffract around the corner. The Mach number of the shock front will vary along the front from the reduced value, M_w , at the wall, to the undisturbed value, M_o , at points on the front ahead of the rarefaction wave. The diffracted overpressure of the shock, P_d , is related to M_w by the Rankine-Huginot relation,

$$P_d = P_A \left[\frac{2\gamma}{\gamma+1} \left(M_w^2 - \frac{\gamma-1}{2\gamma} \right) - 1 \right] , \qquad (1.25)$$

where γ is the ratio of specific heats. Thus, the initial overpressure on the oblique surface may be determined if the value of M_w is known.

Whitham [11] has developed a model for shock diffraction based on a theory of wave propagation along the shock. On this theory, waves propagating along the shock are calculated in a manner analogous to the method of characteristics for plane waves in gas dynamics. For very weak shocks, Whitham obtained the following approximation,

$$\theta \simeq 2^{3/2} \left[(M_w - 1)^{\frac{1}{2}} - (M_o - 1)^{\frac{1}{2}} \right] \qquad (1.26)$$

where:

θ = turning angle of the convex corner, taken to be negative.

M_W = Mach number of the diffracted shock on the wall.

M_o = Mach number of the undisturbed shock.

Equation 1.26 may be solved for M_W to obtain,

$$M_W = \left[\frac{\theta}{2^{3/2}} + (M_o - 1)^{\frac{1}{2}}\right]^2 . \qquad (1.27)$$

Through the Rankine-Hugniot relation, M_o may be related to the overpressure of the undisturbed shock, P_s,

$$M_o = \left[\frac{\gamma-1}{2\gamma} + \frac{\gamma+1}{2\gamma}\ \frac{P_s+P_A}{P_A}\right]^{\frac{1}{2}} \qquad (1.28)$$

Solving for P_s in Equation 1.28, we obtain

$$P_s = P_A\left[\frac{2\gamma}{\gamma+1}\left(M_o^2 - \frac{\gamma-1}{2\gamma}\right) - 1\right] \qquad (1.29)$$

where M_o = Mach number of the undisturbed shock.

Equations 1.25 and 1.29 may be combined to obtain the ratio of diffracted to undisturbed shock pressures,

$$\frac{P_d + P_A}{P_s + P_A} = \frac{M_w^2 - \frac{\gamma-1}{2\gamma}}{M_0^2 - \frac{\gamma-1}{2\gamma}} \quad . \tag{1.30}$$

Substituting the value for M_w given in Equation 1.24 into Equation 1.30 we obtain,

$$\frac{P_d + P_A}{P_s + P_A} = \frac{\left\{\left[\frac{\theta}{(2^{3/2})} + (M_0 - 1)^{\frac{1}{2}}\right]^2 + 1\right\}^2 - \frac{\gamma-1}{2\gamma}}{(M_0^2 - \frac{\gamma-1}{2\gamma})} \tag{1.31}$$

For air, $\gamma \simeq 7/5$, thus Equation 1.31 becomes

$$\frac{P_d + P_A}{P_s + P_A} = \frac{\left\{\left[\frac{\theta}{(2^{3/2})} + (M_0 - 1)^{\frac{1}{2}}\right]^2 + 1\right\}^2 - \frac{1}{7}}{(M_0^2 - \frac{1}{7})} \tag{1.32}$$

Values of $P_d + P_A/P_s + P_A$ as a function of M_0 are shown for various values of θ in Figure 1-8.

Physically, the value of M_w cannot decrease below unity; hence, there is a limit on the value of θ . This limiting value may be obtained from Equation 1.27,

$$\theta\text{lim} = -2^{3/2}\,(M_o - 1)^{\frac{1}{2}} \tag{1.33}$$

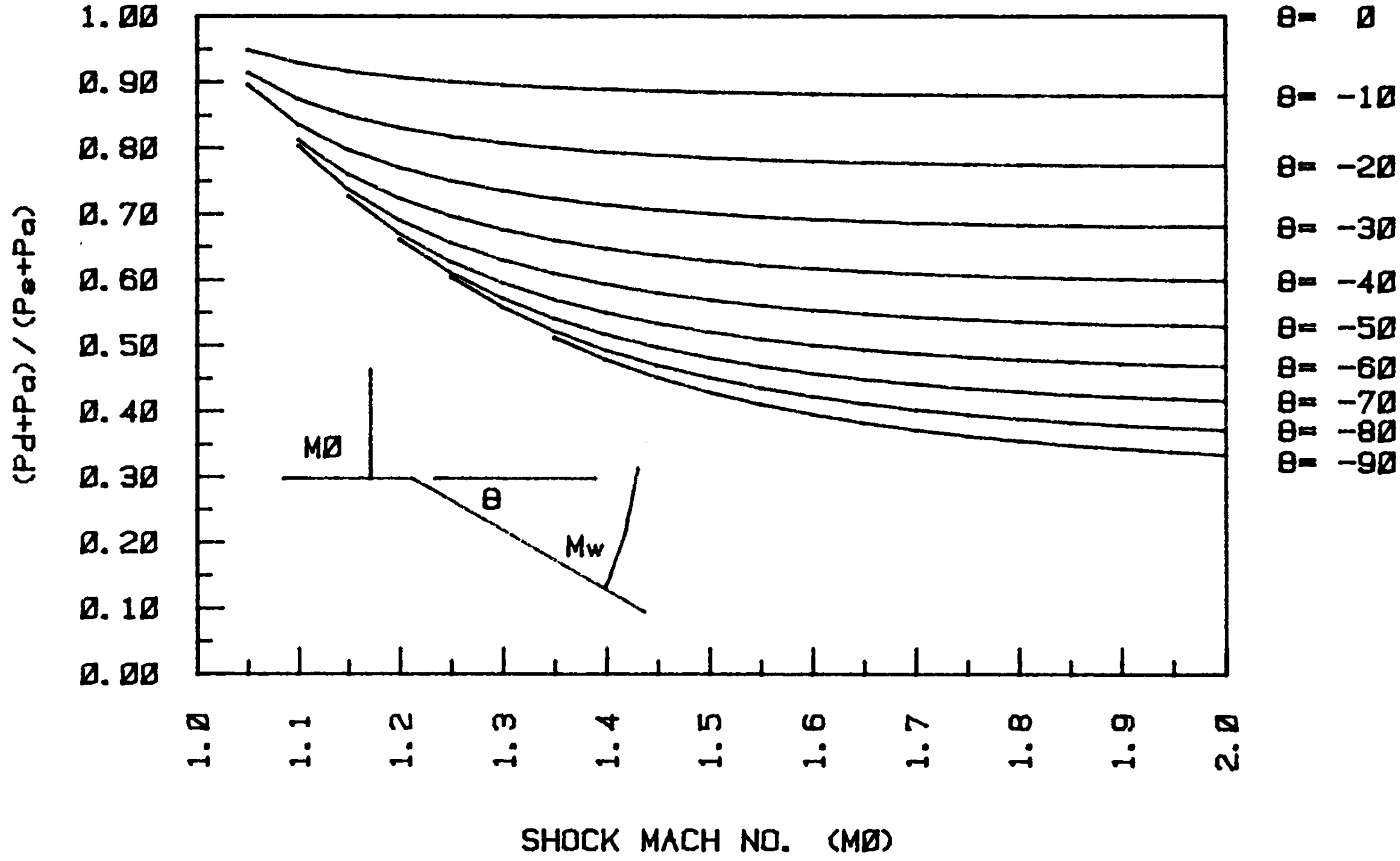

Figure 1-8. Value of the Diffracted to Incident Shock Pressure Ratios as a Function of Shock Mach Number for Various Values of θ.

For values of θ less than θlim the solution breaks down. Presumably, this corresponds to flow separation at the corner. In this case it is assumed that the shock is severely weakened due to vortex action, boundary layer effects, etc., and the overpressure at the "foot" of the shock on the wall is taken to be zero. The flow regimes corresponding to diffraction and separation at the corner are illustrated graphically in Figure 1-9.

One practical problem of interest is to determine the diffracted overpressure of a blast wave on the rear roof of a building (Figure 1-10(A)) or the similar problem of a shock diffracting around a building at oblique incidence (Figure 1-10(B)).

Whitham's solution was developed for the case of a shock initially propagating parallel to a wall (Figure 1-7). However, in these cases the shock is reflected from an oblique surface prior to diffraction. Since the diffraction process is driven by the reflected overpressure P_R , rather than the incident shock overpressure P_s , it is necessary to modify the analysis in order to apply Whitham's theory. Consider the incident shock when it arrives at the point of diffraction. The initial angle of the shock front is unchanged, regardless of the presence of the reflected shock. Therefore, the shock front must turn through the angle θ as

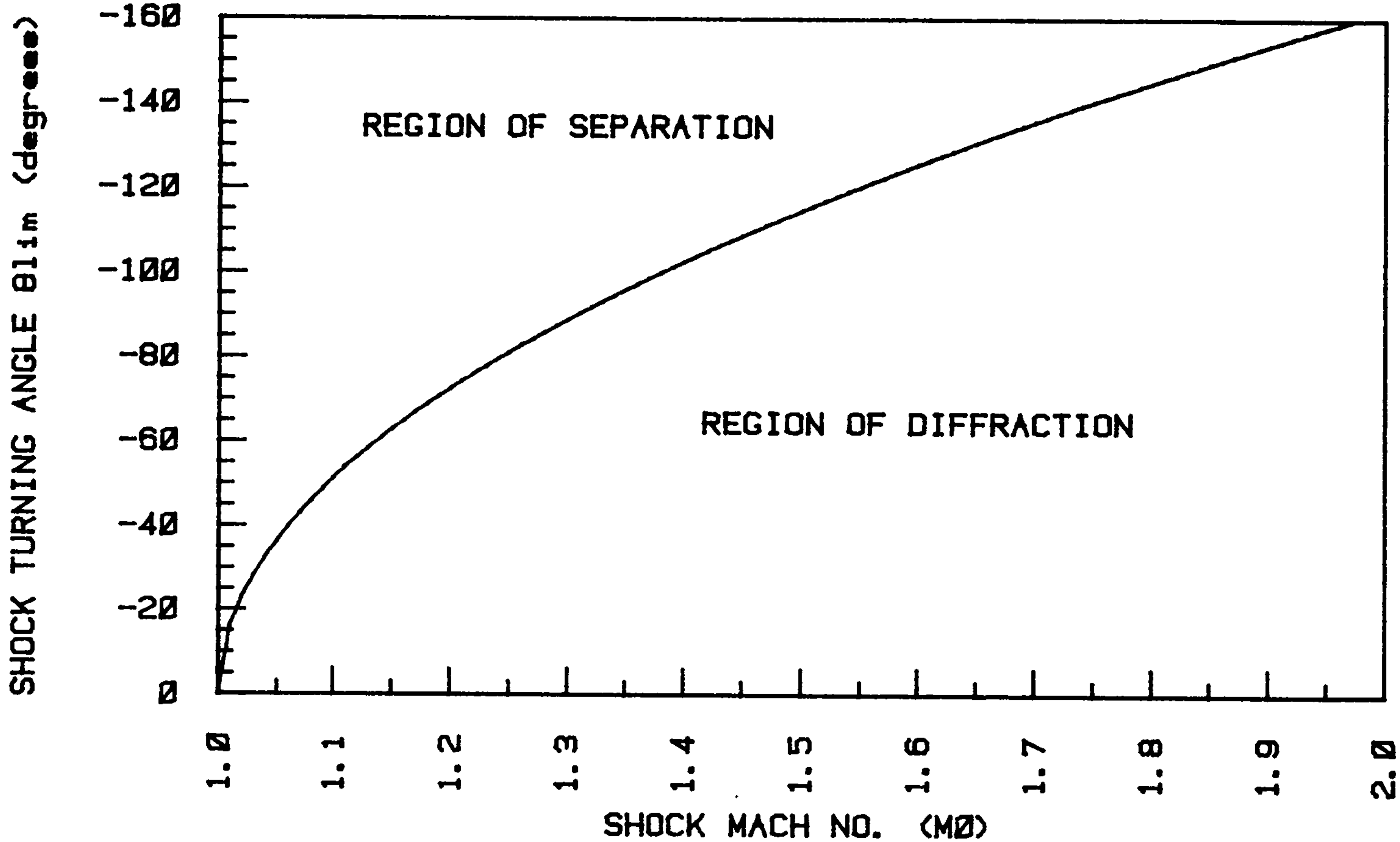

Figure 1-9. Limiting Turning Angle for Flow Separation (θLim) as a Function of Incident Shock Mach Number.

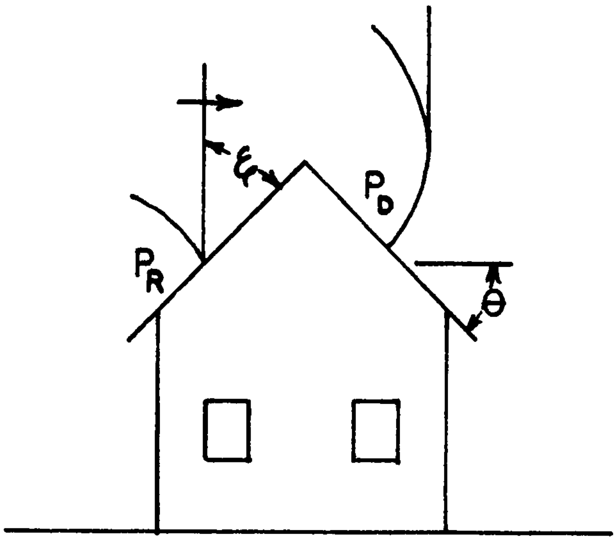

A. Diffraction of a Shock Wave on the Roof of a Building.

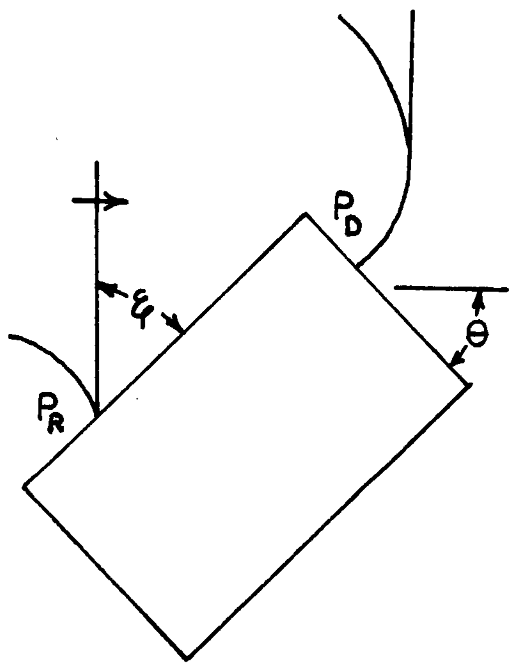

B. Diffraction of a Shock Wave Around One Corner of a Building at Oblique Incidence.

Figure 1-10. Two Similar Problems Involving the Diffraction of a Shock Wave Obliquely Incident on a Surface.

in the case for which Whitham's solution was derived. The pressure at the point of diffraction, however, is equal to P_R rather than P_s , as assumed in Whitham's analysis. Given these considerations, it is possible to transform the problem for oblique interaction into one which is compatible with the assumptions for which Whitham's theory is derived. Let,

$$M_o' = \left[\frac{\gamma-1}{2\gamma} + \frac{\gamma+1}{2\gamma} \quad \frac{P_R+P_A}{P_A}\right]^{\frac{1}{2}} , \qquad (1.34)$$

then the diffracted shock overpressure may be determined if M_o' is substituted for M_o in Equation 1.32. This transformation of the problem is illustrated graphically in Figure 1-11. In general, the solution may be applied for the rearward facing oblique surface if the time scales of the problem are shifted to account for the delay in the wavefront arrival and if the initial overpressure on the wall P_o is taken to be the diffracted overpressure P_d . The value of τ is calculated using the same principles developed in Section 2. The drag co-efficient is chosen to correspond to the oblique geometry.

Equation 1.24 has been compared with empirical models and data from both shock tube and free-field studies. The results are discussed in the following section.

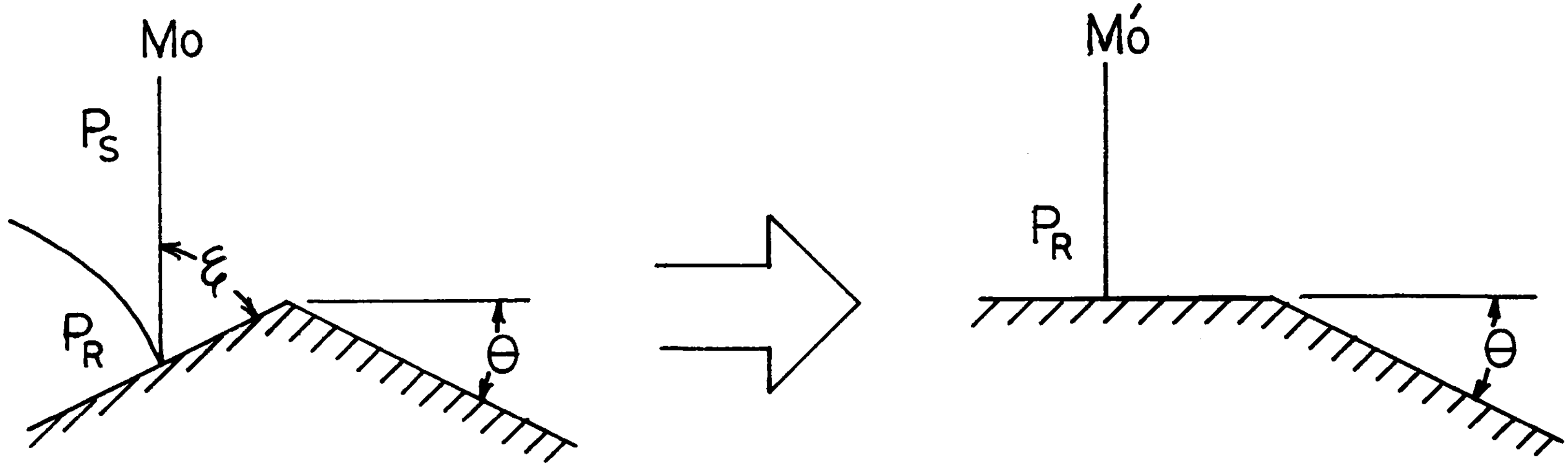

Figure 1-11. Transformation of the Oblique Shock Interaction Problem into an Analogous Problem for which Whitham's Theory Applies.

5. Comparison with Experimental Results

The model developed in Section 2 (Equation 1.24) agrees well with empirical models by Etheridge [2] and experimental data obtained by Coulter in shock tube experiments [12] and free-field explosions [8]. Comparison of the model with the data reveals reasonable agreement for a wide range of overpressures and test configurations, except in those cases where local effects due to vortex formation, etc... dominate the phenomena on the wall.

Etheridge developed empirical models using shock tube data obtained from a study by Taylor [13]. In that study, Taylor exposed a parallelopiped to overpressures ranging from 4.76 to 21.54 psi. Etheridge used the data to obtain empirical curve fits for the average overpressure on both the front and rear walls of a rectangular block structure. These results are given in Appendix B. Target dimensions and gauge positions for the study by Taylor are shown in Figure 1-12.

Equation (1.24) was compared with the models by Etheridge and the data by Taylor for several cases. Shot parameters for these cases are given in Table 1-1. The values of normalized overpressure (P/P_s), calculated using the models by Etheridge (Equations B.1 and B.13) and Equation 1.24 together with the experimental

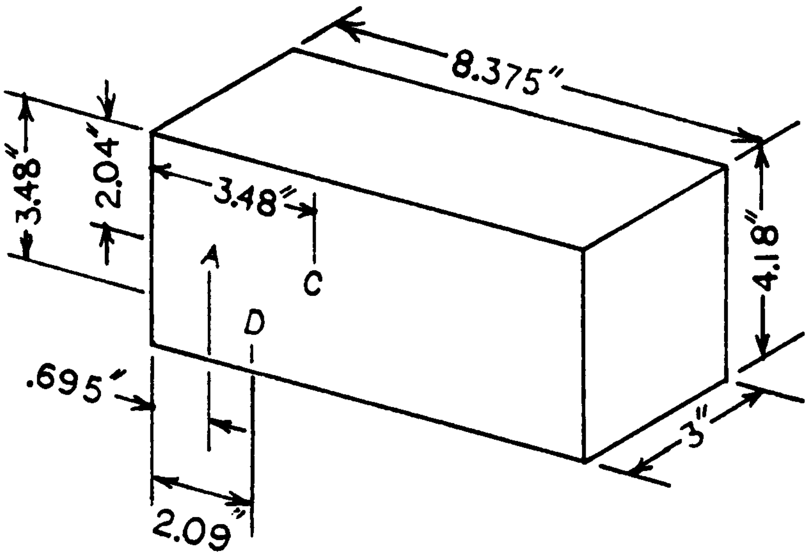

Figure 1-12. Target Dimensions and Gauge Positions Used in the Shock Tube Study by Taylor.[13]

Table 1-1. Shock Tube Test Shot Parameters from the Study by Taylor[13] Used in the Comparison of Equation 1.24 with the Models by Etheridge[2] in Figures 1-14 and 1-15.

Shot	P_s (kpa)	P_A (kpa)	a_o (m/s)	a_5 (m/s)	P_R (kpa)	P_q (kpa)	C_D
1 (3DF)	34.47	101.7	343.5	373.1	78.50	3.981	.8
2 (3DR)	32.96	101.7	344.1	372.5	74.66	3.646	-.5
10(3DR)	148.5	102.0	344.6	446.5	450.4	63.90	-.5
13(3DF)	147.1	102.6	343.9	444.5	444.3	62.55	.8

data of Taylor are shown in Figures 1-13 and 1-14. The data are plotted using the normalized times, $t \cdot a_5 \cdot (R+1)/S$ and $t \cdot a_o/s$, for the front and rear walls respectively. Equation 1.24 agrees very well with both the data and the model by Etheridge for overpressures of approximately 5 psi on both the front and rear walls (Figures 1-13(A) and 1-14(A)). For overpressures of approximately 20 psi, Equation 1.24 continues to agree reasonably well with the data on the front wall (Figure 1-13(B)), but departs significantly from the data on the rear (Figure 1-14(B)).

Shock tube data are available for a 1/15th scale house exposed to incident shock overpressures of approximately 5 psi in a study by Coulter [12]. Sketches of the model dimensions and gauge locations are shown in Figure 1-15. Data were collected for test configurations of 0, 20, and 52½ degrees. These configurations are illustrated in Figure 1-16.

Equation 1.24 was compared with the shock tube data for several cases. Shot parameters and other information used in the calculations are presented in Table 1-2. The results are compared with the data in Figures 1-17 through 1-20.

For the case of normal incidence, Equation 1.24 agrees very well with data on the front wall and front roof of the building (Figure 1-17). A sudden drop in

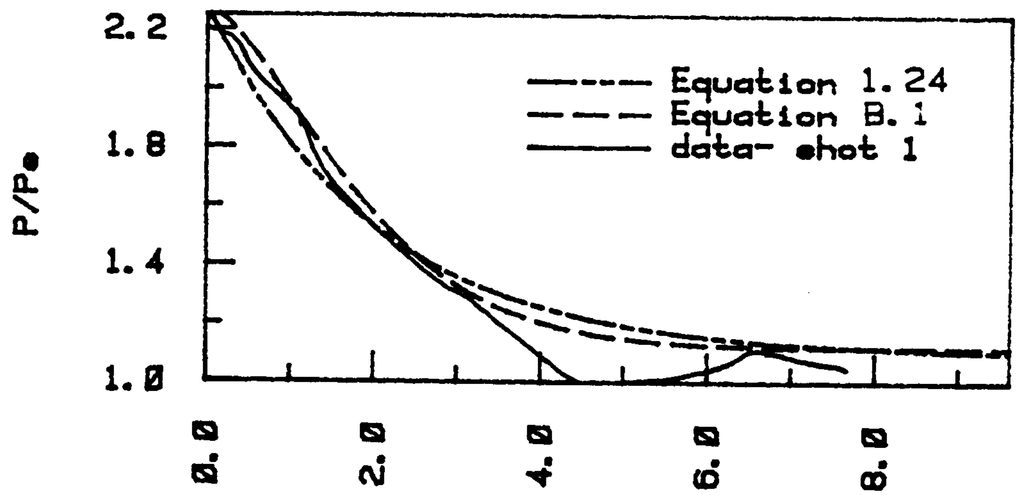

A. 5 Psi

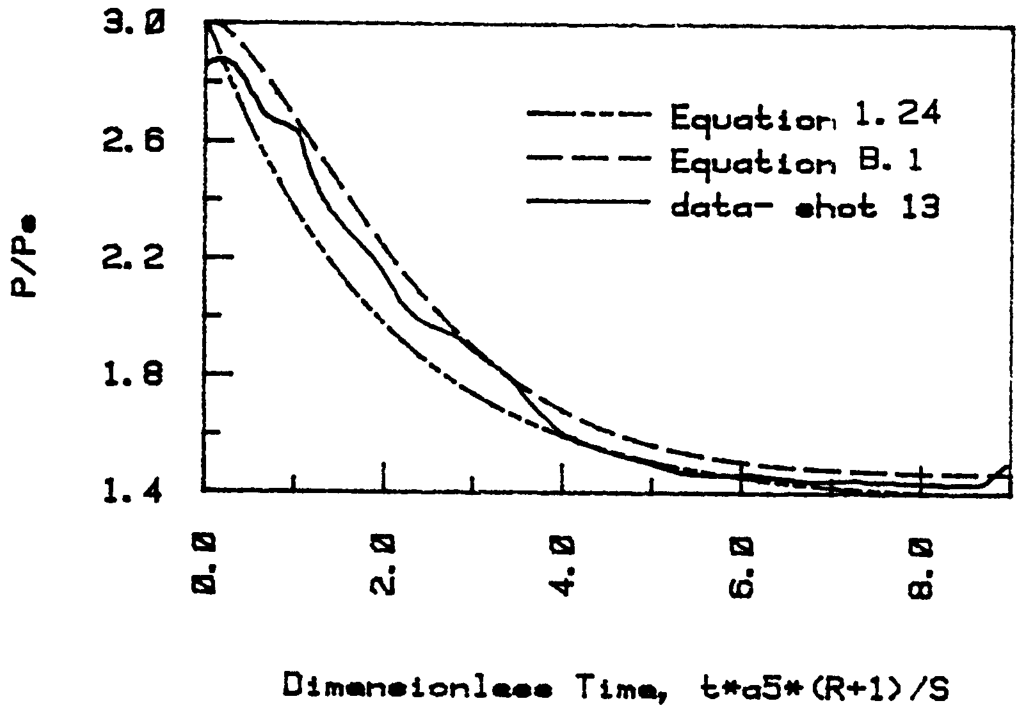

B. 20 Psi

Figure 1-13. Comparison of Equation 1.24 with an Empirical Model by Etheridge[2] (Equation B.1), and Shock Tube Data by Taylor[13] for the Average Overpressure Ratio on the Front of a Rectangular Block Structure Exposed to Overpressures of 5 and 20 Psi at Normal Incidence.

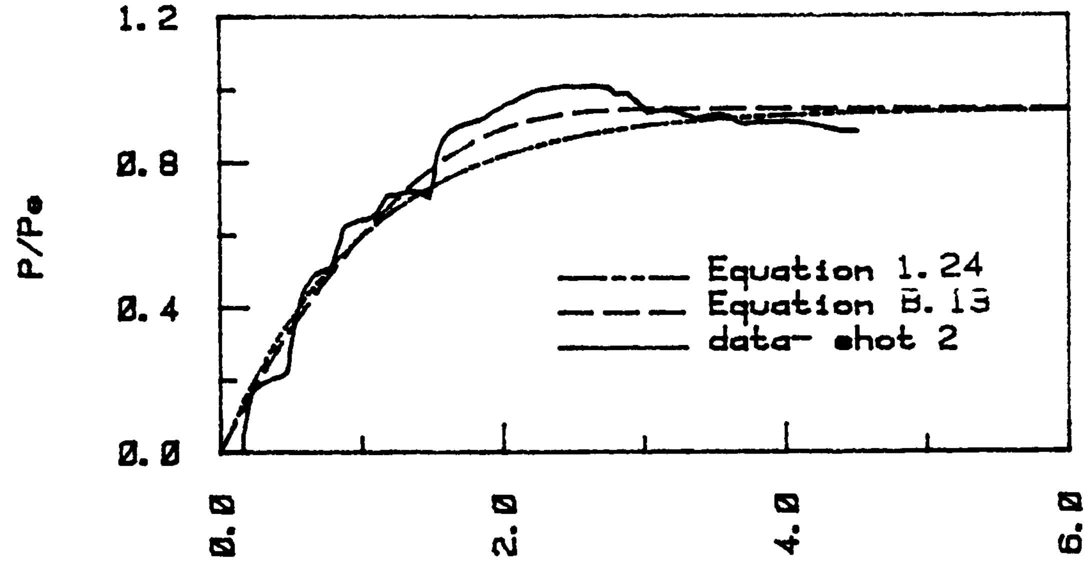

A. 4.78 Psi

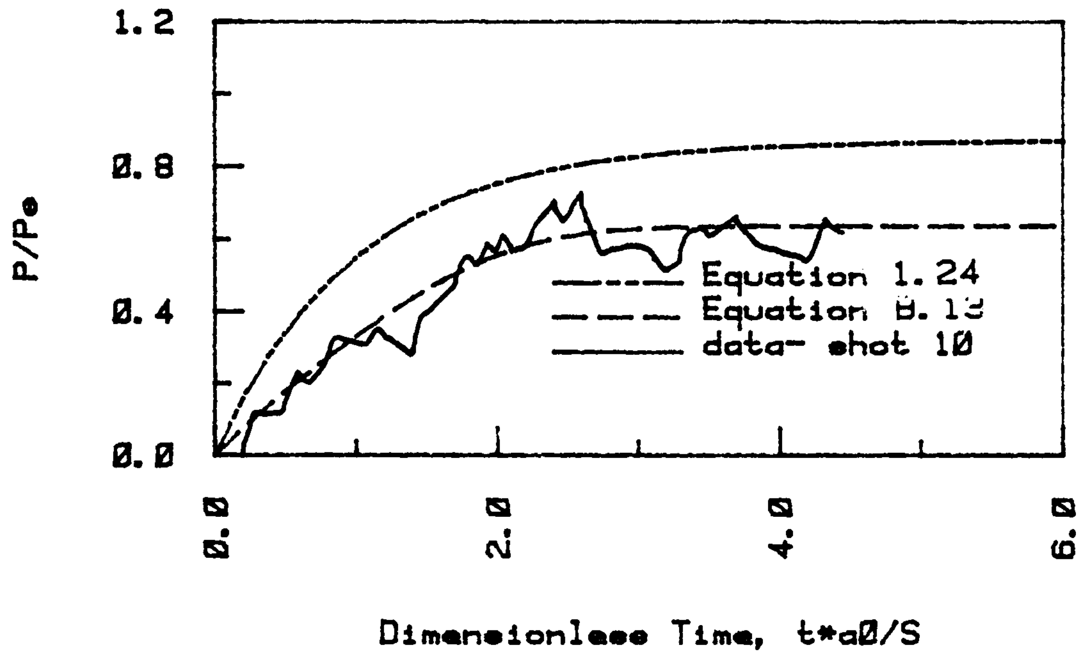

B. 21.5 Psi

Figure 1-14. Comparison of Equation 1.24 with an Empirical Model by Etheridge[2] (Equation B.15), and Shock Tube Data by Taylor[13], for the Average Overpressure on the Rear Surface of a Rectangular Block Structure Exposed to Overpressures of 4.78 and 21.5 Psi at Normal Incidence.

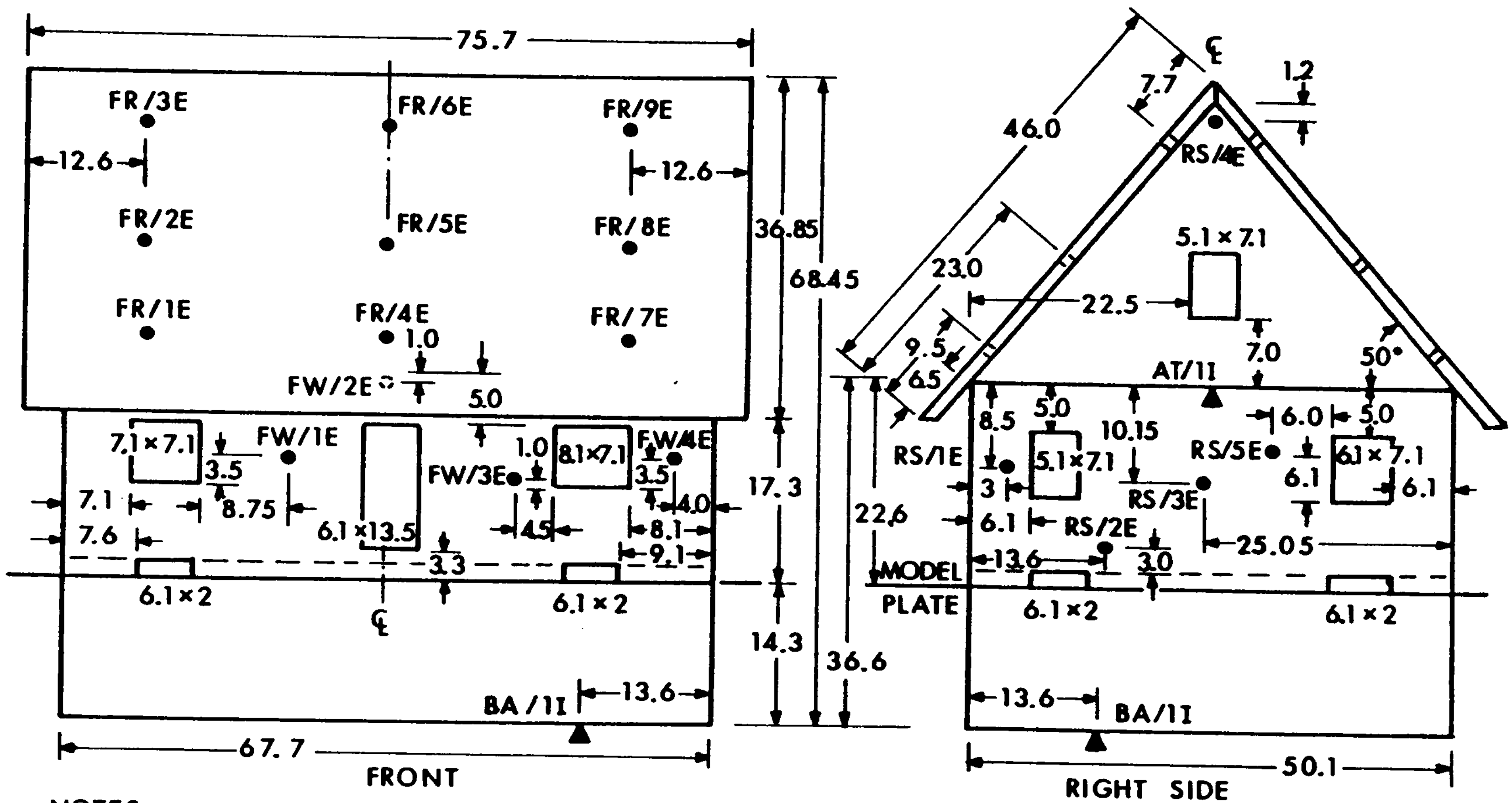

NOTES:
1- DIMENSIONS IN CENTIMETRES
2- DIMENSIONS ARE FOR OUTSIDE

Figure 1-15. Sketch of 1/15 Scale Model House Used In the Shock Tube Study by Coulter[12].

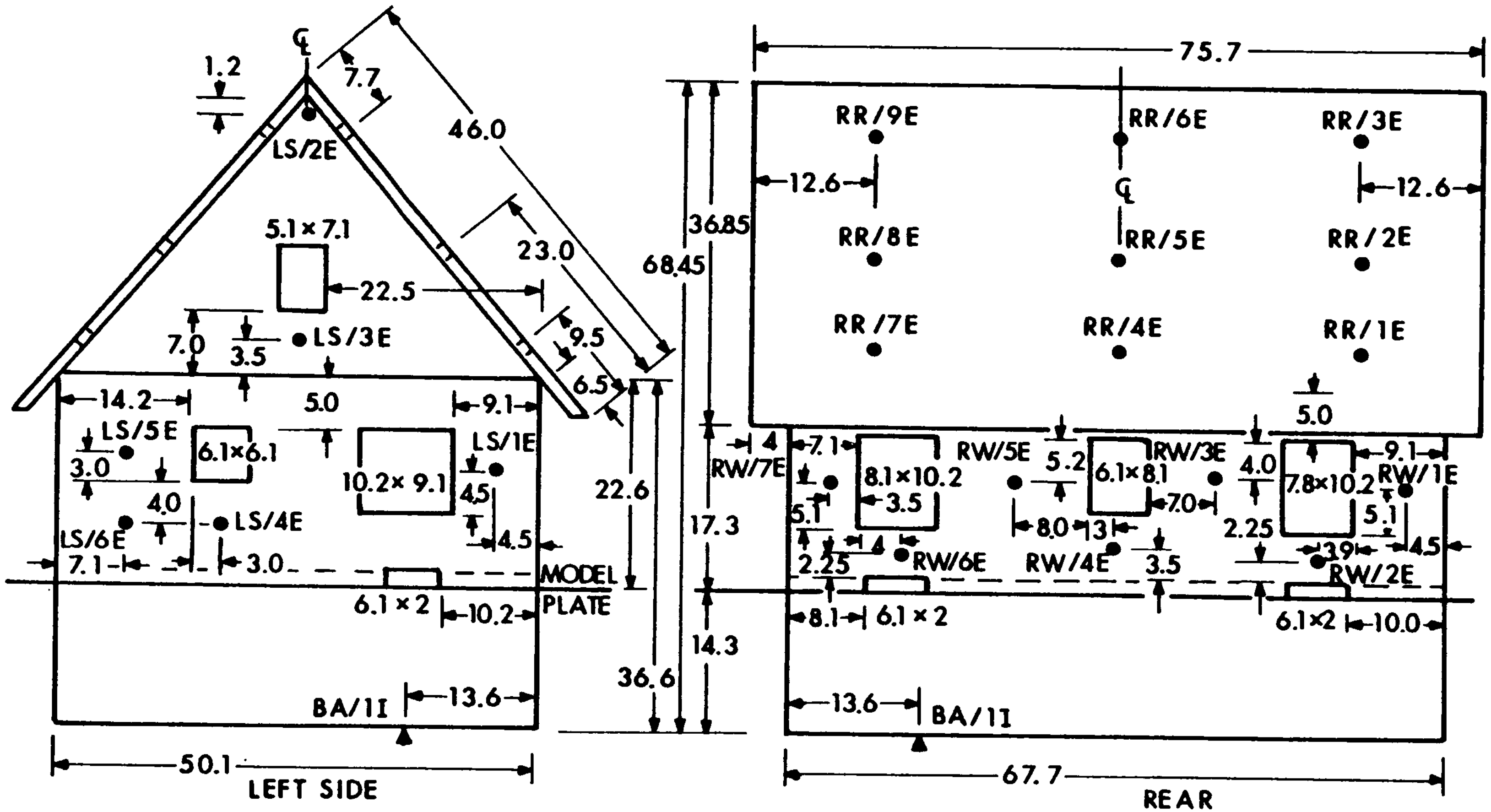

NOTES:
1- DIMENSIONS IN CENTIMETRES
2- DIMENSIONS ARE FOR OUTSIDE

Figure 1-15 (cont.).

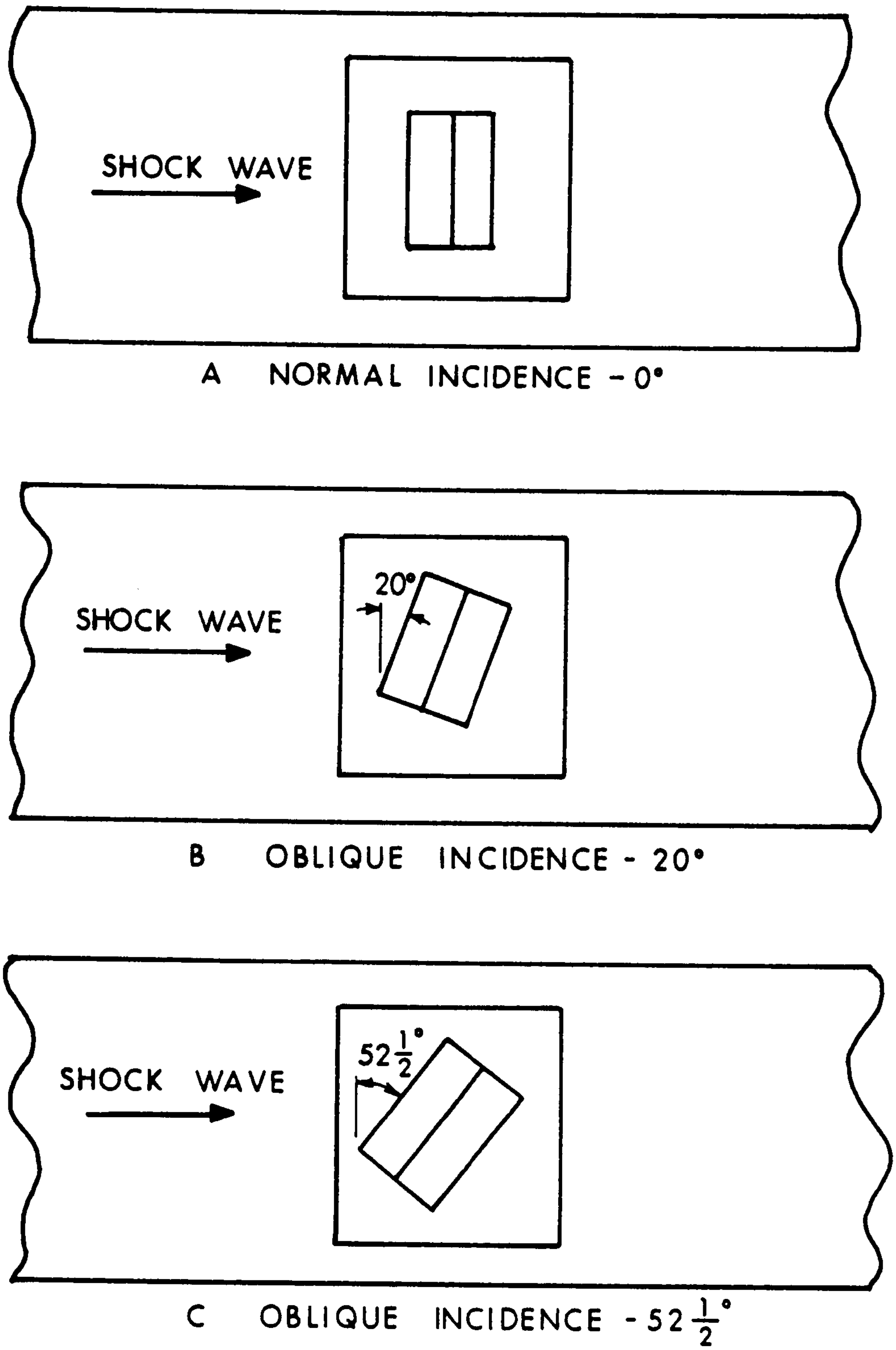

Figure 1-16. Various Test Configurations Used in the Shock Tube Studies by Coulter[12].

Table 1-2. Shot Parameters for Figures 1-17 Though 1-20, from the Shock Tube Study by Coulter[12].

Gauge	Conf.	P_s (kpa)	P_A (kpa)	a_o (m/s)	S (m)	θ degrees	ξ degrees	C_D
FW/1E	0^o	37.9	100.9	346.7	.3385	-	0	.8
FR/8E	0^o	37.9	100.9	346.7	.3785	-	40	.5
RW/3E	0^o	37.4	101.3	351.1	.3385	-90	90	-.5
RR/2E	0^o	37.4	101.3	351.1	.3785	-50	40	-.7
LS/4E	$52\frac{1}{2}^o$	37.8	101.0	348.1	.25	-52.5	52.5	-.7
FW/3E	20^o	38.2	101.9	353.4	.3385	-	20	.8
RR/6E	0^o	37.4	101.3	351.1	.3785	-50	40	-.7

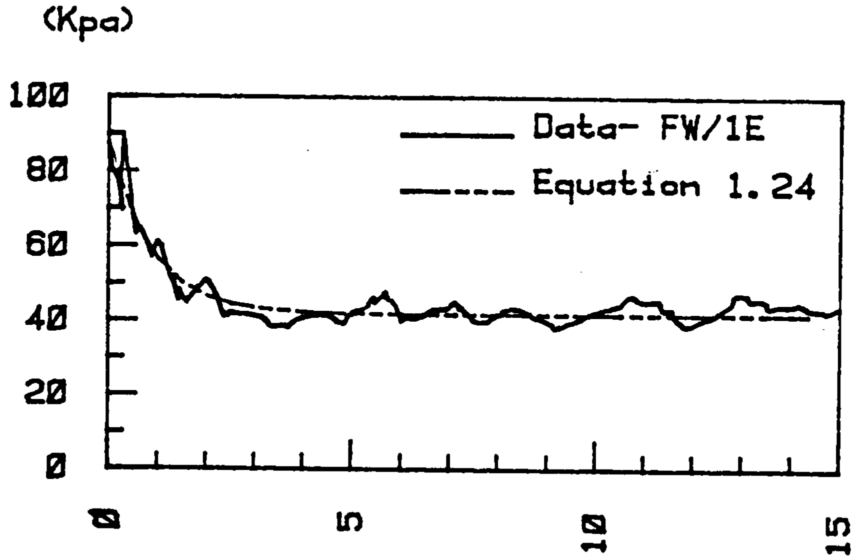

A. Front Wall

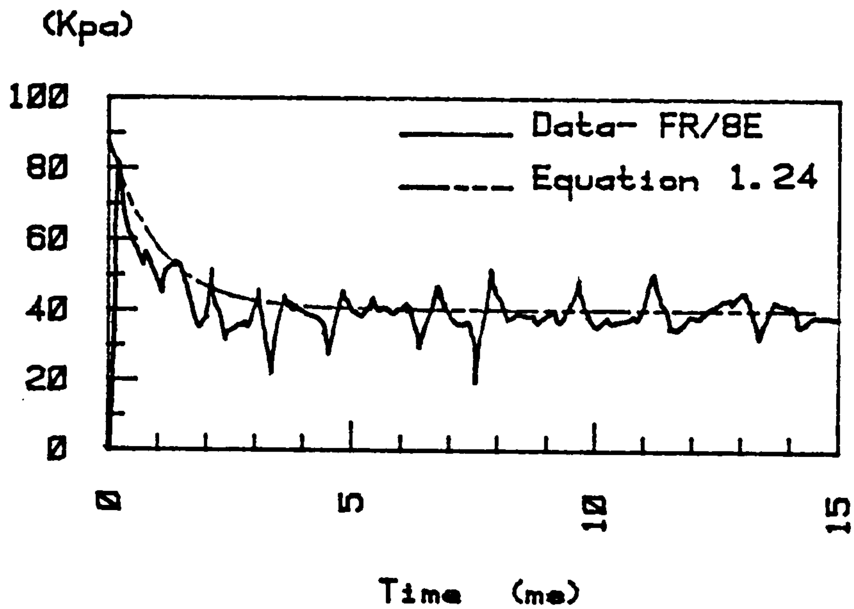

B. Front Roof

Figure 1-17. Comparison of Equation 1.24 with Data from Shock Tube Studies by Coulter[12] for the Front Wall and the Front Roof of a 1/15th Scale Model House (Normal Incidence).

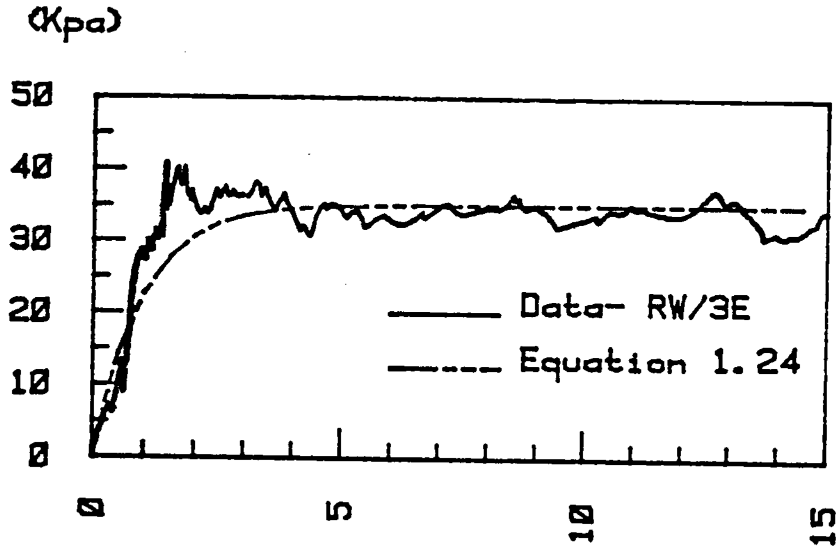

A. Rear Wall

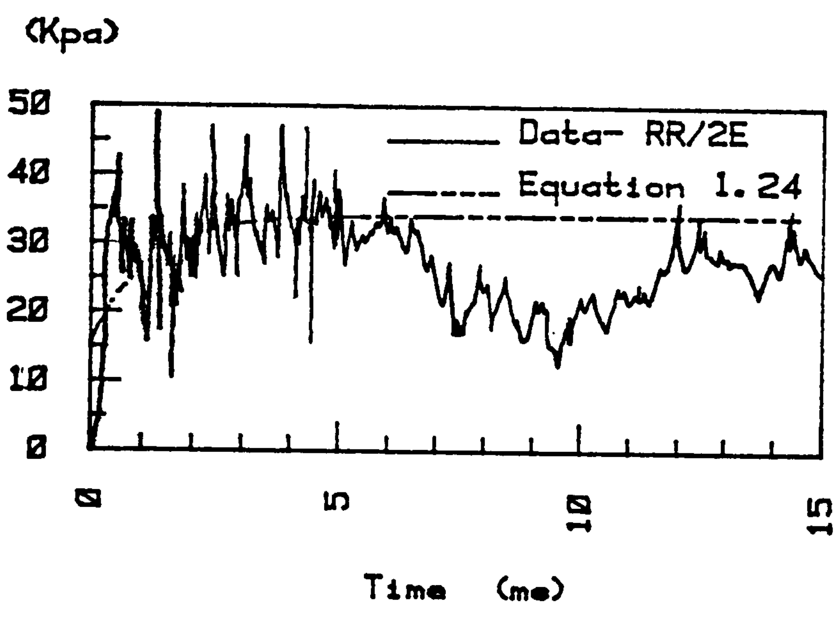

B. Rear Roof

Figure 1-18. Comparison of Equation 1.24 with Data from Shock Tube Studies by Coulter[12] for the Rear Wall and the Rear Roof of a 1/15th Scale Model House (Normal Incidence).

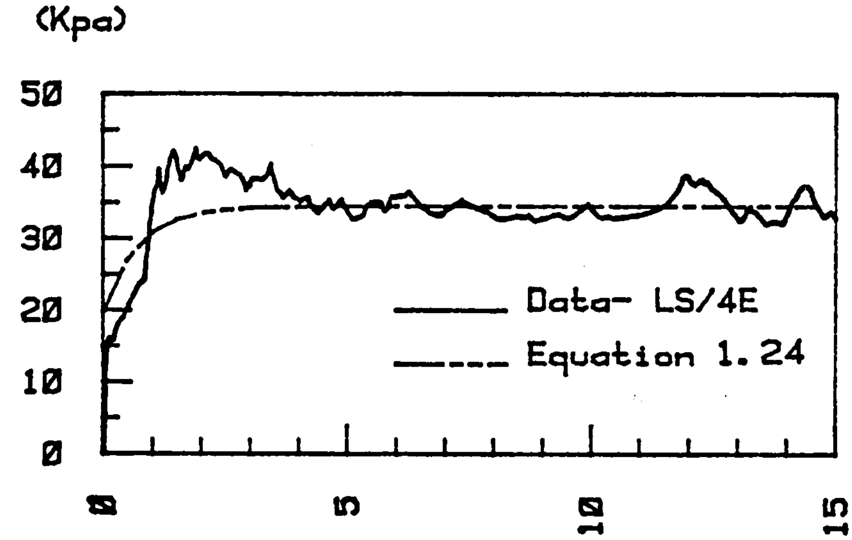

A. Left Side

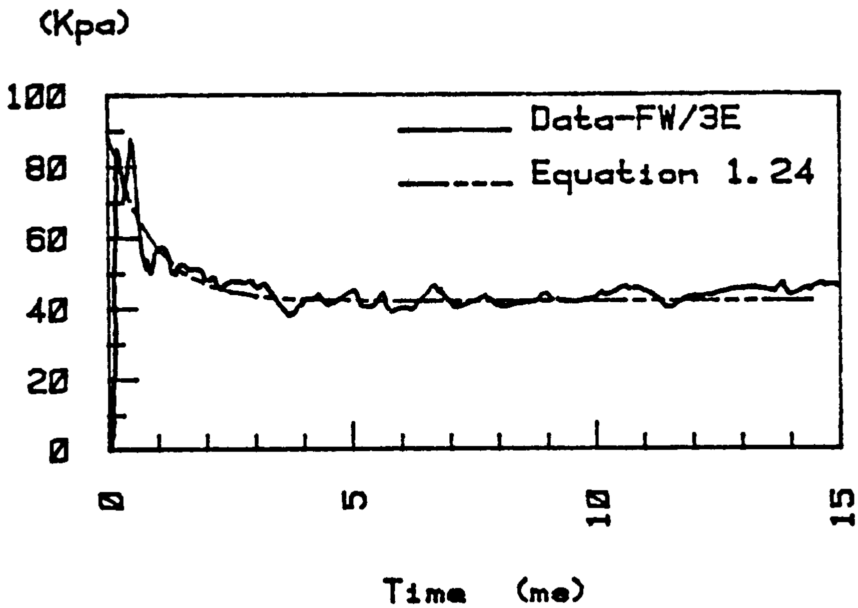

B. Front Wall

Figure 1-19. Comparison of Equation 1.24 with Data from Shock Tube Studies by Coulter[12] for the Left Side and Front Wall of a 1/15th Scale Model House Oriented at Angles of 52½ and 20 Degrees to the Incident Shock Respectively.

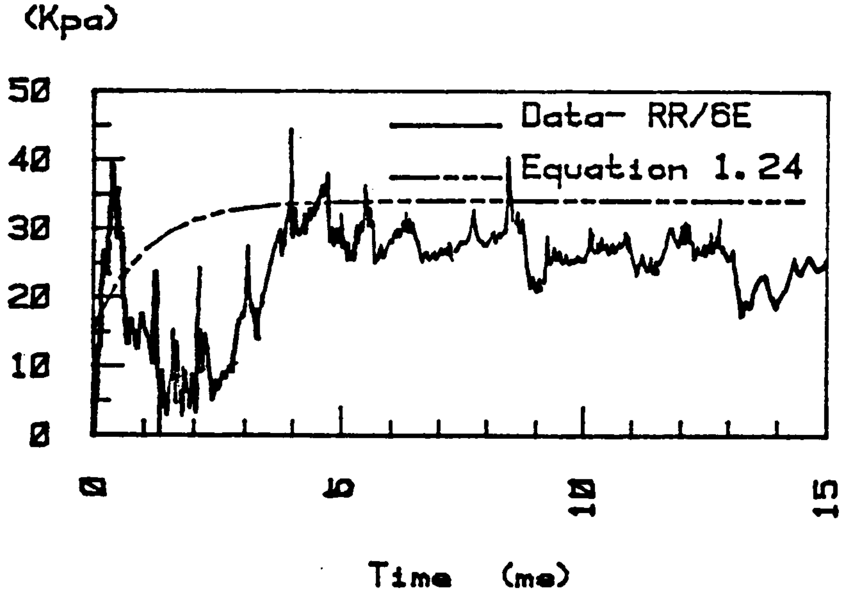

Figure 1-20. Comparison of Equation 1.24 with Data from Shock Tube Studies by Coulter[12] for the Rear Roof of a 1/15th Scale Model House (Normal Incidence). The Presence of a Vortex is Evident for this Station Near the Apex of the Rear Roof.

overpressure is observed on the rear roof of the building, due to the formation of a vortex at the point of diffraction. This vortex is particularly evident at stations near the apex of the roof (Figure 1-20). Diffracted shock overpressures observed in the data for the rear roof approximate the peak overpressure of the incident shock. This initial shock, however, quickly decays and the mean of the data appears to coincide with the solution curve calculated using Whitham's theory to determine the initial condition (Figure 1-18(B)). The solution also agrees very well with data on the rear wall (Figure 1-18(A)).

Two oblique cases were also examined, the left side for the $52\frac{1}{2}^{\circ}$ case, and the front wall for the 20° case. On the left side, the solution fails to predict the shock structure of the early time history, although the initial overpressure predicted by Whitham's theory is approximately correct (Figure 1-19(A)). The solution agrees very well with the data for the front wall at a 20° angle of incidence (Figure 1-19(B)).

Coulter has also obtained data for a 1/8th scale model house exposed to free-field explosions of approximately 4.0 psi overpressure at normal incidence [8]. The model dimensions and gauge locations used in the experiment are shown in Figure 1-21. Shot parameters and other relevant information are presented in Table 1-3.

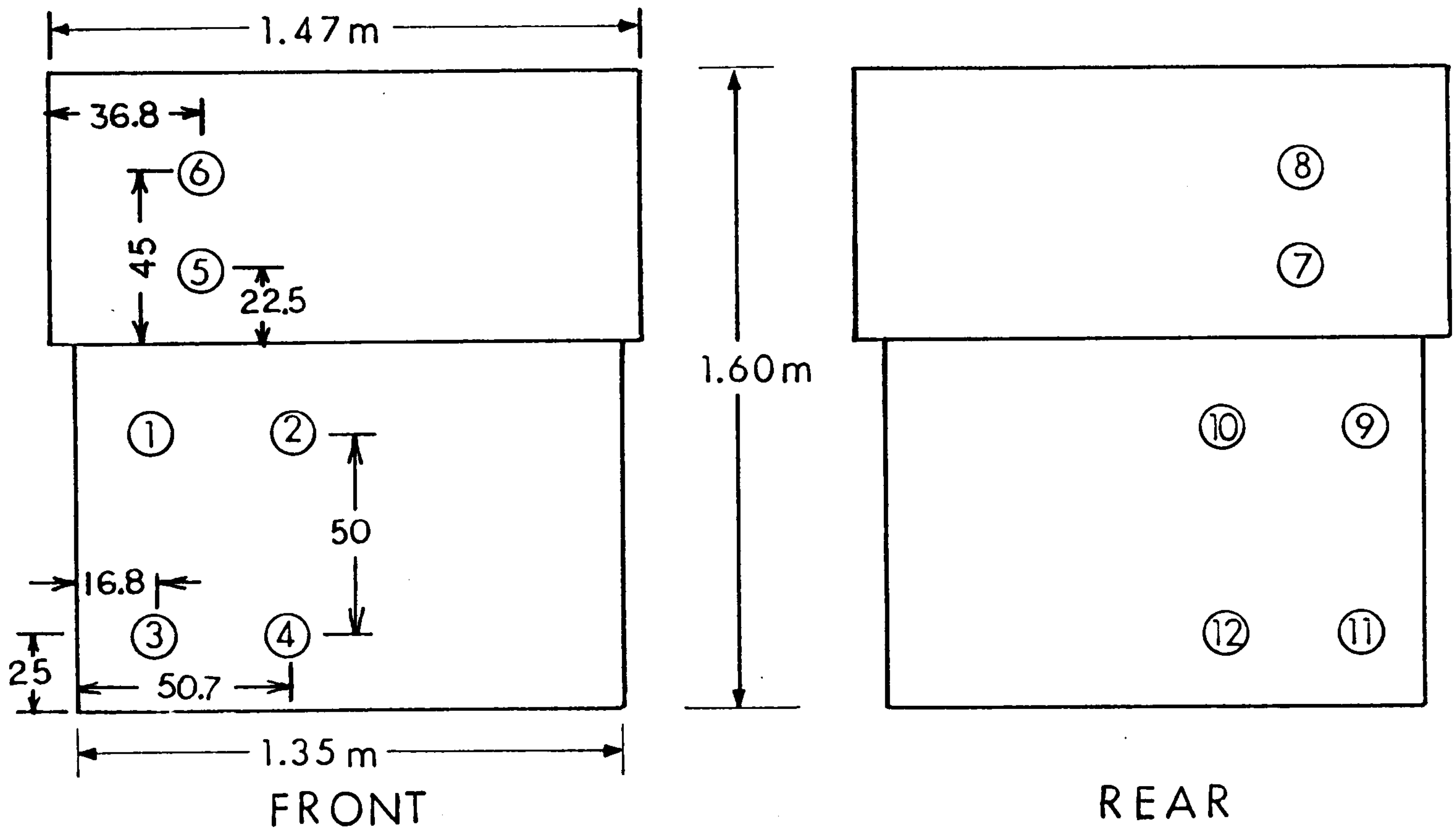

NOTE: ALL DIMENSIONS ARE IN CENTIMETERS UNLESS OTHERWISE SPECIFIED.

Figure 1-21. Sketch of the 1/8 Scale Model House Used in the Free-field Study by Coulter[8].

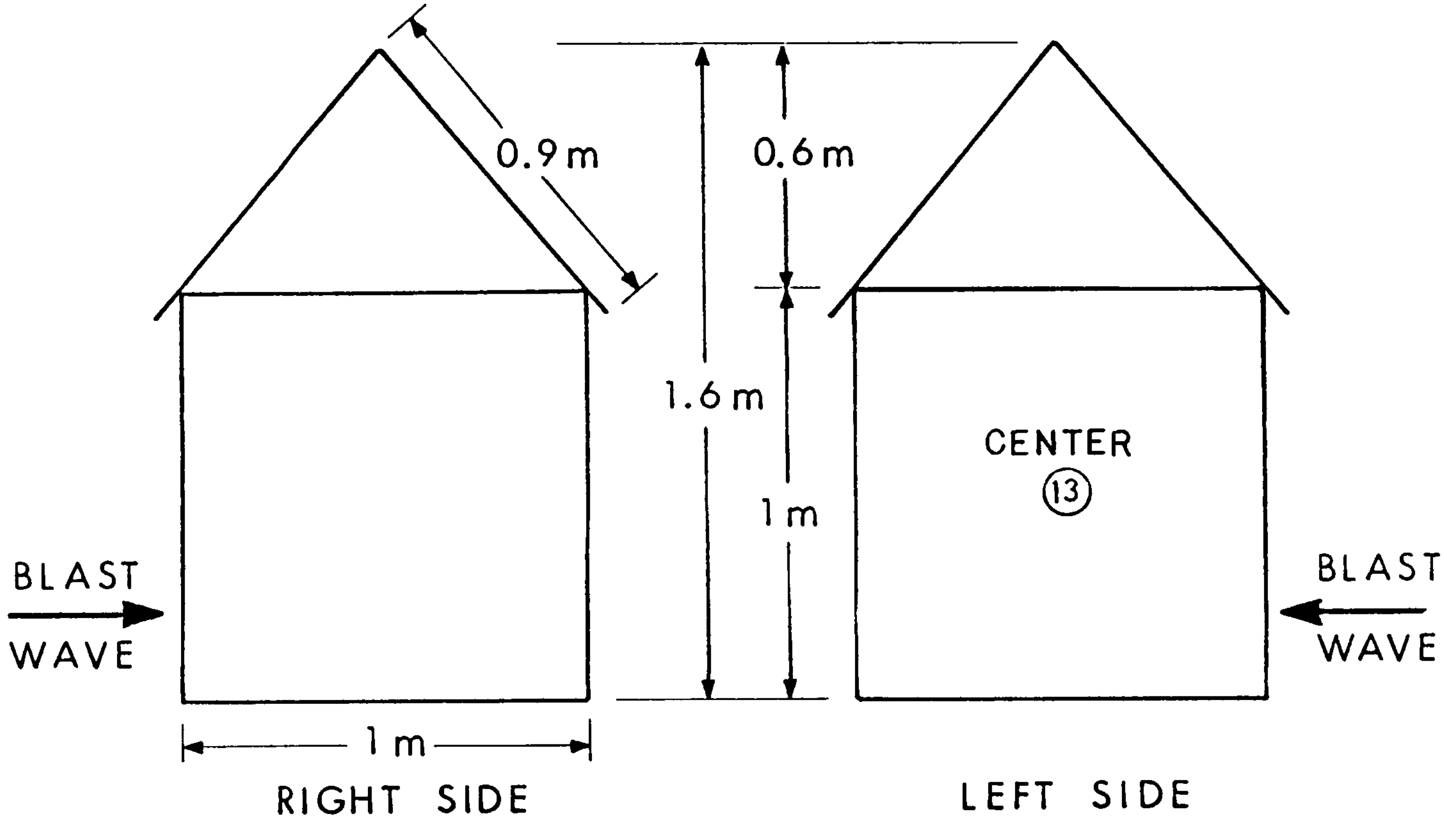

Figure 1-21 (cont.).

Table 1-3. Shot Parameters for Figures 1-22 Through 1-24 from Shot 3 in the Free-field Study by Coulter[8].

Gauge	P_s (kpa)	P_A (kpa)	a_o (m/s)	S (m)	θ degrees	ξ degrees	C_D
0	28	93	346.6	-	-	-	-
1				.675	-	0	.8
5				.735	-	39.8	.5
8				.735	-50.19	29.8	-.7
11				.675	-90	0	-.5

Equation 1.24 was compared with data from the model house for surfaces on the front, rear, and roof of the model. Those results are shown in Figures 1-22 through 1-24. The input wave used to approximate the free-field overpressure is shown in Figure 1-22(A). The solution tends to overestimate the pressure on the front wall and front roof of the model (Figures 1-22(B) and 1-23(A)).

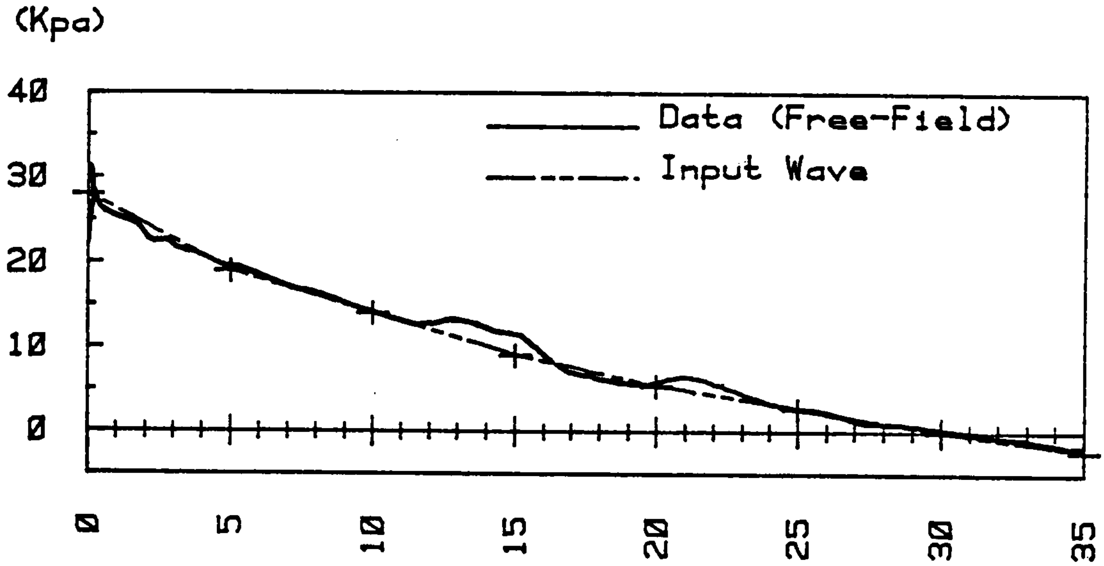

A. Free-field

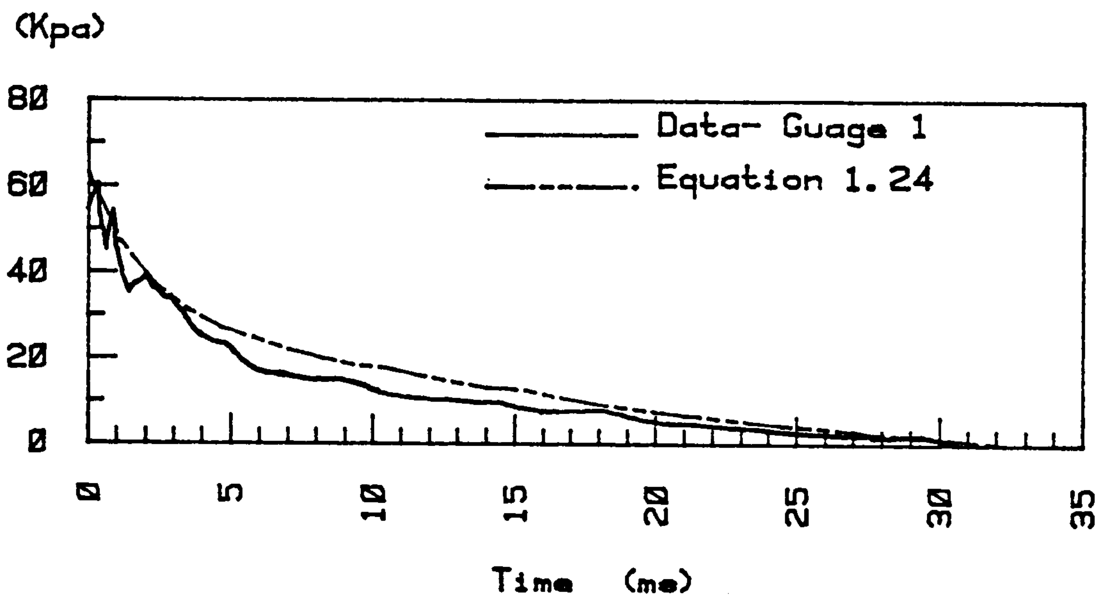

B. Front Wall

Figure 1-22. Input Wave Used to approximate the free-field Data for Calculation Purposes, and Comparison of Equation 1.24 with Data for the Front Wall of a 1/8th Scale Model House Exposed to a Blast Wave at Normal Incidence, from the free-field Studies by Coulter[8].

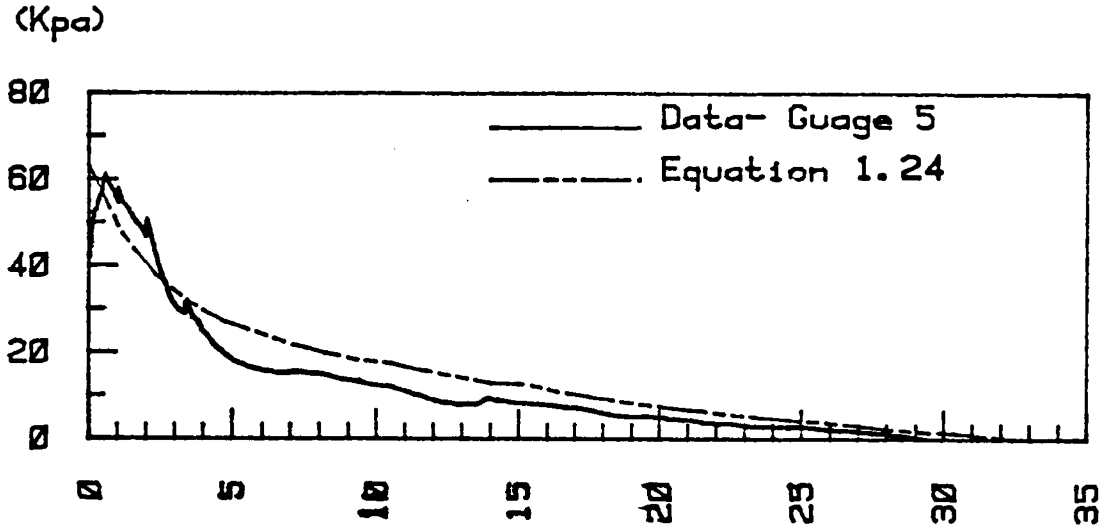

A. Front Roof

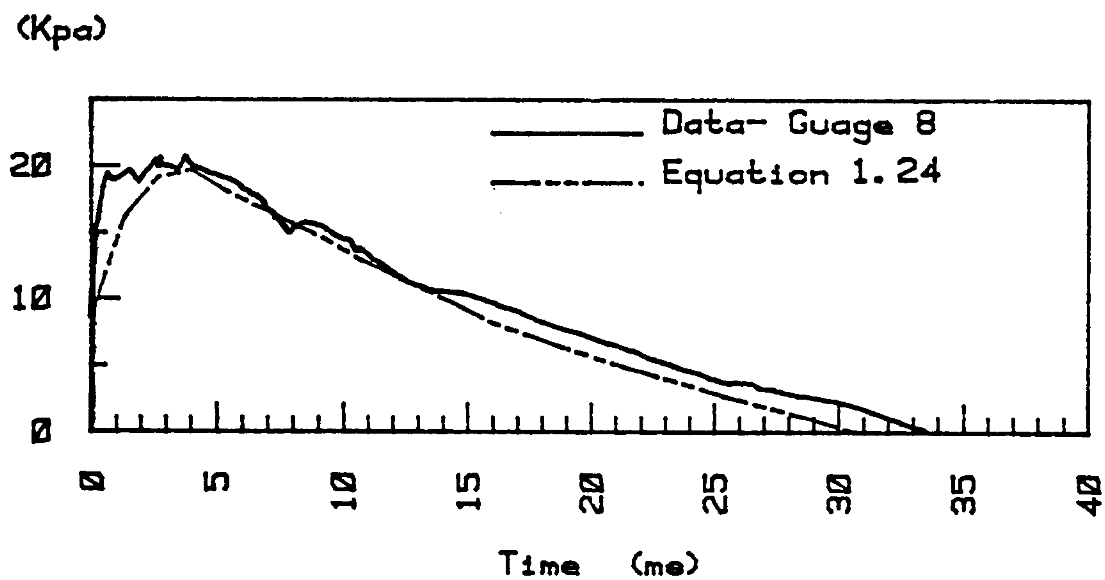

B. Rear Roof

Figure 1-23. Comparison of Equation 1.24 with Data from free-field Studies by Coulter[8] for the Front Roof and Rear Roof of a 1/8th Scale Model House Exposed to a Blast Wave at Normal Incidence.

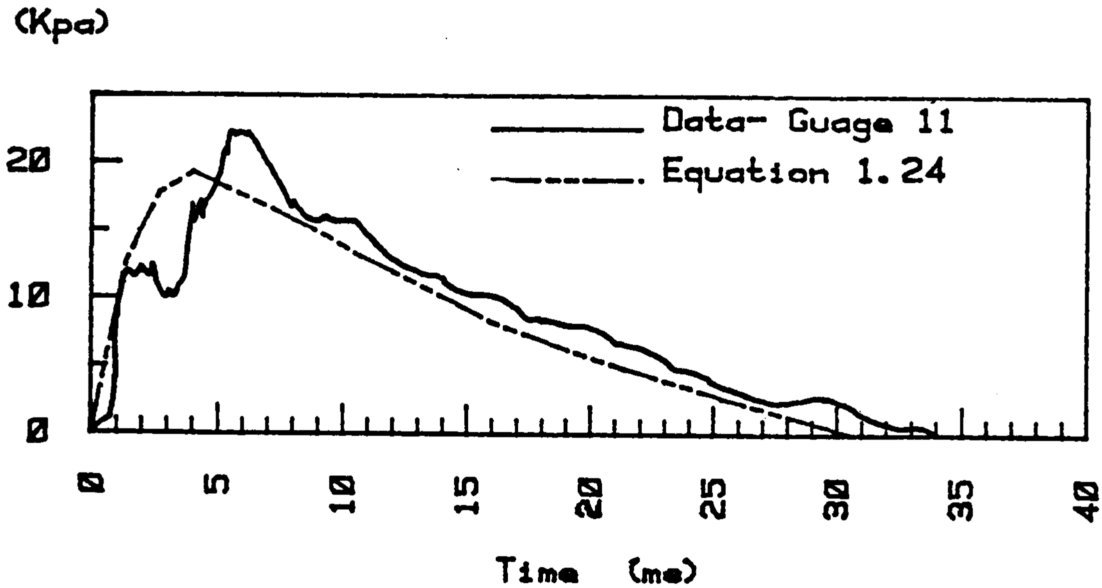

Figure 1-24. Comparison of Equation 1.24 with Data from the free-field Studies by Coulter[8] for the Rear Wall of a 1/8th Scale House Exposed to a Blast Wave at Normal Incidence.

The solution performs well on the rear roof of the model (Figure 1-23(B)). Some shock structure is evident in the data for the rear wall (Figure 1-24) due to a delay in wave arrival between the sides and top of the building and the arrival of a reflected shock from the ground. These effects cannot be treated using this model.

CHAPTER II

BLAST INTERACTIONS WITH MULTI-STRUCTURE COMPLEXES

1. Background

The problem of determining the overpressure on a structure exposed to a blast wave when it is "shielded" by nearby structures if of great practical interest. Models were presented in the previous chapter for the case of isolated buildings. These results may be extended for application in the shielded case.

Coulter [8] has conducted field experiments for a model complex of buildings exposed to blast overpressures of approximately 4.0 psi. This data reveals additional effects which distinguish the shielded case from the unshielded case.

1. Reductions in shock overpressure due to shock diffraction around the surrounding buildings.
2. Appearance of secondary shocks reflected from the surfaces of surrounding buildings.
3. Fluctuations of pressure in the cavities formed between adjacent buildings due to unsteady dynamic effects.

Each of these effects represent a complicated flow interaction problem, ordinarily requiring a detailed and extensive numerical calculation for their solution.

However, since the solution to the shielding effect problem is intended for use with other models for the interior pressures and structural response of the building, it is important that the solution requires a minimum of computational effort. Therefore, the model must rely on the use of simple physical concepts to approximate the actual, highly complex phenomena. Simple models have been developed for these effects and are presented in the following sections.

2. Estimation of Diffracted Shock Overpressure

Consider a plane shock wave propagating at normal incidence to two rectangular buildings, one of which is immediately behind the other. Prior to its arrival on the front of the second building, the shock must diffract around the first building (Figure 2-1).

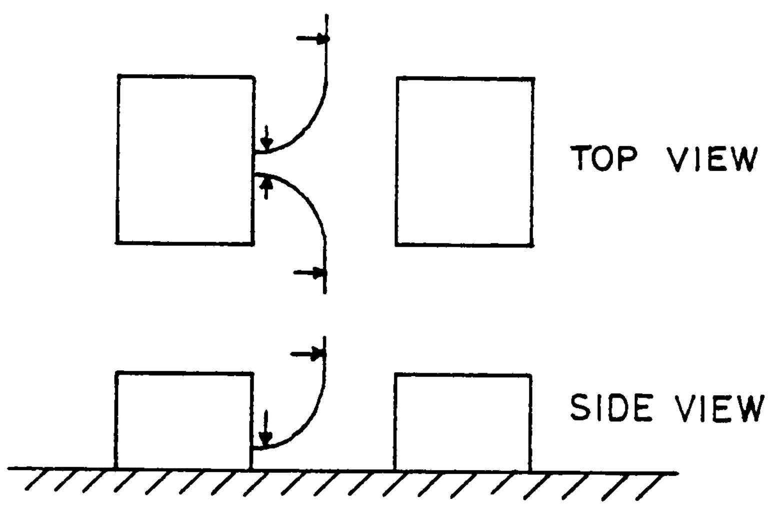

Figure 2-1. Shock Wave Incident on Two Buildings.

The shock is weakened during the diffraction process due to the expansion of the flow on the rear of the first building. Given a sufficiently large distance between the buildings, the shock wave will coalesce and once again resemble a plane wave at the undisturbed state, prior to its arrival on the front of the second building (Figure 2-2).

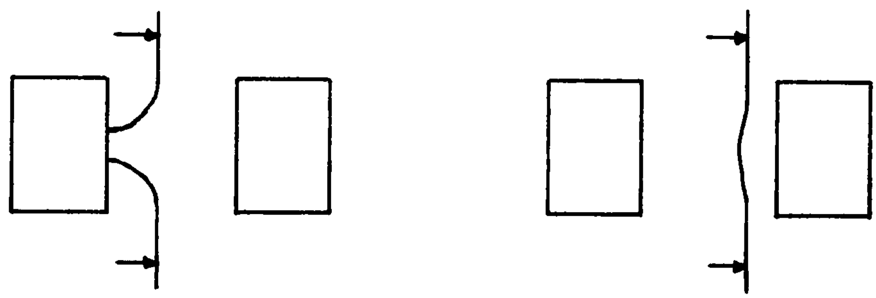

Figure 2-2. Recovery of a Shock Wave Between Buildings.

If the distance is insufficient to permit recovery of the shock, it will strike the second building at a reduced overpressure, P_d ; as a result of the diffraction of the shock around the first building. In order to estimate the loading on the second building, a model for the recovery of the shock and its diffraction strength is needed. Porzel [14] has developed a model based on a method of inverse normal reflection for the similar problem of determining the overpressure of a shock diffracted into a tunnel entrance. Porzel's model, which related the diffracted shock overpressure to the incident shock overpressure is given by

$$F = (D+1)\left(\frac{(3\gamma-1)(D+1) - (\gamma-1)}{(\gamma-1)(D+1) + (\gamma+1)}\right) - 1 \quad , \qquad (2.1)$$

where:

$$D = \frac{P_d}{P_A} \ ,$$

$$F = \frac{P_s}{P_A} \ ,$$

P_d= diffracted shock overpressure

It is also possible to estimate the diffracted shock velocity on the rear of the building. The Rankine-Hugniot relations give the shock velocity, u_o , as a function of the ambient sound speed and shock strength,

$$u_o = a_o \left(\frac{\gamma-1}{2\gamma} + \frac{\gamma+1}{2\gamma}\ (F+1)\right)^{\frac{1}{2}} \qquad (2.2)$$

Applying this same relation to the diffracted shock velocity we obtain,

$$u_d = a_o \left(\frac{\gamma-1}{2\gamma} + \frac{\gamma+1}{2\gamma}\ (D+1)\right)^{\frac{1}{2}} \quad , \qquad (2.3)$$

where u_d is equal to the diffracted shock velocity.

Combining Equations 2.2 and 2.3 we note the following result for the ratio of the diffracted shock velocity to the incident shock velocity,

$$u' = \frac{u_d}{u_o} = \left[\frac{\frac{\gamma-1}{2\gamma} + \frac{\gamma+1}{2\gamma}(D + 1)}{\frac{\gamma-1}{2\gamma} + \frac{\gamma+1}{2\gamma}(F + 1)}\right]^{\frac{1}{2}} \qquad (2.4)$$

Making the substitution $\gamma \simeq 7/5$ for air, Equations 2.1 and 2.4 respectively become,

$$F = \frac{8\ (D+1)^2 - (D+1)}{(D+7)} - 1 \quad , \qquad (2.5)$$

and

$$u' = \frac{u_d}{u_o} = \left[\frac{\frac{1}{7} + \frac{6}{7}\ (D+1)}{\frac{1}{7} + \frac{6}{7}\ (F+1)}\right]^{\frac{1}{2}} \quad . \qquad (2.6)$$

Equation 2.5 may be manipulated to obtain the inverse relation for D in terms of F,

$$D = \frac{\sqrt{(14-F)^2 + 224F} - (14-F)}{16} \quad . \qquad (2.7)$$

Values of D/F and u' are shown as a function of the incident shock overpressure f in Figure 2-3.

The distance for shock recovery may be estimated by considering the phenomenon during diffraction on the rear wall. Upon arrival at the rear wall, the shock front diffracts around the building at velocity u_d (Figure 2-4). At some time t_c later, the shock fronts merge at the center of the rear wall (Figure 2-5). The time

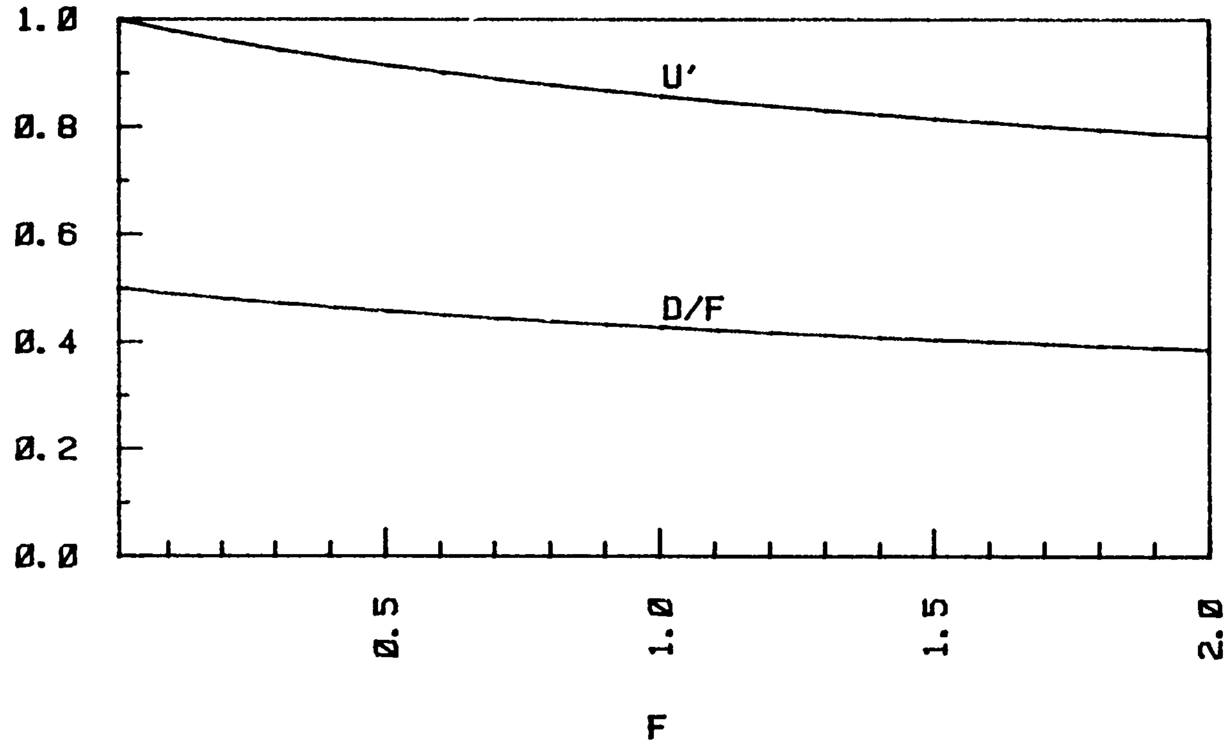

Figure 2-3. Values of the Diffracted to Incident Shock Overpressure Ratio (D/F) and the Diffracted to Incident Shock Velocity Ratio (u'), Plotted as a Function of Incident Shock Overpressure Ratio, F.

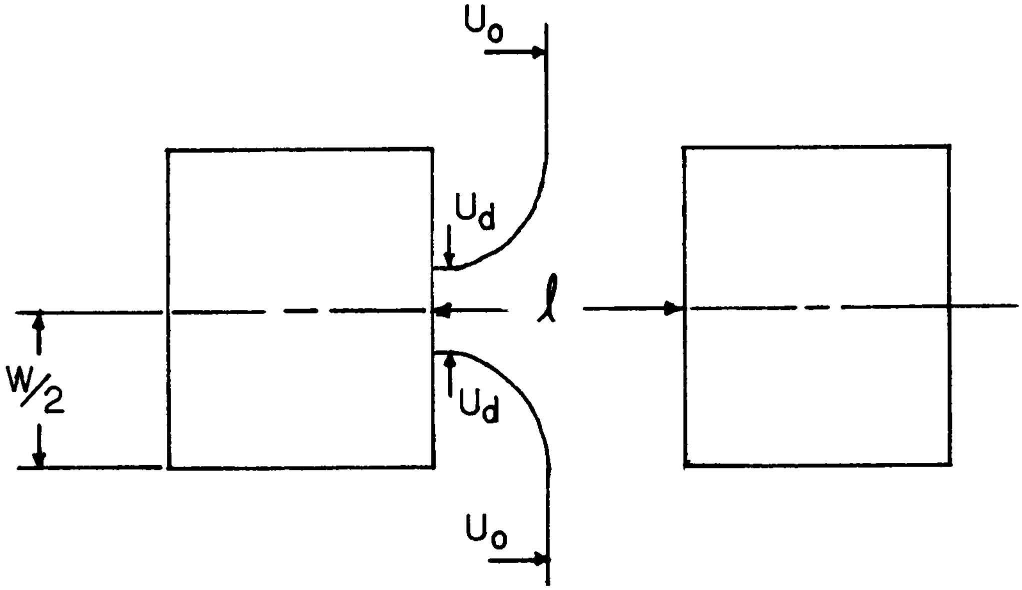

Figure 2-4. Diffraction of a Shock Wave Around a Building.

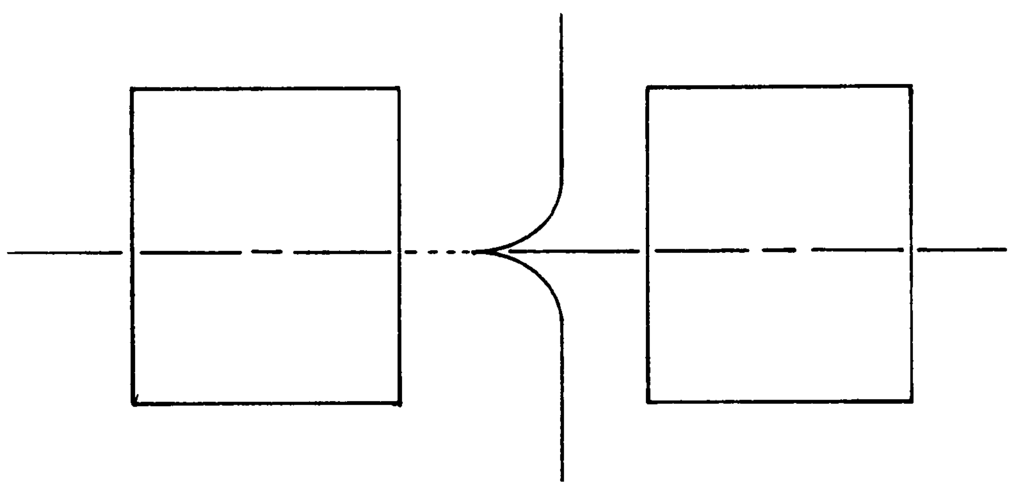

Figure 2-5. Shock Waves Merging at the Rear Wall.

t_c, required for the two fronts to merge is determined by the width of the building, w, and the diffracted shock velocity on the rear wall,

$$t_c = \frac{w}{2u_d} \tag{2.8}$$

At this point the shock front resembles a plane wave which is disturbed over a small region. At the point of merger, the front is strengthened due to stagnation of the flow and hence propagates forward at a higher velocity than the rest of the front. This process has the effect of "smoothing out" the perturbation on the shock. Thus, some short time after merger the disturbance essentially will have disappeared, and the shock will return to the undisturbed state.

Assuming that the overpressure of the perturbed shock approximates the undisturbed state, this perturbation may be neglected and the minimum recovery time may be approximated by:

$$t_r \simeq t_c = \frac{w}{2u_d} \tag{2.9}$$

Given this approximation for the recovery time, it is possible to develop a criterion for recovery of the shock wave in terms of the distance between buildings, ℓ and the width of the shielding building, w . The transit time, t_t , required for the shock to travel between the buildings is given by:

$$t_t = \frac{\ell}{u_o} \quad . \tag{2.10}$$

The shock is assumed to have recovered during this time if $t_r < t_t$, hence the criterion for shock recovery;

$$\frac{t_r}{t_t} < 1 \quad . \tag{2.11}$$

Substituting the values for t_r and t_t (Equations 2.9 and 2.10) into Equation (2.11) yields the result,

$$\frac{w}{2\ell} \; \frac{1}{u'} < 1 \quad . \tag{2.12}$$

Where u' is the shock velocity ratio as given by Equation 2.6.

If half the building width is greater than the building height, then the shock wave from the top of the building will arrive at the ground before the waves from the sides merge. In this case, the shock is assumed to recover when it collides with the ground and t_r becomes,

$$t_r = \frac{h}{u_d} \quad . \tag{2.13}$$

Substituting (2.13) into (2.11) together with (2.10) yields the criterion for shock recovery,

$$\frac{h}{\ell} \; \frac{1}{u'} < 1 \; . \tag{2.14}$$

Summarizing, the criterion for shock recovery is given by

For $\frac{w}{2h} < 1$,

the shock wave will recover if,

$$\frac{w}{2\ell} \; \frac{1}{u'} < 1 \quad . \tag{2.15}$$

For $\frac{w}{2h} > 1$,

the shock wave will recover if,

$$\frac{h}{\ell} \; \frac{1}{u'} < 1 \quad . \tag{2.16}$$

If the "target" building is closely surrounded by buildings (Figure 2-6) on all sides, then the shock will be weakened on either side due to interaction with other buildings. In this case, the downward traveling shock front is predominant and Equation 2.16 alone must be used to determine the recovery of the shock.

If the criterion for shock wave recovery is met, then the loading for the shielded building may be approximated by the free-field shock wave overpressure. If the criterion for recovery is not met, then the diffracted shock overpressure as given by Equation (2.7) is used to approximate the loading on the shielded building.

3. Effects of Reflected Shocks

The effects of reflected shocks must be considered in the case where the building is shielded by nearby structures. These secondary shocks decay rapidly, but may be of sufficient strength to influence the assessment of structural damage during the initial portion of the blast wave interaction.

Nuclear test data suggests that for overpressures greater than approximately 5 psi, structures are damaged greatly in almost all cases. It is the lower overpressure regime which is of primary concern, where the amount of damage is uncertain. Shock strengths within

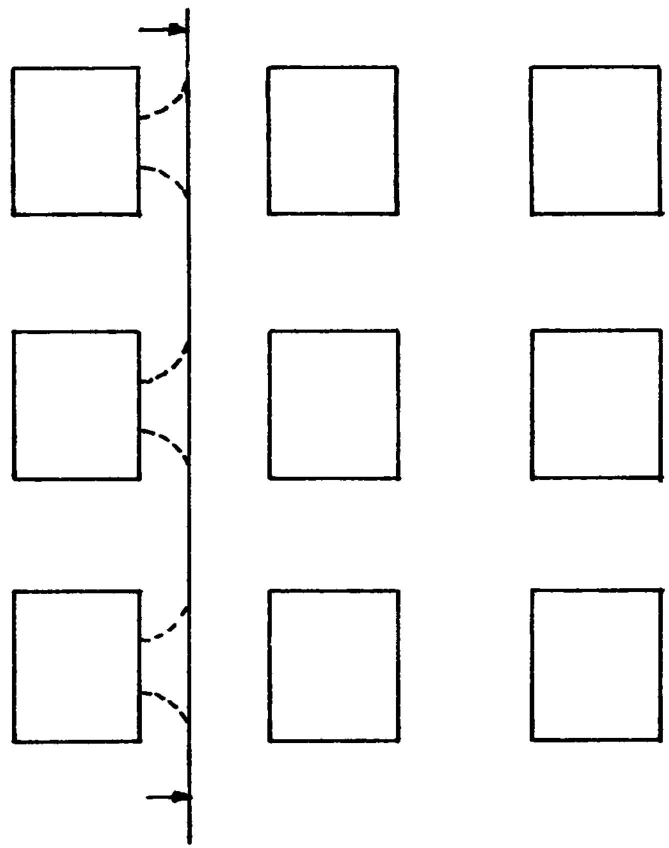

Figure 2-6. Shock Wave Propagating Across a Complex of Buildings.

this regime are low enough to be considered as "weak shocks" and hence behave similar to sound waves. An acoustic treatment of the problem is advantageous, as it leads to a linear analysis in which the waves may be superimposed.

It is assumed in this analysis that there is an overall loss co-efficient which may be applied to each successive reflected shock to determine its overpressure. This loss co-efficient is actually the result of two loss factors, the loss due to reflection at the wall and a "geometric" loss due to expansion of the curved shock front as it propagates. Consider a shock reflecting between two buildings (Figure 2-7).

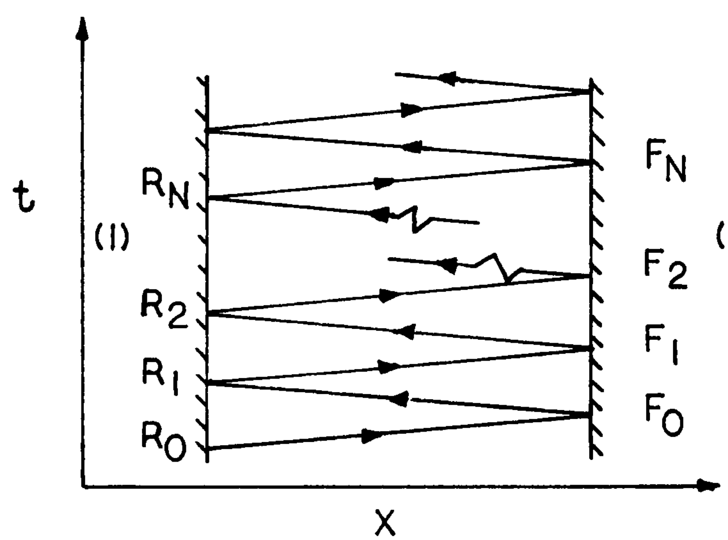

Figure 2-7. Illustration of the Reflecting Shock Process

Initially, the shock diffracts around the rear of building (1). Due to flow separation and other effects, the initial shock on the rear of building (1) is degraded and generally may be neglected. Eventually, the shock will reach the front of building (2), at which point it may or may not have recovered from its loss in diffraction. The diffracted overpressure of the incident blast upon arrival at the front wall may be determined using the criterion for shock recovery given in Section 2-2. The value of the reflected overpressure, F_o , may then be estimated using the relation for normal reflection of shocks (Equation A.1) or the value for oblique reflection (Porzel [10]), depending on the angle of incidence. Following reflection from the front wall of building (2), the shock will be weakened due to adsorption by the wall, and expansion of the shock front prior to its return to the rear of building (1). Thereafter, the shock is weakened further as this process is repeated. This sort of analysis suggests the following form for the decay of the shock on a single transit,

$$W_{N+1} = \alpha W_N \tag{2.17}$$

where: W_{N+1} is the reduced overpressure at the end of the (N+1)th transit,

α is a number less than one, describing the loss,

and W_N is the overpressure at the beginning of the Nth transit.

It will be assumed in this analysis that following the initial reflection, each shock is weakened a sufficient amount to be treated as an acoustic wave. Hence, the reflected overpressure of the secondary shocks is approximately equal to twice the incident overpressure of the shock.

Generalized equations for the reflected overpressure of the Nth reflecting shock on both the front and rear walls may be written:

On the front surface,

For $N = 0$, F_o is determined by the criterion for shock recovery and the relations for normal or oblique shock reflection

$$\text{For } N \geq 1; \; F_N = 2P_I \, \alpha^{2N} \; . \tag{2.18}$$

On the rear wall,

$$\text{For } N = 0, \; R_o = 0 \; . \tag{2.19}$$

$$\text{For } N \geq 1, \; R_N = 2P_I \, \alpha^{2N-1} \; , \tag{2.20}$$

where:

$P_I = P_d$, the diffracted overpressure (Equation (2.1) if the criterion for shock recovery is not met.

$P_I = P_s$, if the criterion for shock recovery is met.

F_N = the reflected overpressure of the Nth shock on the front wall

R_N = the reflected overpressure of the Nth shock on the rear wall.

Normalized values of overpressure for successive reflections on the front and rear walls are shown in Figures 2-8 and 2-9 respectively for various values of α.

The determination of the loss co-efficient poses a difficult problem due to the non-uniform, three dimensional nature of the reflected shock front. Therefore, the loss co-efficient must be determined from empirical results.

The model for reflected shocks is easily incorporated into the model for buildup and reduction of pressure. Essentially, the shocks are treated as discontinuities in the solution which instantaneously change the value of pressure on the wall. Consider the solution for the wall, Equation 1.24, before and after the arrival of a shock. Prior to arrival of the shock, the solution approaches the input curve as the pressure on the wall equalizes with the free-field (Figure 2-10).

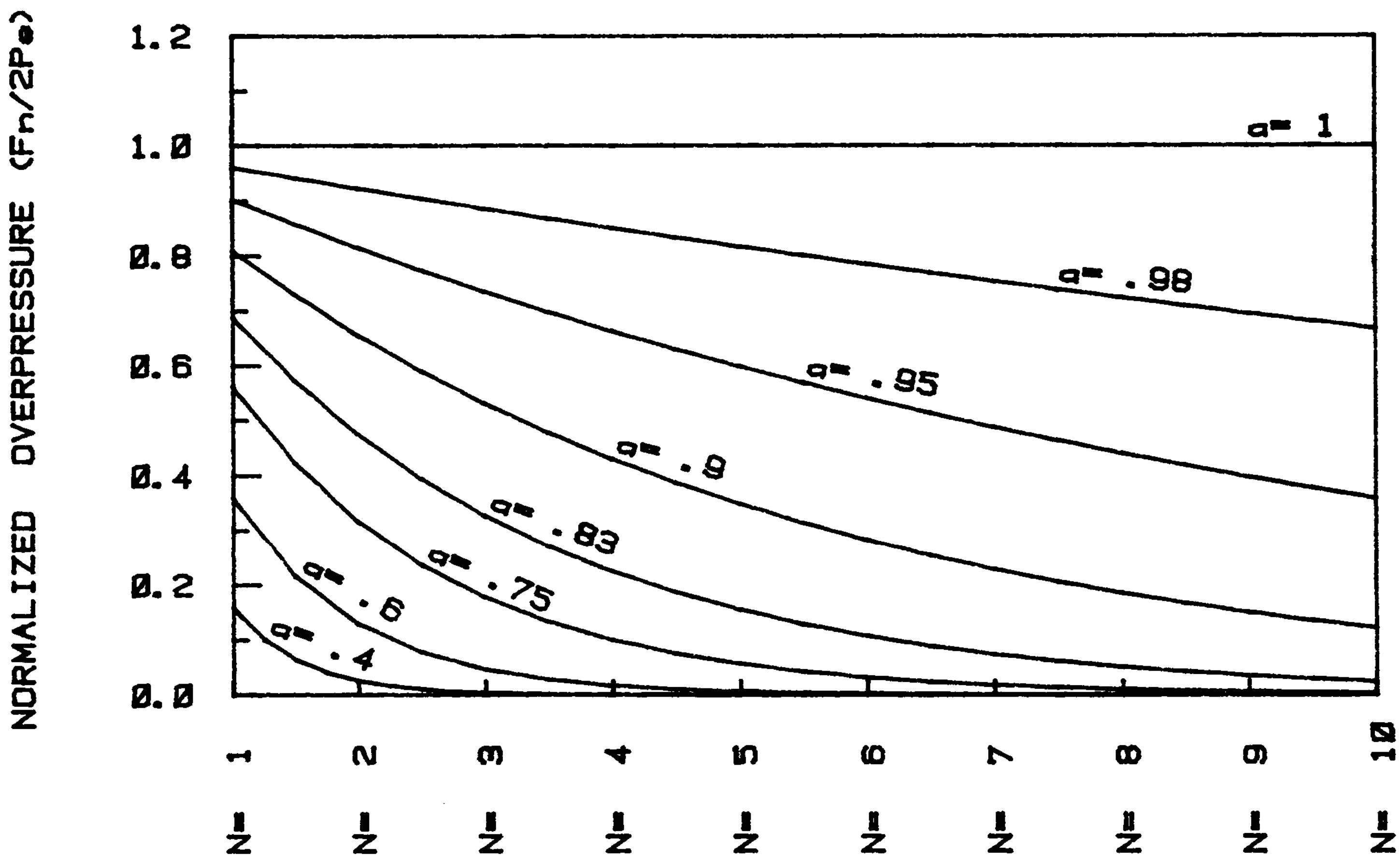

Figure 2-8. Normalized Reflected Overpressure on the Front Wall as a Function of Shock Index for Various Values of Loss Coefficient, α .

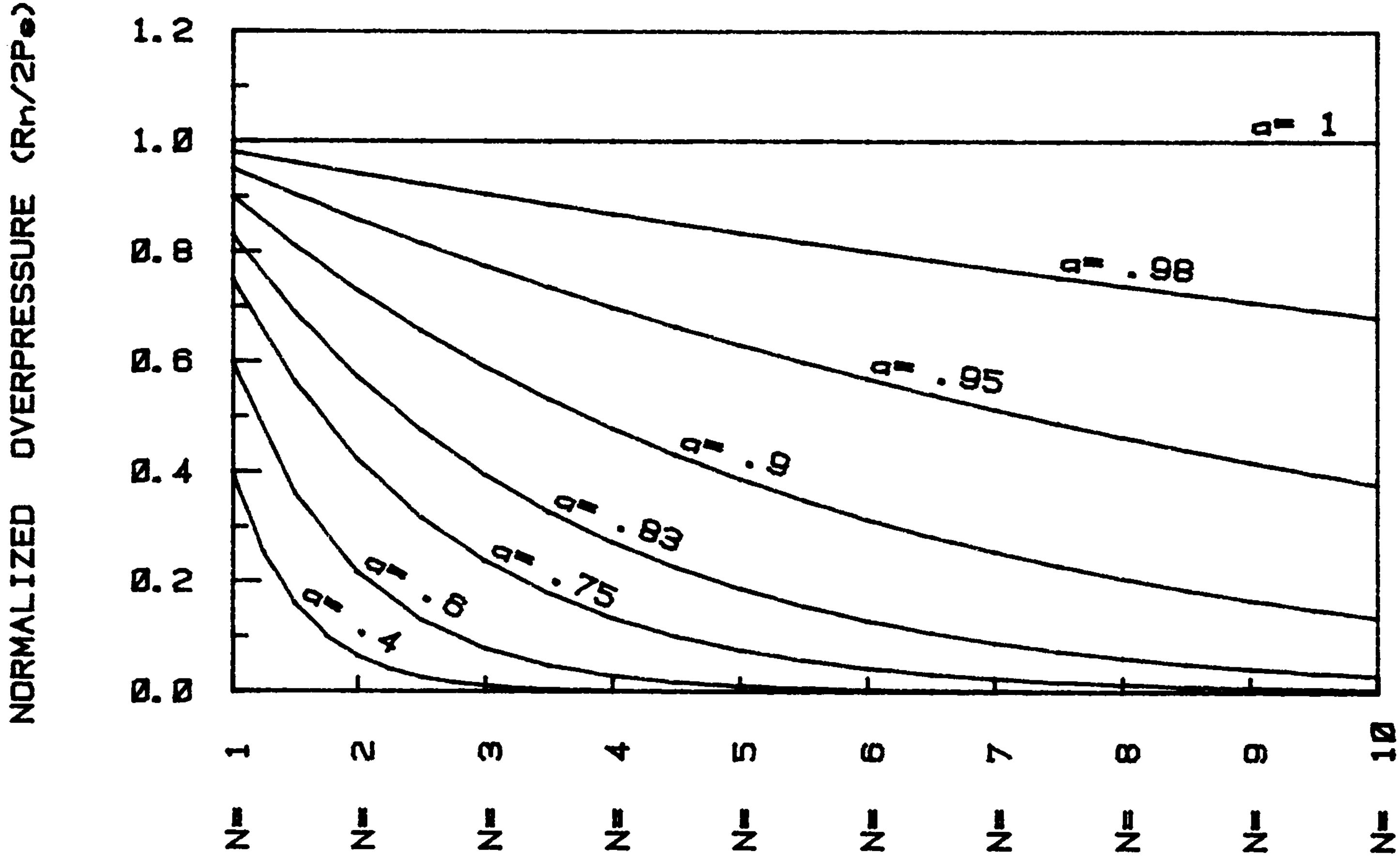

Figure 2-9. Normalized Reflected Overpressure on the Rear Wall as a Function of Shock Index for Various Values of Loss Coefficient, α .

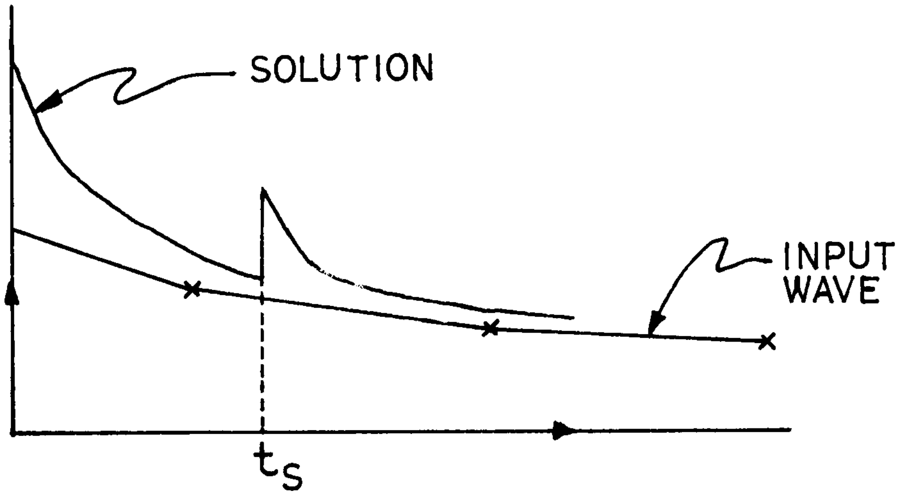

Figure 2-10. Effect of a Reflected Shock on the Solution.

When the reflected shock arrives at the wall at time t_s , the solution is instantaneously increased by the linear superposition of the reflected shock overpressure. This amounts to setting $\hat{t}_N = 0$ and re-evaluating the constant p_N at $t = t_s$ in Equation 1.24. The solution is restarted after this modification for the reflected shock. This process is repeated each 2N multiple of the shock transit time across the intervening space between the buildings.

4. Treatment of Unsteady Dynamic Effects

Data by Coulter [8] suggests the presence of a fluctuating negative dynamic component of overpressure in the cavity formed between adjacent buildings exposed to a blast wave. In his experiments, Coulter exposed two configurations of shielded buildings (Figures 2-11 and 2-12) to free-field explosions of approximately 4.0 psi overpressure. Analysis of these pressure records reveals a significant oscillating negative flow component which is not observed in the isolated case. These effects are particularly evident in those cases where the buildings are closely spaced.

Experimental results are available from East [15] concerning the oscillation of pressure in cavities immersed in a steady flow. It has been determined from these experiments that an oscillating shear layer is formed over the mouth of the cavity if the flow velocity is above a certain critical speed. This phenomenon is closely related to the shedding of vortices from the leading cavity edge. In certain instances, the cavity resonant modes may couple with this shear layer to induce a bulk oscillation of pressure within the cavity. Plumblee [16] has developed a model for determining the resonant frequencies at which the cavity may oscillate. Estimates of the critical speed are given by Covert [17] in his theoretical investigation of shear layer stability. It should be noted that the theoretical results

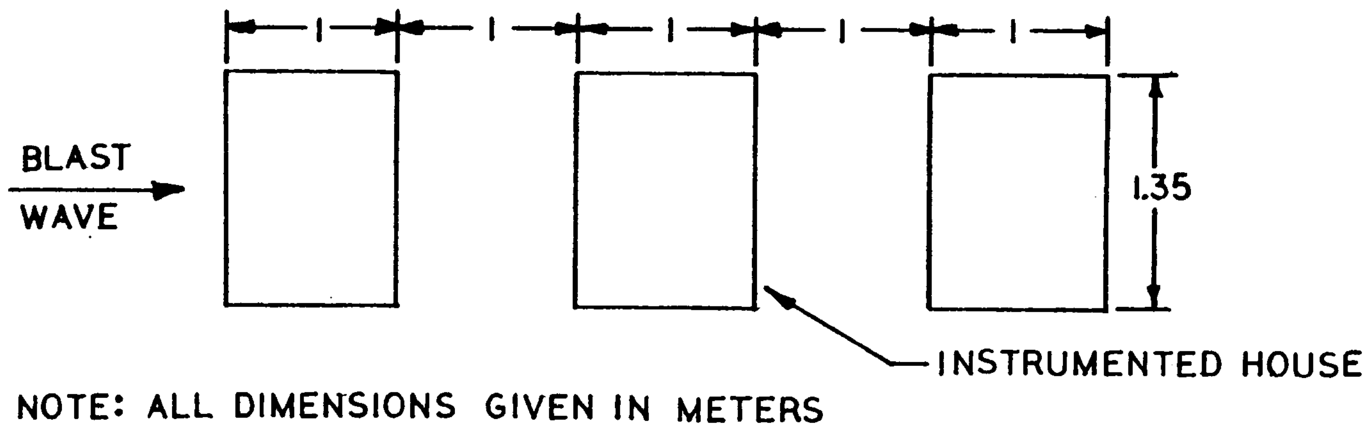

Figure 2-11. Test Configuration for In-Line Shields, From the Free-field Study by Coulter.[8] (Normal Incidence)

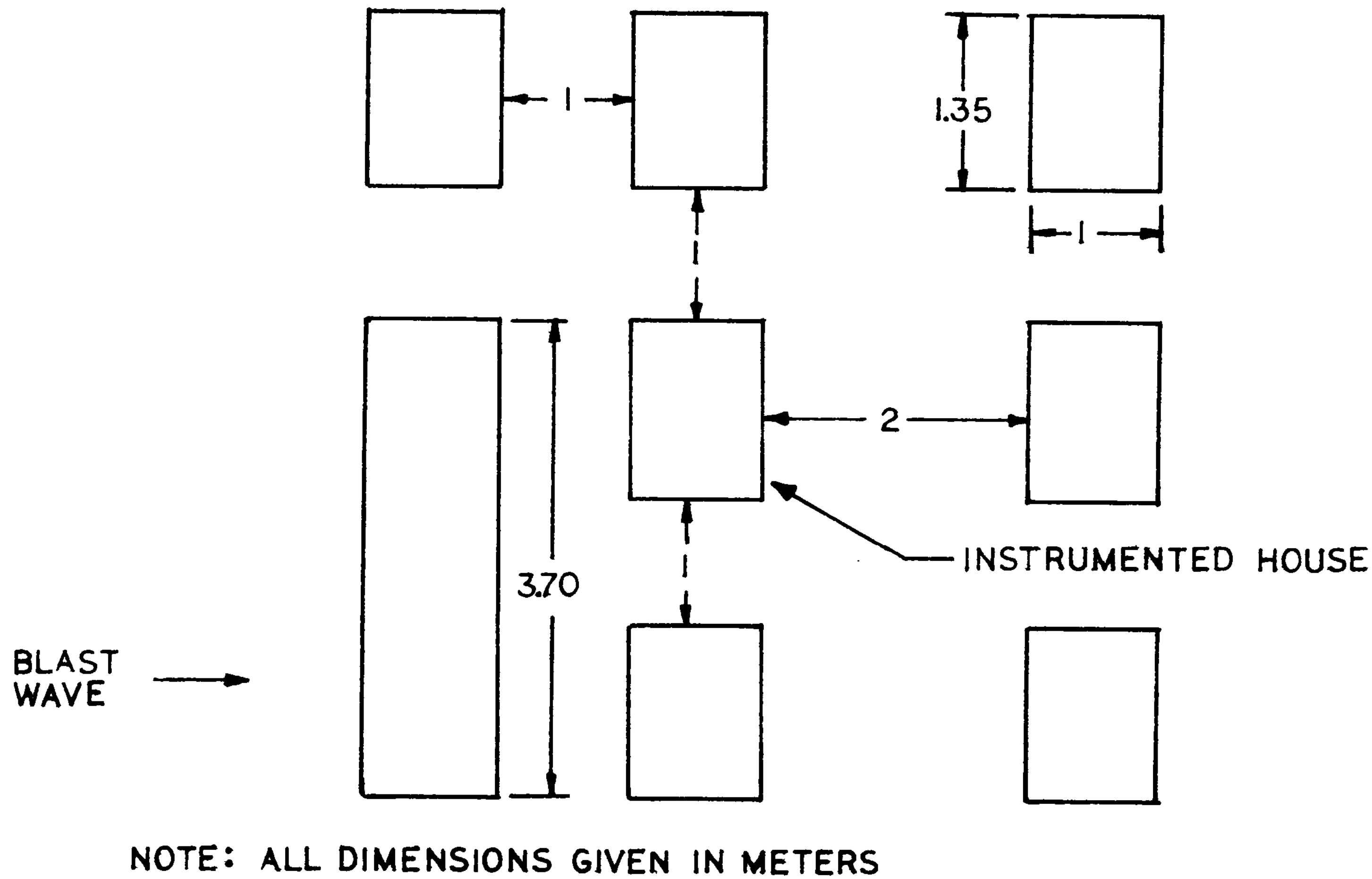

Figure 2-12. Complex of Model Houses Used in the Free-field Study by Coulter[8].

by Plumblee predict the frequency of oscillation observed in the data by Coulter for both configuration of shielded buildings, particularly for latter times. The peak flow velocities behind the shock in the experiments by Coulter are also greater than the critical velocity given by Covert. However, these results are of little value since none of these models predict the peak amplitude or phase of the cavity oscillation.

These oscillatory effects are not accounted for in this model due to the difficulties previously mentioned. Instead, a negative dynamic component of pressure is assumed to exist due to the acceleration of the external flow into the cavity (Figure 2-13).

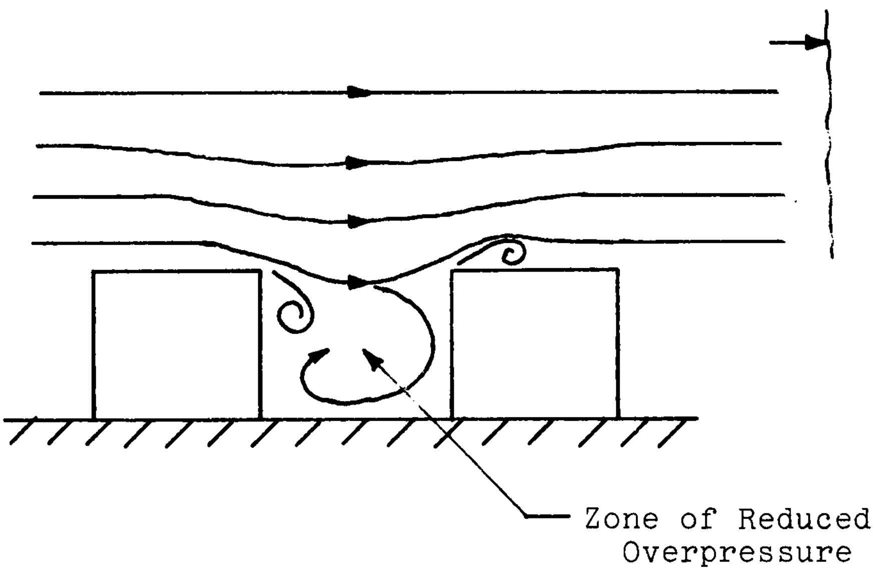

Figure 2-13. Acceleration of the External Flow Into the Cavity Between Adjacent Buildings.

For this purpose, a drag co-efficient of -.5 is assumed for all building walls within the cavity.

5. Comparison with Experimental Results

The model developed in Chapters One and Two was compared with data from free-field studies by Coulter [8] for the configuration of in-line shields (Figure 2-11) and the 1/8 scale model city complex (Figure 2-12). The solution agrees reasonably well with the data in the early time history for most cases. However, anomalous effects are observed in the data for which the model does not account. These effects may be due to oscillations of pressure within the cavity between buildings, transient dynamic effects, vortex action or any combination of the above. Although these effects cause the solution to depart from the data, the agreement is well enough to indicate that the model is fundamentally sound in terms of describing the general behavior and magnitudes observed in the data.

The relevant parameters used in the calculations for the case of in-line shields are given in Table 2-1. The shock loss co-efficient, α , was estimated from the data for each case studied. The parameter, D , in the table is the shortest distance from the location of the gauge on the model to the nearest shield. This parameter was used to estimate

Table 2-1. Parameters Used for Calculation of the Loading on the Shielded Building for the Configuration of In-Line Shields (Figure 2-11) From the Free-field Study by Coulter.[8] (Normal Incidence)

Gauge	P_s (KpA)	P_A (KpA)	a_o (m/s)	S (m)	D (m)	ξ (Degrees)	θ (Degrees)	C_D	α	Comments
2	26.3	94.4	340.4	.675	1.0	0	-	-.5	.75	Front Wall
6				.735	1.3	39.8		.5	.25	Front Roof
8				.735	1.3	39.8	-50.2	-.7	.25	Rear Roof
10				.675	1.0	-	-90.0	-.5	.75	Rear Wall
13				1.0	-	0	-	-.7	-	Side Wall

the transit time of the reflected shocks. All other parameters have been defined previously.

Calculations were made for the front wall, front roof, rear roof, rear wall and side of the model using a BASIC computer program (Appendix D) utilizing principles developed in Chapters I and II. These results are given in Figures 2-14 through 2-16. The input wave used for calculation is given in Figure 2-14A.

On the front wall (Figure 2-14B) a significant oscillation is evident in the data which the solution does not include. The reflected shocks decay more rapidly than those calculated though the magnitudes are approximately correct.

For the front roof (Figure 2-15A), the solution was calculated assuming no reduction in peak overpressure due to the effect of the shield building. However, the data reveals a slight reduction in peak overpressure. The model developed will not predict this slight variation as it actually predicts only the minimum or maximum possible value as determined by the criterion for shock recovery (Section 2-2).

The solution on the rear roof (Figure 2-15B) agrees very well with the data. Only one reflected shock appears in this case for the very small loss co-efficient (α = .25) assumed from the data.

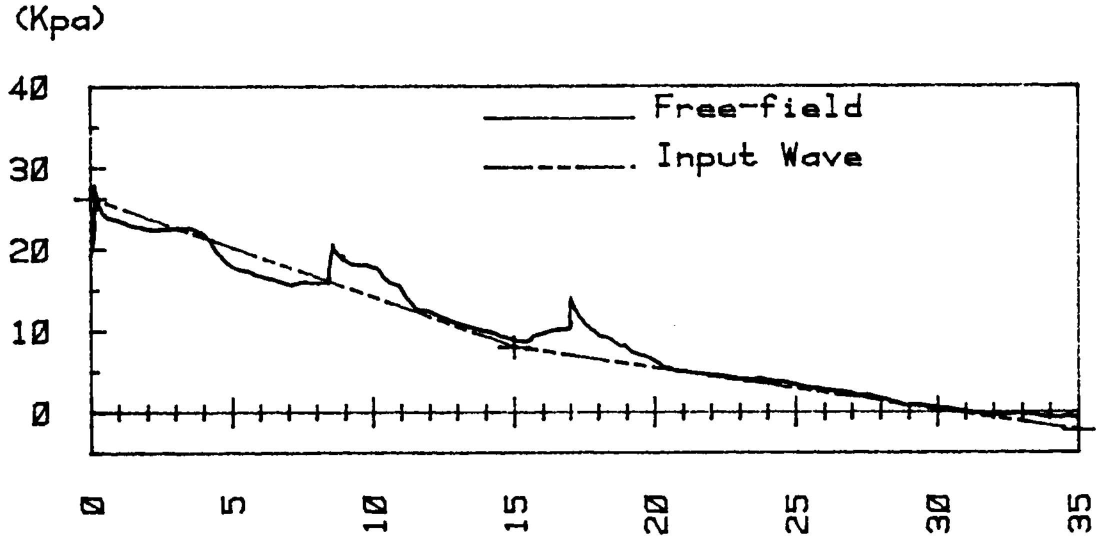

A. Free-field

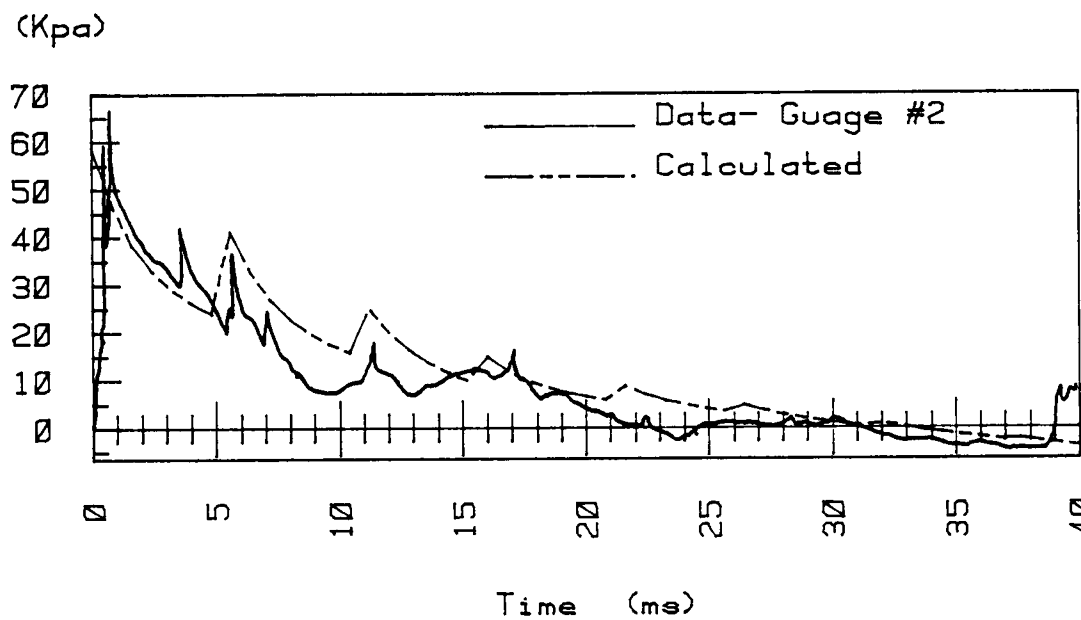

B. Front Wall

Figure 2-14. The Input Wave Used to Approximate the Free-field Data for Calculation Purposes, and Comparison of Calculated Results With Data for the Front Wall of a 1/8th Scale Model House in the In-line Shields Configuration From the Free-field Experiments by Coulter.[8] (Normal Incidence)

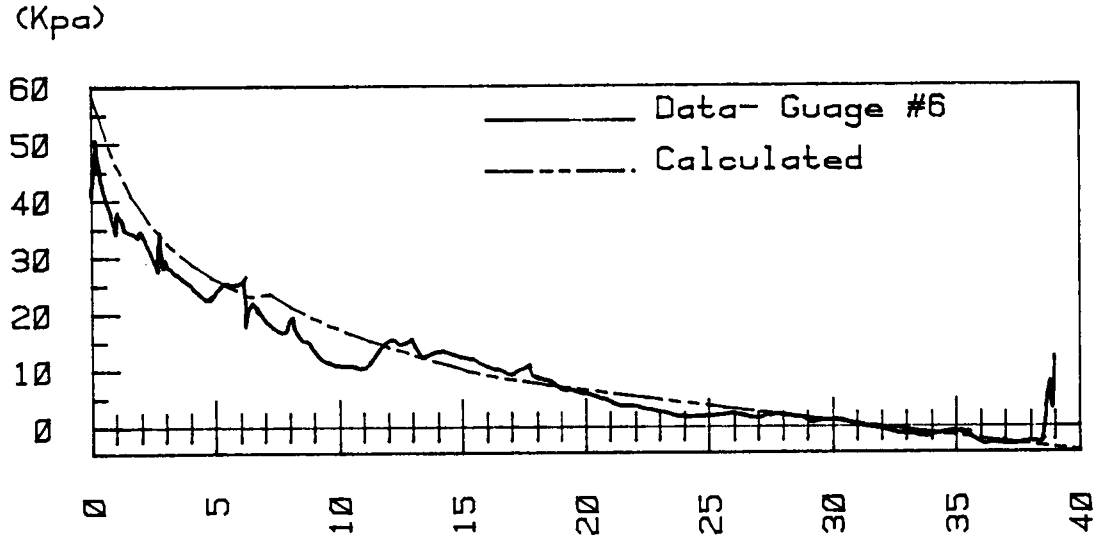

A. Front Roof

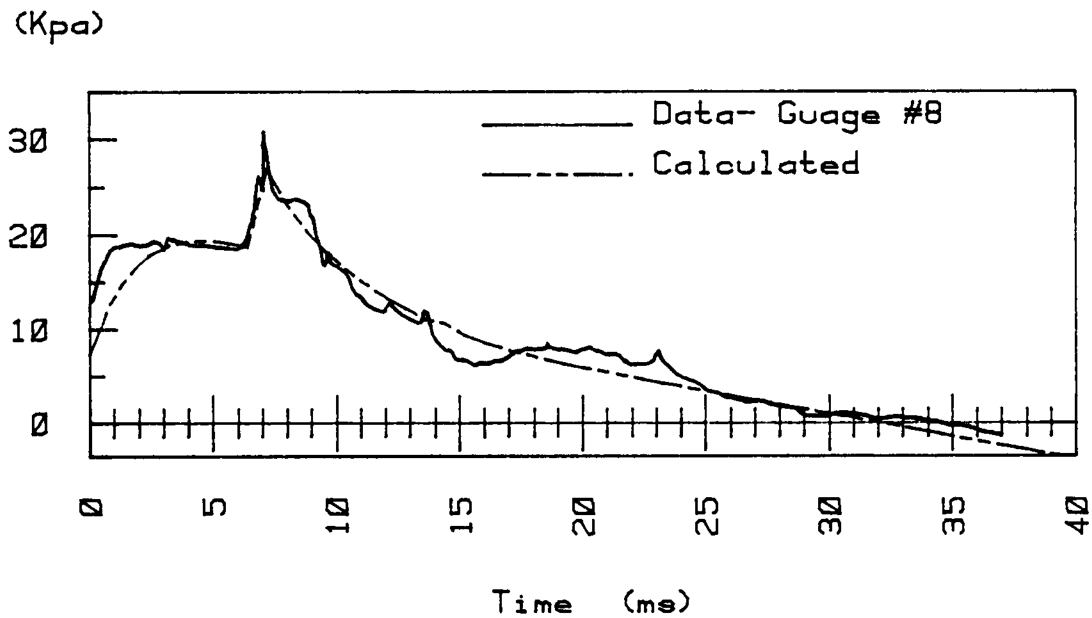

B. Rear Roof

Figure 2-15. Comparison of Calculated Results With Data For the Front Roof and Rear Roof of a 1/8th Scale Model House in the In-line Shields Configuration From the Free-field Experiments by Coulter.[8] (Normal Incidence)

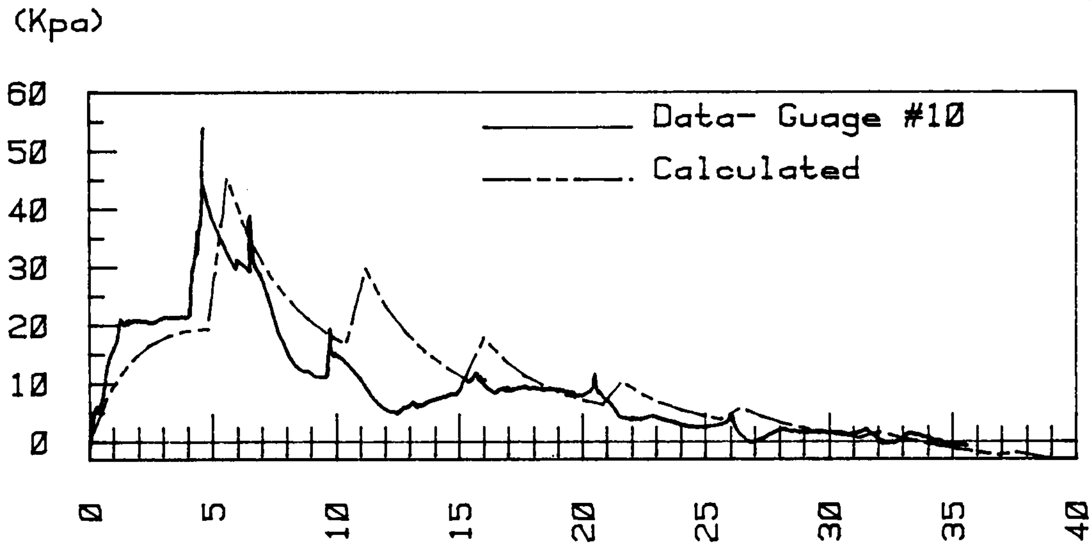

A. Rear Wall

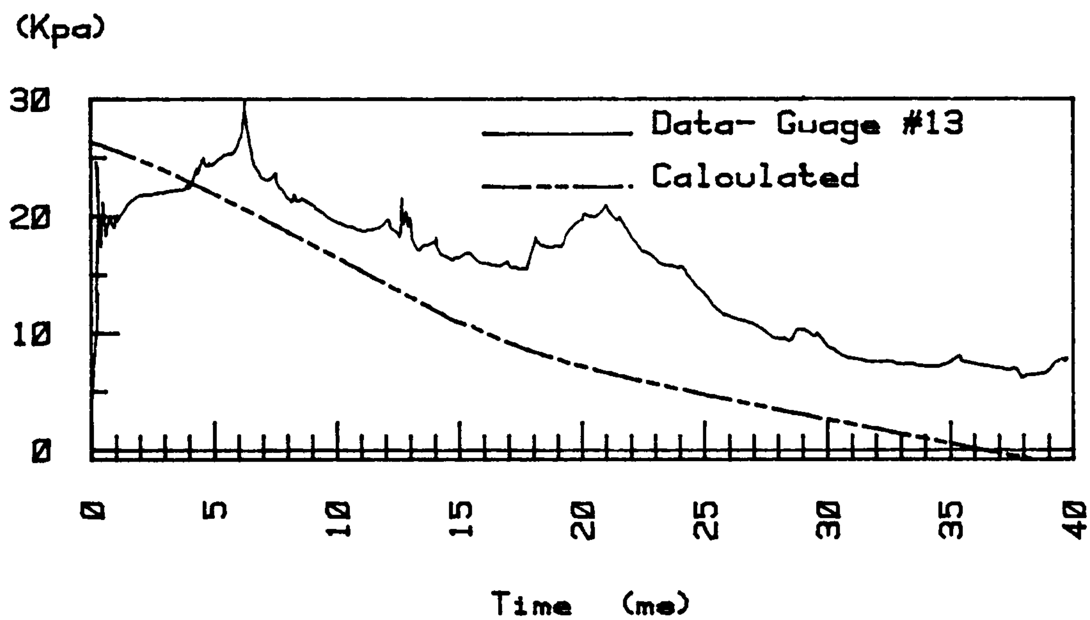

B. Side Wall

Figure 2-16. Comparison of Calculated Results With Data For the Rear Wall and the Side Wall of a 1/8th Scale Model House in the In-line Shields Configuration From the Free-field Experiments by Coulter.[8] (Normal Incidence)

On the rear wall (Figure 2-16A) a slight oscillation appears to be present in the data. The reflected shocks in the data decay more rapidly than those in the solution as well, contributing much less total impulse than is predicted.

On the side wall, (Figure 2-16B), the model developed predicts a behavior similar to the free-field record, modified by a negative dynamic component. However, the data exhibits a strange behavior in this case in which the pressure maintains a higher value than the free-field all during the positive phase of the blast.

Calculations were also made for the instrumented house in the model city complex examined by Coulter.[8] The relevant parameters used in these calculations are presented in Table 2-2. Calculations were made using the BASIC program in Appendix D for all surfaces of the building. These results are given in Figures 2-17 through 2-19. The input wave used to approximate the free-field data is given in Figure 2-17A.

On the front wall (Figure 2-17B), the diffracted overpressure (Section 2-2) was used for the peak value of the incident shock, in order to determine the reflected overpressure. This method accurately predicted the magnitude of pressure on the wall for early times. For latter times an oscillation is evident which reduces the pressure below that predicted. Reflected shocks, other than the first, are also strangely lacking in the data.

Table 2-2. Parameters Used for Calculation of the Loading on the Shielded Building for the Complex of Buildings (Figure 2-12) from the Free-field Study by Coulter [8].

Gauge	P_s (KpA)	P_A (KpA)	a_o (m/s)	S (m)	D (m)	ξ (Degrees)	θ (Degrees)	C_D	α	Comments
2	26	93.3	349.4	.675	1	90	-	-.5	.75	Front Wall
6				.735	1.3	39.8	-	.5	.25	Front Roof
8				.735	2.27	39.8	-50.2	-.7	.15	Rear Roof
10				.675	2	-	-90	-.5	.15	Rear Wall
13				.675	-	0	-	-.7	-	Side Wall

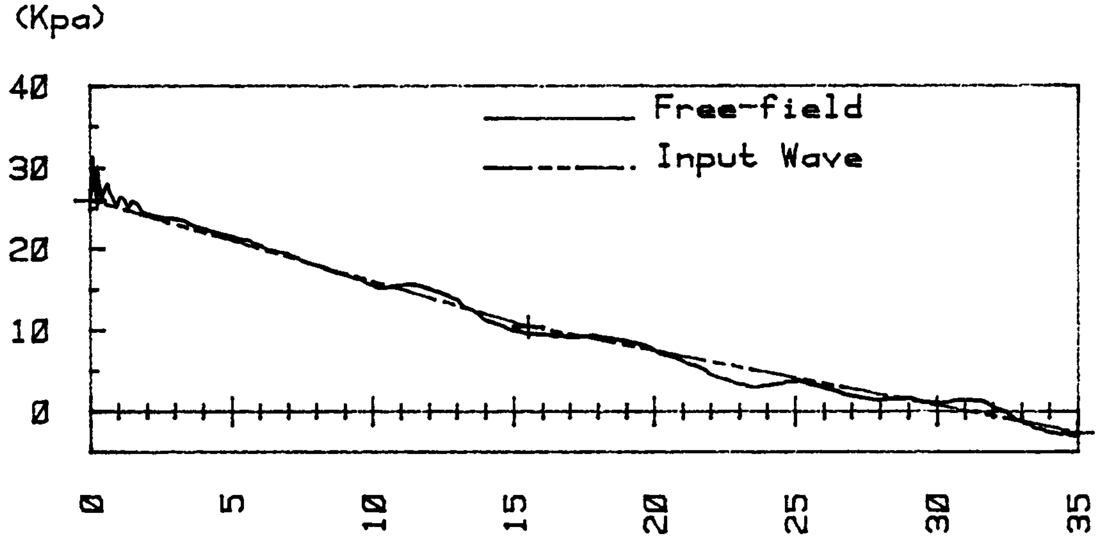

A. Free-field

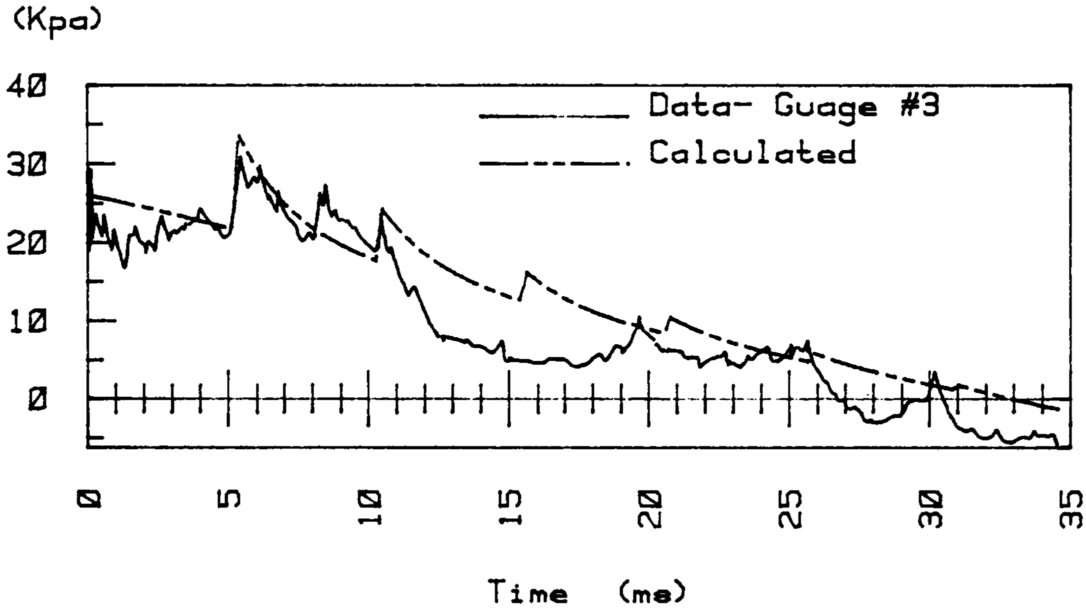

B. Front Wall

Figure 2-17. Input Wave Used to Approximate the Free-field Data for Calculation Purposes, and Comparison of Calculated Results With Data for the Front Wall of a 1/8th Scale House in the Model City Complex From the Free-field Experiments by Coulter.[8] (Normal Incidence)

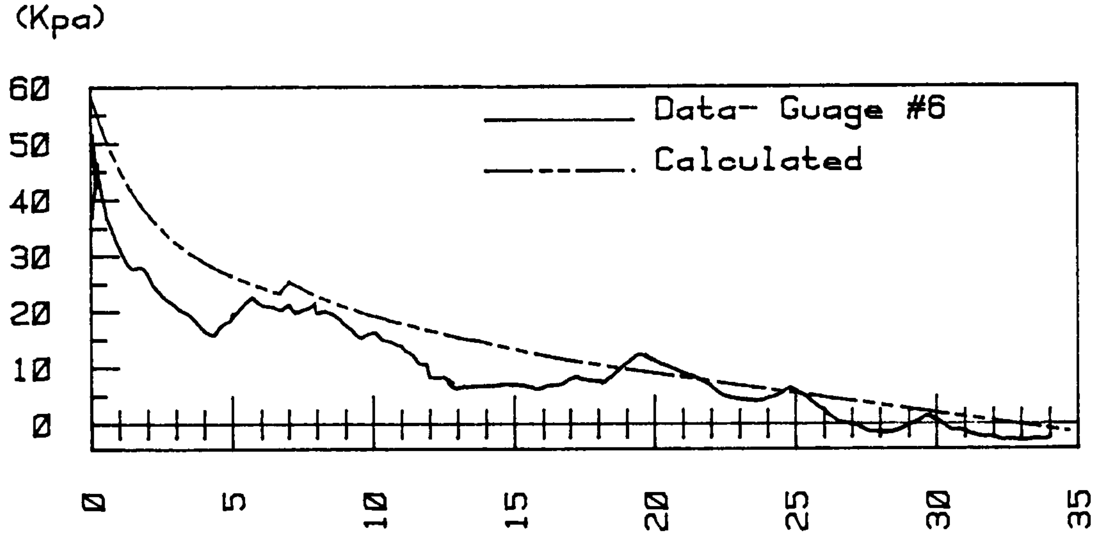

A. Front Roof

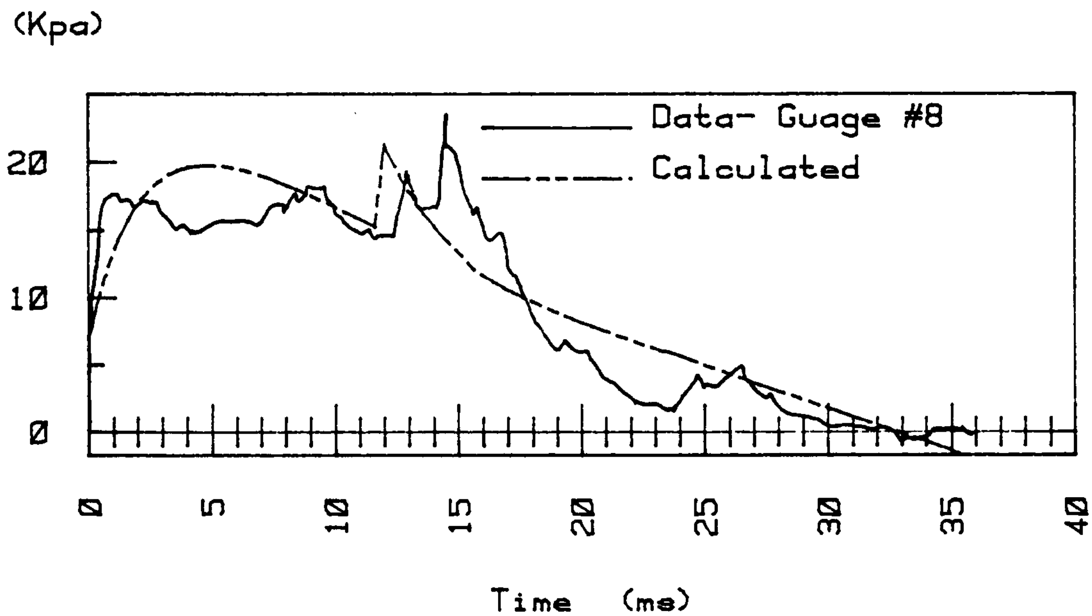

B. Rear Roof

Figure 2-18. Comparison of Calculated Results With Data For the Front Roof and Rear Roof of a 1/8th Scale Model House in the Model City Complex From the Free-field Experiments by Coulter.[8] (Normal Incidence)

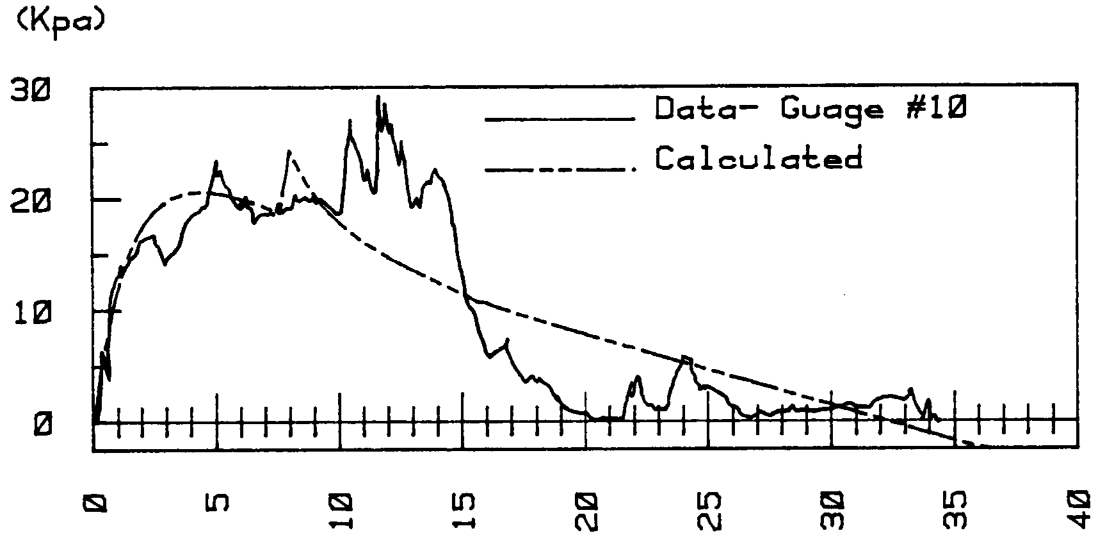

A. Rear Wall

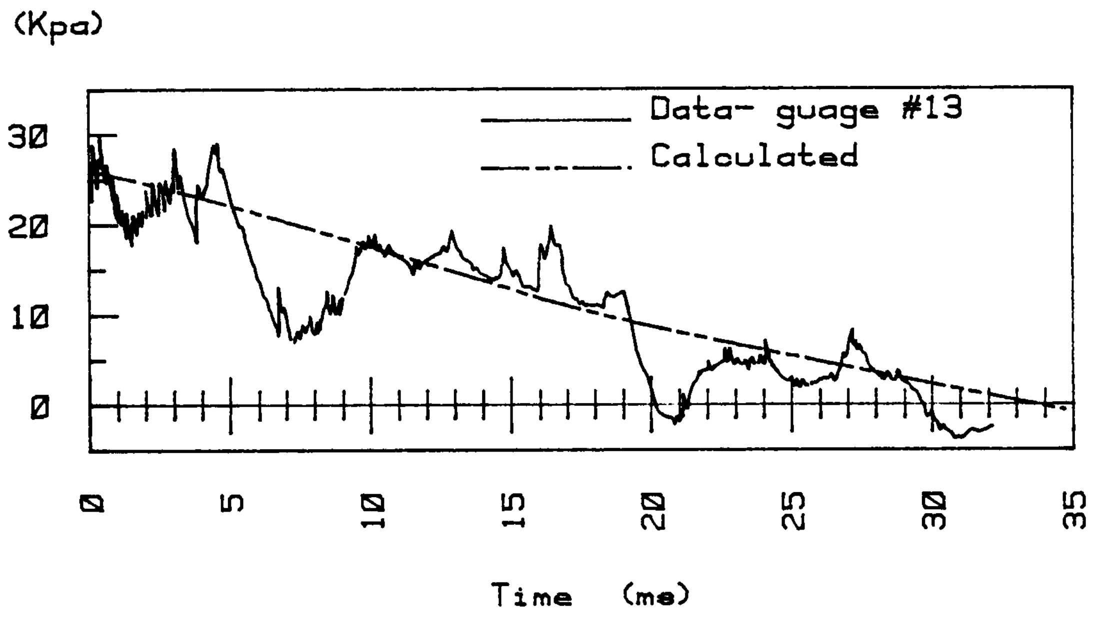

B. Side Wall

Figure 2-19. Comparison of Calculated Results With Data For the Rear Wall and Side Wall of a 1/8th Scale House in the Model City Complex From the Free-field Experiments by Coulter.[8] (Normal Incidence)

On the front roof, (Figure 2-18A) no reduction was assumed for the incident blast. As a result, the solution overestimates the peak reflected value of overpressure on the roof. A very small loss co-efficient was assumed for the reflection of shocks ($\alpha = .25$) to correspond to the similar geometry for the case of in-line shields. Thus, the model predicts a very small reflected shock although only a gradual rise and fall of significant impulse is evident in the data at this point.

For the rear roof (Figure 2-18B) the overpressure observed is somewhat less than that predicted by the solution in the initial portion of the blast wave interaction. The data also exhibits a sharp drop in overpressure following the arrival of the first reflected shock. However, the solution provides a good estimate of the data regardless of these differences.

The solution for the rear wall (Figure 2-19A) agrees very well with the data for early times. The reflected shocks observed in the data arrived later than expected, followed by a sharp drop in overpressure which the model does not predict.

On the side wall (Figure 2-19B) the model provides a solution which resembles the free-field reduced by a dynamic component. The solution well approximates the data in this instance with the exception of two sharp reductions in overpressure which may be the result of vortices traveling along the wall.

CHAPTER III

SUMMARY

A model has been developed to approximate the loading on a building exposed to blast waves from large scale chemical or nuclear explosions. This model is applicable to buildings which are either isolated or shielded by nearby structures. Overpressure calculations based on this model have been compared with both empirical models and experimental data and were found to be in reasonable agreement. The model agrees very well with the experimental data for isolated buildings obtained by Coulter [8,11] for both free-field and shock tube explosions. Good agreement is also reached with empirical models by Etheridge[2] for overpressures of approximately 5 psi. However, the model does not account for local effects such as vortices which are frequently observed in the data.

The model predicts the general behavior and magnitudes observed in the data for the shielded case except where transient dynamic effects are predominant. These effects are characterized by an abrupt reduction of overpressure between adjacent buildings, often accompanied by subsequent oscillations. These effects may be due to the formation of an unstable vortex sheet in the wake of the shielding building.

A criterion for the recovery of the shock wave between buildings has been proposed, based on a model by Porzel [14] for the overpressure of a shock diffracted into a tunnel entrance. This model predicts the gross attenuation of shock strength observed on the front wall of the shielded building, although it does not provide an estimate for the slight reductions observed on the roof.

The effects of shock waves reflected between adjacent buildings have also been included in the model. These shock waves are assumed to decay in a geometric progression described in terms of an empirical loss coefficient. Although the model somewhat overestimates the impulse of these reflected shocks, the overall behavior of the reflected shocks are reasonably well predicted.

The blast loading predictions provided by this model should be useful as input to existing models for blast damage to structures. The model provides reasonable estimates of blast loading for all surfaces of either shielded or isolated structures while requiring a minimum of computational effort. In some cases anomalous effects have been observed which are not accounted for by the model; however, the results are sufficiently accurate for the purpose of estimating structural damage due to large scale explosions.

LIST OF REFERENCES

LIST OF REFERENCES

1. Glasstone, Samuel and Dolan, Phillip J., "The Effects of Nuclear Weapons," Dept. of the Army, Pamphlet No. 50-3, March 1977.

2. Etheridge, Noel H., "Blast Diffraction Loading On the Front and Rear Surfaces of a Rectangular Parallelopiped," BRL Memorandum Report No. MR 2784, September 1977.

3. Gentry, R. A., et al., "Three Dimensional Computer Analysis of Shock Loads on a Simple Structure," BRL Report No. CR 219, March 1975.

4. Rempel, J. R., "Room Filling From Air Blast," Appendix E to "Slanting for Combined Nuclear Weapon Effects: Examples with Estimates and Air Blast Room Filling," SRI Project No. 1219-1, Stanford Research Institute, Menlo Park, California, 1973.

5. Keefer, D., "Modeling of Room Response to Air Blasts," Final Report, Contract No. DAAG29-79-G-0049, U.S. Army Research Office, P.O. Box 12211, Research Triangle Park, NC, August 1979.

6. Vaidya, P. G., "The Acoustic Response of Rooms with Open Windows to Airborne Sounds," J. Sound and Vibration, 25, pp. 505-532, 1972.

7. Rempel, J. R., Private Communication.

8. Coulter, G. A., "Shielding From Blast Effects - 1/8th Scale Model City Complex," Draft Copy, BRL Memorandum Report, April 1980 (To Be Published).

9. Salman, A. and Gould, P. L., "Dynamic Response of Structures to Wind and Earthquake Loading," Halstead Press, 1980.

10. Porzel, F. B., "Height of Burst for Atomic Bombs, 1954. Part II, Theory of Surface Effects," Report No. LA-1665, Los Alamos Scientific Laboratory, May 1954.

11. Whitham, G. B., "A New Approach to the Problems of Shock Dynamics - Part I. Two Dimensional Problems," J. Fluid Mechanics, 2 , pp. 145-171, Jan-Aug 1957.

12. Coulter, G. A., "Blast Wave Loading of a 1/15th Scale Model House," BRL Report No. ARBRL-MR-03031, July 1980.

13. Taylor, W. J., "A Method for Predicting Blast Loads During the Diffraction Phase," Shock and Vibration Bulletin, Part 4, Bulletin 42, The Shock and Vibration Information Center, Naval Research Laboratory, Washington, D.C., Jan. 1972.

14. Porzel, F. B., "Study of Shock Impedance Effects in a Rough Walled Tunnel," Research Paper No. P-330, Institute for Defense Analysis, Science and Technology Division, Arlington, VA, March 1969.

15. East, L. F., "Aerodynamically Induced Resonance in Rectangular Cavities," J. Sound and Vibration, 3, pp. 277-287, 1966.

16. Plumblee, H. E., et al., "A Theoretical and Experimental Investigation of the Acoustic Response of Cavities in an Aerodynamic Flow," Report No. WADD-TR-61-75, Wright Patterson AFB, 1962.

17. Covert, E. E., "An Approximate Calculation of the Onset Velocity of Cavity Oscillations," AIAA Journal, Vol. 8, No. 12, pp. 2189-2194, Dec. 1970.

APPENDICES

APPENDIX A

USEFUL RELATIONS

1. Reflected overpressure, P_R , behind a shock wave reflected from a wall at normal incidence (for air).

$$P_R = P_A \left[1 + \frac{7}{\frac{6P_A}{P_s + P_A} + 1} \right] , \qquad (A.1)$$

where P_A is the ambient atmospheric pressure, and P_s is the peak overpressure of the incident shock wave.

2. Speed of sound, a_5 , behind a shock wave reflected from a surface at normal incidence (for air).

$$a_5 = a_o \left(\frac{(8z+7)(2z+7)}{7(7+6z)} \right)^{\frac{1}{2}} , \qquad (A.2)$$

where a_o is the ambient speed of sound and $z = P_s/P_A$.

3. Peak dynamic pressure, P_q , of the flow behind a shock wave.

$$P_q = \frac{5}{2} \frac{P_s^2}{7P_A + P_s} \tag{A.3}$$

APPENDIX B

EMPIRICAL MODELS FOR THE BLAST DIFFRACTION LOADING ON THE FRONT AND REAR OF A RECTANGULAR PARALLELEPIPED

Etheridge [2] has developed empirical models for the average loading on the front and rear surfaces of a rectangular block structure using shock tube data obtained by Taylor [13]. For the front surface, Etheridge chose the following form of equation to fit the data,

$$\frac{p(t)}{P_R} = \left(1 - \frac{P_L}{P_R}\right)e^{-A\eta^B} + \frac{P_L}{P_R} \quad , \tag{B.1}$$

where p(t) is the average overpressure on the surface and P_R is the reflected overpressure on the surface,

$$P_R = 2P_s\ (4z + 7)/(z + 7) \quad . \tag{B.2}$$

The overpressure approached as a limit, P_L, is equal to the stagnation overpressure P_{STAG},

$$P_L = P_{STAG} = (P_s + P_A)\left[1 + \frac{5z^2}{7(z+1)(z+7)}\right]^{7/2} - P_A, \quad (B.3)$$

where:

P_s = overpressure of the incident shock,

P_A = ambient pressure of the atmosphere,

$$z = P_s/P_A \quad , \qquad (B.4)$$

$$A = .265Z^{-.2} \quad , \qquad (B.5)$$

$$B = 1.5R + (1-R)(.97 + e^{-.177z^{.37}\eta}) \quad , \qquad (B.6)$$

$$\eta = ta_5\,(1 + R)/S \quad , \qquad (B.7)$$

and,

t = time.

The velocity of the rarefaction wave behind the shock, a_5 , is given by,

$$a_5 = a_o\sqrt{\frac{(8z+7)(2z+7)}{7(7+6z)}} \quad , \qquad (B.8)$$

where:

a_o = ambient sound velocity.

The ratio of the edges, S_1 and S_2, of the minimum rectangular area on the surface which must be examined, R , is given by,

$$R = S_1/S_2 \tag{B.9}$$

if $S_1 < S_2$, and

$$R = S_2/S_1 \tag{B.10}$$

if $S_1 > S_2$.

The minimum area on the surface which must be examined is shown for several configurations in Figure B-1. The minimum distance, S , to traverse the loaded area is taken to be S_1 or S_2 , whichever is smallest.

Equation B.1 was developed for a shock wave which does not decay in time, as in the case of a shock tube. Etheridge has modified Equation B.1 to account for the decay of the incident blast by reducing the pressure predicted by an amount proportional to the reduction in P_{STAG} with time utilizing this method Etheridge obtained,

$$p(t) = \left[P_R\left(1 - \frac{P_{STAG}}{P_R}\right)e^{-A\eta^B} + P_{STAG}\right] \cdot \frac{P_{STAG(t)}}{P_{STAG}} , \tag{B.11}$$

$P_{STAG}(t)$ is the stagnation overpressure of the blast wave at time t given by,

$$P_{STAG}(t) = (p_s(t) + P_A)\left[1 + \frac{2p_q(t)}{7(p_s(t) + P_A)}\right]^{7/2} - P_A , \tag{B.12}$$

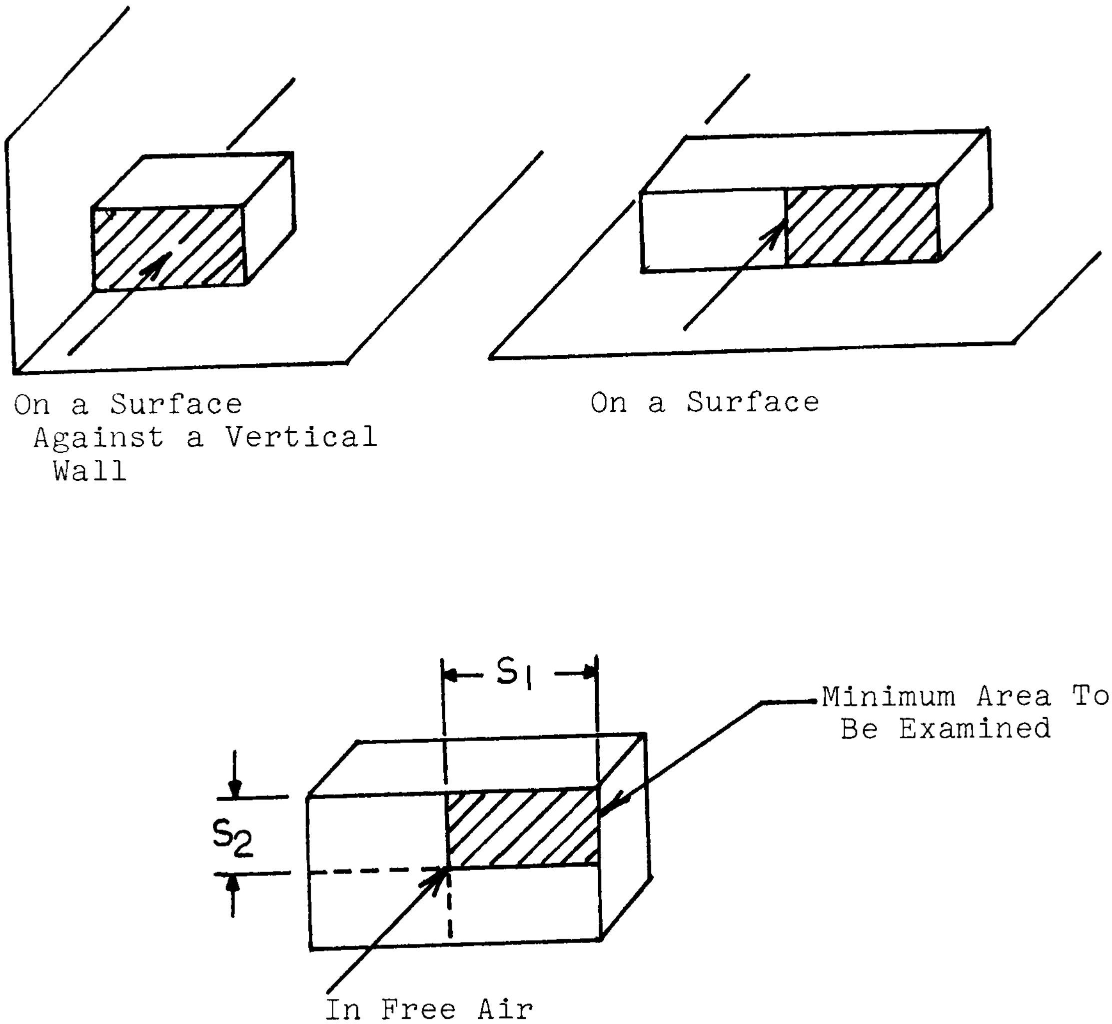

Figure B-1. Minimum Area To Be Examined In Order To Determine The Loading On A Surface Of A Building Exposed To A Blast Wave For Several Exposure Conditions.[2]

where:

$p_s(t)$ = the overpressure of the blast wave at time t,

and

$p_q(t)$ is the dynamic overpressure of the blast wave at time t.

For the rear surface, where the incident blast does not decay with time, Etheridge obtained the following equation to fit the data,

$$\frac{p(t)}{P_s} = \left\{ e^{-(.73-.41R)Z^{.5+1.4e^{-.83z}}} \right\} \left[1-e^{-.94e^{-.27z}\zeta(1+.16\zeta^2} \right] \tag{B.13}$$

where:

$$\zeta = t \cdot a_o/S \tag{B.14}$$

Etheridge noted that Equation B·13 may be modified to account for the decay of the incident blast. If it is assumed that the average pressure on the rear wall be reduced in proportion to the reduction in incident pressure from its peak value, then the decay can be accounted for by substituting $p_s(t)$ for P_s in Equation B 13.

APPENDIX C

DRAG CO-EFFICIENTS FOR THE FACES OF A STRUCTURE WITH A GABLED ROOF.

Drag Co-efficients have been given by Salmon [9] for the faces of a structure with a gabled roof exposed to wind (Figure C-1).

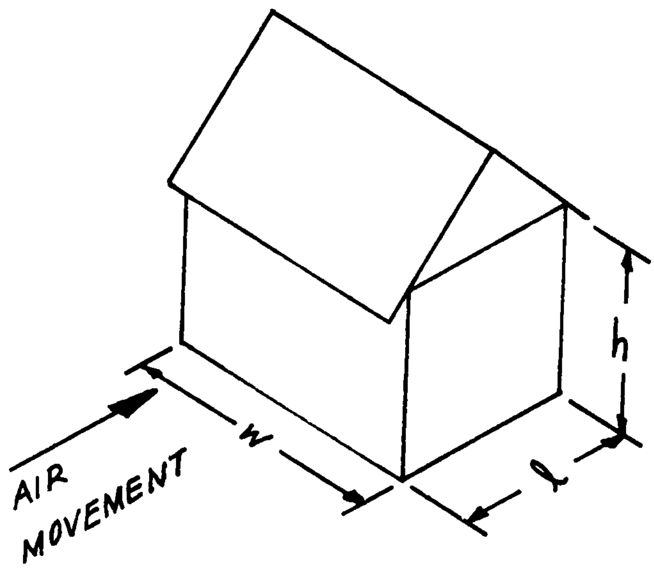

Figure C-1. Structure With a Gabled Roof Exposed to Wind.

These results are given in Tables C-1 and C-2 for the sides and roof of the structure respectively.

Table C-1. Drag Co-efficients for the Sides of a Building.

FACE	DRAG COEFFICIENT
Front	.8
Side	-.7
Rear ($h/\ell \geq 2.5$)	-.6
Rear ($h/\ell < 2.5$)	-.5

Table C-2. Drag Coefficients for the Roof of a Building.

Type of Roof										
Windward	h/w	10-15°	20	25	30	35	40	45	50	$\geqq$60
	$\leq$.3	.01θ*	.2	.25	.3	.35	.4	.45	.5	.01θ
	.5	-1	-.75	-.5	-.2	.05	.3	.45	.5	.01θ
	0.0	-1	-1	-.8	-.55	-.3	-.05	.2	.45	.01θ
	$\geq$1.5	-1	-1	-1	-.9	-.6	-.35	-.1	.2	.01θ
Leeward	all	-.7	for all θ							
Flat	<2.5	-.7								
	$\geq$2.5	-.8								

*Except for roofs using from ground level(h/w = o) a co-efficient of -1.0 shall be used when $10^\circ < \theta < 15^\circ$.

APPENDIX D

BASIC PROGRAM

```
20 REM
30 REM                              BASIC PROGRAM
40 REM
50 REM
60 REM
70 REM          THIS PROGRAM WILL CALCULATE BLAST LOADING ON STRUCTURES
80 REM    EXPOSED  TO LARGE SCALE CHEMICAL OR NUCLEAR EXPLOSIONS. THE
81 REM    PROGRAM IS BASED ON MODELS DEVELOPED BY R. H. ESKRIDGE AND
82 REM    D.R. KEEFER IN A FINAL REPORT ENTITLED 'PREDICTION OF BLAST
83 REM    INDUCED OVERPRESSURES ON ISOLATED AND SHIELDED STRUCTURES'.
84 REM    THIS WORK WAS SPONSORED BY THE ARMY RESEARCH OFFICE UNDER
85 REM    CONTRACT NO. DAAG29-79-C-0127.
90 REM          THE PROGRAM ACCEPTS SAMPLED DATA POINTS FROM ANY ARBITRARY
100 REM BLAST WAVE AS INPUT. THE OUTPUT IS IN THE FORM OF OVERPRESSURE ON
110 REM A PARTICULAR BUILDING FACE AS A FUNCTION OF TIME.  THE
120 REM PROGRAM IS APPLICABLE TO BUILDINGS WHICH ARE EITHER ISOLATED
130 REM OR SHIELDED BY THE PRESENCE OF NEARBY STRUCTURES. FOR ISOLATED
140 REM BUILDINGS, THE PROGRAM WILL MAKE CALCULATIONS FOR ALL FACES OF
150 REM THE BUILDING FOR ANY ANGLE OF INCIDENCE OF THE INCIDENT BLAST.
160 REM WAVE.   FOR THE SHIELDED CASE, THE PROGRAM IS APPLICABLE FOR THE
170 REM CASE OF NORMAL INCIDENCE ONLY.
190 REM          THE EFFECTS OF SHOCKS REFLECTED BETWEEN ADJACENT BUILDINGS
200 REM ARE ACCOUNTED FOR IN THIS PROGRAM.  THESE SHOCKS ARE ASSUMED TO
210 REM DECAY IN A GEOMETRIC PROGRESSION DETERMINED BY AN EMPIRICAL LOSS
220 REM COEFFICIENT.  THE LOSS INCURRED BY THE BLAST WAVE AS IT DIFFRACTS
230 REM AROUND ADJACENT BUILDINGS IS ALSO ACCOUNTED FOR.  THIS LOSS IS
240 REM DETERMINED BY A CRITERION FOR SHOCK RECOVERY DEVELOPED FROM
250 REM A TUNNEL ENTRY DIFFRACTION MODEL BY F.B.PORZEL . A MODEL
260 REM BY G.B. WHITHAM  HAS ALSO BEEN ADAPTED FOR USE IN PREDICTING
270 REM THE INITIAL OVERPRESSURE OF AN OBLIQUE SHOCK DIFFRACTED AROUND
280 REM A CORNER.
290 REM          A SIMPLE LINEAR MODEL HAS BEEN DEVELOPED TO APPROXIMATE
300 REM THE BUILDUP OR REDUCTION OF PRESSURE UPON A WALL EXPOSED TO AN
310 REM INCIDENT SHOCK WAVE.  IN THIS MODEL, THE RATE OF REDUCTION  IS
320 REM DETERMINED BY THE "CHARACTERISTIC TIME" FOR THE SURFACE. THIS
330 REM "CHARACTERISTIC TIME" IS EASILY CALCULATED IF THE GEOMETRY AND
340 REM SPEED OF SOUND ARE KNOWN .  DYNAMIC EFFECTS ARE ALSO INCLUDED
350 REM BY THE USE OF AN EMPIRICAL DRAG COEFFICIENT.
355 REM
356 REM ---------------------------------------------------------------
360 SET MULTIPLE
370 DIM T(10),PS(10),I(10),A(10)
380 PI=3.14159
390 REM ---------------------------------------------------------------
400 REM INPUT SECTION
410 REM ---------------------------------------------------------------
420 PRINT LIN(1)," INPUT SECTION  ",LIN(1)
430 INPUT " AMBIENT SPEED OF SOUND                 (M/S) ",A0
440 INPUT " AMBIENT ATMOSPHERIC PRESSURE           (KPA) ",PA
450 REM SIDE SURFACE MEANS SURFACE PARALLEL TO FLOW
460 INPUT " FRONT, REAR, OR SIDE SURFACE (F,R OR S)       ",S$
470 IF S$="S" THEN 490
480 INPUT " SHIELDED CASE (Y/N)                           ",SHIELD$
490 INPUT " CHARACTERISTIC DISTANCE                  (M) ",S
500 INPUT " DRAG COEFFICIENT                              ",CD
510 REM ***************************************************************
520 REM **** READ INPUT WAVE-  TIME(MS), PEAK-SIDE-ON OVERPRESSURE
```

```
530 REM -----------------------------------------------------------------
540 NPTS=3                              ! NPTS IS NO. OF INPUT DATA POINTS
550 DATA 0,26.3,15,8,40,-3.0
560 PRINT LIN(2);" INPUT WAVE","TIME (SEC)","PRESSURE (KPA)";LIN(1)
570 FOR N=1 TO NPTS\ READ T(N),PS(N)\T(N)=T(N)/1000\ PRINT " ",T(N),PS(N)
580 NEXT N\ PRINT LIN(1)
590 Z=PS(1)/PA
600 IF SHIELDS="Y" THEN GOSUB 1970 ELSE PPEAK=PS(1)
610 IF SHIELDS<>"Y" THEN TT=10000000  ! DISABLE REFLECTED SHOCKS
620 IF SS="S" THEN 2290
630 IF SS="F" THEN GOSUB 1360 ELSE GOSUB 1570
640 BETA=1/TAU
650 REM -----------------------------------------------------------------
660 REM **** MODIFY INPUT WAVE TO ACCOUNT FOR DYNAMIC EFFECTS
670 REM -----------------------------------------------------------------
680 PQ=2.5*(PS(1)^2/(7*PA+PS(1)))  ! PEAK DYNAMIC OVERPRESSURE (KPA)
690 CONSTANT=CD*PQ/PS(1)+1
700 FOR N=1 TO NPTS
710 I(N)=CONSTANT*PS(N)             ! I(N) IS MODIFIED INPUT
720 NEXT N
730 REM ------------------------------------------------------------------
740 REM **** CALCULATE SEGMENT SLOPES
750 REM ------------------------------------------------------------------
760 FOR N=1 TO (NPTS-1)
770 A(N)=(I(N+1)-I(N))/(T(N+1)-T(N))    ! A(N) IS SEGMENT SLOPE
780 NEXT N
790 GOSUB 1240                       !  SETUP ROUTINE FOR PLOTTING
800 N=1                             ! N IS INPUT SEGMENT INDEX
810 M=1                             ! M IS INDEX FOR SHOCK REFLECTION(=J+1)
820 DELT=(XMAX-XMIN)/70/1000        ! DELT IS SIZE OF TIME STEP
830 REM -------------------------------------------------------------------
840 REM *********BEGIN TIME LOOP**********
850 REM -------------------------------------------------------------------
860 FOR T=XMIN/1000 TO XMAX/1000 STEP DELT
870 IF T>=(2*TT*M/1000) THEN GOSUB 1120 ! TEST FOR ARRIVAL OF REFLECTED SHOCK
880 IF T>=T(N+1) THEN GOSUB 960     ! TEST FOR END OF INPUT SEGMENT
890 GOSUB 1030                       ! CALCULATE OVERPRESSURE
900 PHOLD=P
910 PLOT (T*1000,P)                 ! PLOT OUTPUT - OVERPRESSURE ON SURFACE
920 PRINT T*1000,P
930 NEXT T                          ! T IS TIME IN SECS.
940 REM
950 REM -------------------------------------------------------------------
960 REM  SUBROUTINE TO UPDATE INPUT SEGMENT
970 REM -------------------------------------------------------------------
980 N=N+1
990 P0=PHOLD
1000 T0=T-DELT/2
1010 RETURN
1020 REM ------------------------------------------------------------------
1030 REM  SUBROUTINE TO CALCULATE OVERPRESSURE ON THE WALL
1040 REM ------------------------------------------------------------------
1050 TERM1=(BETA*(T-T0)-1)*A(N)/BETA
1060 TERM2=(P0+(A(N)/BETA)-I(N))*EXP(-BETA*(T-T0))+I(N)
1070 P=TERM1+TERM2
1080 RETURN
1090 REM ------------------------------------------------------------------
1100 REM SUBROUTINE TO CALCULATE STRENGTH OF REFLECTED SHOCKS
1110 REM ------------------------------------------------------------------
1120 I(N)=I(N+1)+(A(N)*(T-T(N+1))) ! INTERPOLATE OVERPRESSURE
1130 T0=T-DELT                    ! RESET TIME "ZERO"
1140 M=M+1                         ! INCREMENT SHOCK INDEX
1150 J=M-1
1160 IF SS="F" THEN 1170 ELSE 1190
1170 P0=PHOLD+PPEAK*2*ALPHA^(2*J)        !FRONT SURFACE
1180 GOTO 1210
1190 P0=PHOLD+PPEAK*2*ALPHA^(2*J-1)      ! REAR SURFACE
1200 PHOLD=P0
1210 RETURN
1220 END
1230 REM -------------------------------------------------------------------
1240 REM PLOT SETUP SUBROUTINE  (FOR HP 2647A GRAPHICS TERMINAL)
1250 REM -------------------------------------------------------------------
1260 PRINT LIN(2)," INPUT WINDOW SIZE (USER UNITS) ";LIN(1)
1270 INPUT "XMIN,XMAX ",XMIN,XMAX
1280 INPUT " YMIN,YMAX ".YMIN,YMAX
```

```
1290 PLOTR
1300 LOCATE (15,175,10,90)
1310 SCALE (XMIN,XMAX,YMIN,YMAX)
1320 FXD (0,0)
1330 FRAME
1340 LAXES (1,5,0,0,5,2)
1350 RETURN
1360 REM -----------------------------------------------------
1370 REM SUBROUTINE TO DETERMINE PARAMETERS FOR FRONT SURFACE
1380 REM -----------------------------------------------------
1390 PRINT LIN(1)
1400 INPUT " NORMAL OR OBLIQUE CASE (N OR O) ",A$
1410 IF A$="N" THEN 1470
1420 INPUT " ANGLE OF INCIDENCE (DEGREES) ",AIN
1430 IF AIN>40 THEN 1440 ELSE 1470
1440 PRINT LIN(1),"TRANSITION REGION",LIN(1)
1450 INPUT " REFLECTED OVERPRESSURE ",PR
1460 GOTO 1490
1470 PR=PPEAK*(1+(1+1/6)/(PA/(PPEAK+PA)+1/6))
1480 PRINT LIN(1),"PR= ";PR
1490 Z1=PPEAK/PA
1500 PO=PR
1510 PRINT LIN(2),"INITIAL OVERPRESSURE= ";PO
1520 A5=A0*((8*Z1+7)*(2*Z1+7)/7/(7+6*Z1))^.5
1530 TAU=S/A5
1540 PRINT "CHARACTERISTIC TIME= ",TAU
1550 PRINT "SPEED OF SOUND BEHIND REFLECTED SHOCK= ",A5
1560 RETURN
1570 REM
1580 PRINT LIN(2)
1590 REM -----------------------------------------------------
1600 REM SUBROUTINE TO DETERMINE PARAMETERS FOR REAR SURFACE
1610 REM -----------------------------------------------------
1620 INPUT " NORMAL OR OBLIQUE CASE (N OR O) ",A$
1630 IF A$="N" THEN 1770
1640 PRINT " INITIAL ANGLE OF INCIDENCE OF SHOCK TO SURFACE "
1650 INPUT " PRIOR TO DIFFRACTION (DEGREES) ?",AIN
1660 IF AIN=90 THEN 1810
1670 IF AIN>40 THEN 1710 ELSE 1740
1680 PRINT " "
1690 PRINT " FOR ANGLES OF INCIDENCE > 40 DEGREES , NEAR REGION OF MACH"
1700 PRINT " TRANSITION REGION , INPUT REFLECTED OVERPRESSURE"
1710 INPUT " REFLECTED OVERPRESSURE ",PR
1720 Z=PR/PA
1730 GOTO 1810
1740 PR=PS(1)*(1+(1+1/6)/(PA/(PS(1)+PA)+1/6))
1750 Z=PR/PA
1760 GOTO 1810
1770 THETA=(-PI/2)  ! FOR NORMAL INCIDENCE
1780 AIN=90
1790 GOTO 1830
1800 PRINT " "
1810 INPUT " SHOCK TURNING ANGLE FOR DIFFRACTION (DEGREES) ? ",THETA
1820 THETA=THETA*PI/180
1830 M0=(1/7+(6/7)*(Z+1))^.5
1840 PRINT "INITIAL SHOCK MACH NO.,  M0= ";M0
1850 THETALIM=-1*(2^1.5*(M0-1)^.5)
1860 PRINT " "
1870 PRINT "LIMITING TURNING ANGLE ,THETALIM = ",THETALIM*180/PI;" DEGREES"
1880 TERM1=(((THETA/(2^1.5))+(M0-1)^.5)^2+1)^2
1890 TERM1=(TERM1-1/7)/(M0^2-1/7)
1900 IF AIN=90 THEN PR=PS(1)
1910 PD=((PR+PA)*TERM1)-PA
1920 PRINT " DIFFRACTED OVERPRESSURE, PD = ",PD
1930 IF THETA<THETALIM THEN PO=0 ELSE PO=PD
1940 PRINT "PO= ";PO,LIN(1)
1950 TAU=S/A0
1960 RETURN
1970 REM -----------------------------------------------------
1980 REM SUBROUTINE TO DETERMINE PARAMETERS FOR SHIELDED CASE
1990 REM -----------------------------------------------------
2000 INPUT " SHORTEST DISTANCE FROM GUAGE TO ADJACENT BUILING",DSHORT
2010 INPUT "SHOCK LOSS COEFFICIENT                    ",ALPHA
2020 U0=A0*(1/7+6*(Z+1)/7)^.5  ! SHOCK VELOCITY
2030 TT=DSHORT/U0*1000         ! TRANSIT TIME
2040 PRINT LIN(1)," SHOCK TRANSIT TIME =  ",TT;" MS ",LIN(1)
```

```
2050 INPUT " IS THIS A ROOF? (Y/N)  ",ROOF$
2060 IF ROOF$="Y" THEN 2240 ! ROOF IS TREATED AS ISOLATED CASE
2070 REM MODE OF SHOCK DIFFRACTION MAY BE PRIMARILY VERTICAL
2080 REM (AS WHEN THE TARGET IS COMPLETELY SURROUNDED BY BUILDINGS)
2090 REM OR BOTH VERTICAL AND HORIZONTAL( AS WHEN BUILDINGS ARE
2100 REM ONLY IN FRONT   AND/OR BEHIND THE TARGET)
2110 INPUT " MODE OF SHOCK DIFFRACTION( V OR VH) ",E$
2120 INPUT " WIDTH OF SHIELD       (M) ",W
2130 INPUT " HEIGHT OF SHIELD WALL (M) ",H
2140 D=((((14-Z)^2+224*Z)^.5)+Z-14)/16 ! D IS PD/PA (PORZEL, REF. 14)
2150 UD=A0*(1/7+6*(D+1)/7)^.5
2160 UPRIME=UD/U0                     ! SHOCK VELOCITY RATIO
2170 L=DSHORT
2180 HR=W/2/L/UPRIME       ! CRITERION FOR SHOCK RECOVERY
2190 VR=H/L/UPRIME
2200 IF E$="V" THEN 2230
2210 IF HR<1 THEN 2240
2220 IF VR<1 THEN 2240 ELSE 2260
2230 IF VR<1 THEN 2240 ELSE 2260
2240 PPEAK=PS(1)  ! SHOCK RECOVERS
2250 GOTO 2270
2260 PPEAK=D*PA    ! SHOCK DOESN'T RECOVER
2270 PRINT LIN(1),"PEAK OVERPRESSURE = ";PPEAK,LIN(1)
2280 RETURN
2285 REM ------------------------------------------------------------
2290 REM INITIALIZE ROUTINE FOR SIDE SURFACE
2295 REM ------------------------------------------------------------
2300 P0=PS(1)
2310 TAU=S/A0
2320 GOTO 640
2330 END
```

VITA

Richard H. Eskridge was born in Memphis, Tennessee, on July 3, 1957. He attended elementary schools in Dyersburg, Tennessee, and was graduated from Dyersburg High School in June 1975. He attended Dyersburg State Community College until June 1977. He entered the University of Tennessee at Martin in September 1977 and began study towards a Bachelor of Science degree in Mechanical Engineering Technology. This degree was awarded with high honors in June 1979. He accepted a graduate research assistantship with the University of Tennessee Space Institute immediately thereafter and began study towards a Master of Science degree with a major in Engineering Science. This degree is the object of the present work.

The author is married to the former Kathy Vance of Dyersburg, Tennessee.